Interleaved spread spectrum orthogonal frequency division multiplexing for system coexistence

Pingzhou Tu
University of Wollongong

Interleaved Spread Spectrum Orthogonal Frequency Division Multiplexing for System Coexistence

Pingzhou Tu

A thesis submitted for the degree Doctor of Philosophy
University of Wollongong

School of Electrical, Computer and Telecommunication Engineering
July 2008

Abstract

Various kinds of wireless communication devices and systems provide a number of different functions and services to meet different demands for people. Some of these devices and systems coexist in the same area and share the common frequency bands according to some coexistence mechanisms such as cooperative and non-cooperative mechanisms. These mechanisms including power control, frequency hopping and time division multiplexing technique can handle electromagnetic interference between coexistence devices to some extent, but for the coexistence systems the interference problems between these systems are still very serious issues which affect coexistence system performance. In this thesis we consider the system coexistence interference problems in the spectrum shared environments.

Rather than applying the techniques of power control, frequency control, time control and spatial control to avoid interference, we attempt to address the fundamental nature of system transmission. The general philosophy is to combine the orthogonal frequency division multiplexing (OFDM) technique with a spectrum spread method to generate an interleaved spectrum spread OFDM (ISS-OFDM) multiple subband signal, so that the system transmission subbands are selected adaptively and system coexistence interference is avoided and suppressed. This approach reveals the potential ability of system coexistence.

Simulated results on system performance such as peak to average power ratio (PAR), signal frequency diversity and time diversity, and system bit error rate (BER) are presented to verify that system transmission bandwidth can be adaptively selected to avoid interference of coexistence systems and improve system performance. We then consider the implications of choosing or dropping the subbands with different levels of interference from the multiple subbands of the ISS-OFDM signal, and show that (i) it is possible to implement the information transmission without

information loss by selecting some of the subbands with an interference level below the threshold, and dropping the subbands with an interference level over the threshold, and (ii) it is possible to derive the interference thresholds, based on which the adaptive selection subband transmission is implemented. We also show that it is possible to replace the interference thresholds over multipath fading channels by the interference thresholds over the Gaussian channels, so that the derivation process of interference thresholds over the multipath fading channels is greatly simplified.

Through the theoretical analysis and investigations, we show that the ISS-OFDM technique can be applied to the coexisting systems sharing the frequency bands in the industrial, scientific and medical (ISM) band. Coupled with a technique for cognitive radios, the ISS-OFDM can be applied to a wide class of problems covering the interference suppression and spectrum efficiency improvement.

Declaration

This is to certify that the work presented in this thesis is solely my own, except where due reference is made in the text.

No work in this thesis has been submitted for degree to any other university or institutions.

Signed

Pingzhou Tu

July 18, 2008

Acknowledgements

The work presented in this thesis would not have been possible without the help and the support of the following people.

My supervisor Associate Professor Xiaojing Huang, with his guidance, insight, enthusiasm and unique wit, has inspired me to advance towards the Ph.D goals step by step.

My co-supervisor Professor Eryk Dutkiewicz, with his many helpful suggestions on this work and his generous financial support, has made me concentrate on my Ph.D study without any disturbance.

My wife, Gang Xu, and my two lovely sons, Robert Tu and Michael Tu, have encouraged and pushed me to work very hard toward my career destination.

My fellow students in the Wireless Technologies Laboratory and ICT Research Institute and stuff of the School provided me with a lot of advice and help in my daily research work.

Contents

List of Figures

List of Tables

List of Abbreviations

AFD-OFDM	adaptive frequency diversity OFDM
AP	access point
AWGN	additive white Gaussian channel
BER	bit error rate
BPSK	binary phase shift keying
BS	base station
CDMA	code division multiple access
CES	complex exponential spreading
CI	convolutional interleaving
CR	cognitive radios
CSMA/CA	carrier sense multiple access/collision avoidance
CTS	clear to send
CP	cyclic prefix
CDF	cumulative distribution function
DAB	digital audio broadcast
DFS	dynamic frequency selection
DSSS	direct sequence spread spectrum
FDD	frequency division duplex
FDMA	frequency diversion multiple access
FFT	fast Fourier transform
MWT	modified Walsh transform
FH	frequency hopping
FH-SS	frequency hopped spread spectrum
FSK	frequency shift keying
FD-OFDM	frequency diversity OFDM
GFSK	Gaussian frequency shift keying
ICI	inter channel interference
IFFT	inverse fast Fourier transform

ISI	inter symbol interference
ISM	industrial, scientific and medical
ISS-OFDM	interleaved spread spectrum orthogonal frequency division multiplexing
LOS	line-of-sight
MAC	medium access control
MB-OFDM	multiband OFDM
MBOA	multiband OFDM alliance
MBOA-UWB	MBOA ultra-wideband
MIMO-OFDM	multiple-input multiple-output OFDM
MRC	maximum ratio combining
MC-CDMA	multicarrier CDMA
OESI	odd-even symmetric interleaver
OFDM	orthogonal frequency division multiplexing
PAM	pulse amplitude modulation
PAR	peak-to-average power ratio
PC	power control
PCB	printed circuit board
PDA	personal digital assistant
PDF	probability density function
PI	periodic interleaving
QAM	quadrature amplitude modulation
QPSK	quadrature phase shift keying
RF	radio frequency
RTS	request to send
RS	Reed-Solomon
RSSI	received signal strength indicator
SDMA	spatial division multiple access
SDR	software designed radio
SI	spread interleaving
SINR	signal to interference noise ratio
SIR	signal to interference ratio
SS	subscriber station

SS-MC-MA	spread-spectrum multiple-carrier multiple-access
SS-OFDM	spread spectrum OFDM
TA	time agility
TDD	time division duplex
TDMA	time division multiple access
UHF	ultra high frequency
UWB	ultra-wideband
VHF	very high frequency
VISA	virtual subcarrier assignment
VoIP	voice over Internet protocol
WBAN	wireless body area networks
WiMAX	worldwide interoperability for microwave access
Wi-Fi	wireless fidelity
WLAN	wireless local area networks
WMAN	wireless metropolitan area network
WPAN	wireless personal area network

Chapter 1

Introduction

The wireless communication technologies are widely and deeply penetrating the daily lives of people to create a new information and communication environment in the modern society. The use of wireless communication services will enable people to study, play, work and shop anywhere they want [1]. The significance of the "space" and "place" is quite different from our conventional thinking, which are surrounded by various wireless devices and networks coexisting in the same space. Some of these wireless devices and systems are sharing the same spectrum environments to complete communication services. Although some cooperative and non-cooperative mechanisms [2, 3] are adopted in the sharing of the same spectrum, the conflicts of the electromagnetic frequency spectrum, the interference between different systems, are still serious issues that need to be solved. Until recently, very few papers studied the operation of several different wireless systems in the same frequency band [4].

1.1 Wireless Coexistence Environment

The coexistence environments of wireless communication systems can be a home, a small office, a campus, a hospital, an industry company, and even the same metropolis or a nation. In an office environment, for example, different groups of electronic devices may constitute different wireless local area networks (WLANs) [5] to serve different people or sections. When the different WLANs are operating in the same frequency bands at the same time, there may be conflict in the use of the frequencies. The conflict can cause significant damage for the performance of the coexistence systems, and decrease the coexistence ability of systems [6].

Coexistence is the ability of one system to perform a task in a given shared environment in which there are other systems that may or may not be using the same set of rules [7]. Simply speaking, coexistence is the ability that multiple systems collocate in the same radio frequency environment sharing the common frequency bands and performing their own functions.

1.2 Coexistence Modes

Many different modes in wireless communication system coexistence can be run. According to the shared frequency band, it can be classified into system coexistence sharing a licensed frequency band and system coexistence sharing a non-licensed frequency band. According to coexistence locations, system coexistence can be categorized into coexistence devices in a single chip or single printed circuit board (PCB) [8], or in a certain range of area. According to the system coexistence solution mechanism, system coexistence can be divided into collaborative mechanisms and non-collaborative mechanisms.

In a shared licensed frequency band, since the electromagnetic spectrum natural resource is very limited, its use by transmitters and receivers is licensed by radio management government regulatory agencies. The licensed users are sharing the common frequency bands by using some kinds of frequency access technologies, such as the time division multiple access (TDMA) [9], frequency diversion multiple access (FDMA) [10], and code division multiple access (CDMA) [11-14]. Recently,

some researchers proposed cognitive radio (CR) techniques [15-19] combining orthogonal frequency division multiplexing (OFDM) techniques [20-25] to realize spectrum sharing and improve the efficiency of spectrum utilization. It is believed that in many frequency bands, the spectrum access is more significant than physical scarcity of spectrum. In a large part of the licensed frequency band, due to the legacy command-to-control regulation, the ability of access spectrum of users is limited severely. In a great range of rural areas, even in rich revenue urban areas, some of the frequency bands are largely unoccupied most of the time; some other frequency bands are partially occupied; only small portions of the spectrum are densely occupied. Thus, researchers proposed the idea of the combination of CR and OFDM to efficiently use the spectrum holes, which are lots of discrete frequency bands assigned to primary users, but at a particular time and at a specific geographic location, the bands are not being occupied by the primary users. Thus, the efficiency of the spectrum utilization can be greatly improved by assigning the spectrum holes to the unlicensed secondary users. For the coexistence system sharing unlicensed frequency bands such as in industrial, scientific and medical (ISM) bands [26] , the spectrum can be used by some users without license. ISM bands were originally reserved internationally for the use of radio frequency (RF) electromagnetic fields for industrial, scientific and medical purposes other than communications [27]. However, in recent years these bands have also been shared with license-free error-tolerant communications applications such as WLANs and cordless phones in the 915 MHz, 2450 MHz, and 5800 MHz bands. Since the ISM frequency bands are shared with license-free devices, more and more devices are using the ISM frequency bands. Thus, many systems and devices coexist and share radio frequency bands in ISM bands.

The coexistence systems collocated in the same printed circuit board or chip can be easily controlled by using some access technologies. The typical example experiments produced for the collocated coexistence devices are the coexistence between WLAN IEEE 802.11b and Bluetooth [28]. For realization of system coexistence, some experimental products have already integrated the devices of short-range IEEE802.11b/g WLAN and Bluetooth into a single printed circuit board [29, 30].

The more common system coexistence is that multiple systems are collocated in a certain area, such as office, building, campus, hospital and even in the same metropolis. For many people, the most commonly encountered ISM device is the home microwave oven operating at 2.45 GHz. In the future wireless networks, 802.16a wireless metropolitan area network (WMAN) [31, 32] or the worldwide interoperability for microwave access (WiMAX) will be capable of providing wireless backhaul connectivity to homes and offices, while IEEE802.11b may offer complementary local area network capability in a home, office or campus. Since the IEEE802.16a will be able to operate in unlicensed spectrum bands, spectral resources would also have to be shared with other wireless systems such as ultra-wideband (UWB) devices [33, 34].

Figure 1.1 reviews the wireless communications environments which have already been developed or will be developed in the near future. These coexistence systems include WiMAX, wireless fidelity (Wi-Fi) [35, 36] [37], Bluetooth, multiband OFDM (MB-OFDM), and wireless body area networks (WBAN) [34, 38]. These systems could be collocated in an office, room or a building and share the unlicensed ISM frequency bands from 2GHz to 66GHz.

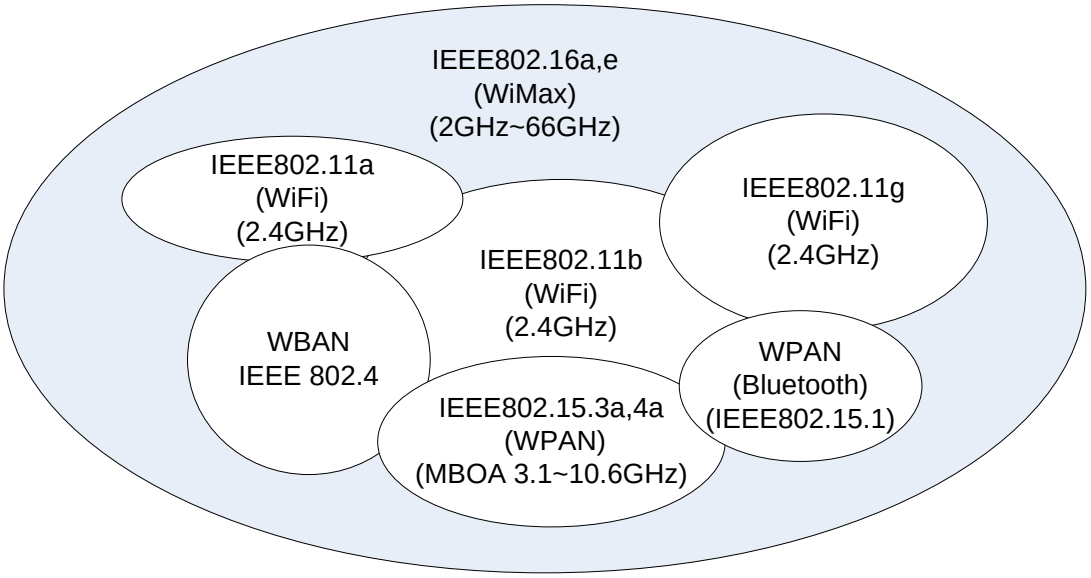

Figure 1.1 Review of systems coexistence.

Wi-Fi is a set of WLAN standards including IEEE 802.11a, IEEE 802.11b and IEEE 802.11g. The working frequency bands are 2.4GHz for IEEE 802.11b and IEEE 802.11g, 5GHz for IEEE 802.11a [8]. The data rate of IEEE 802.11a, IEEE 802.11b and IEEE 802.11a is from 11Mbps to 54 Mbps. Their transmission distance is less than 100 meters. Both IEEE 802.11a, and IEEE 802.11g adopt the OFDM modulation scheme, except that IEEE 802.11b uses DSSS modulation [39, 40]. The key access feature is carrier sense multiple access/collision avoidance (CSMA/CA) and virtual carrier sense. The transmitter checks if the subcarrier is available. If it is free, then the transmitter sends a request to send (RTS) short packet which includes the source and destination address and the duration for the subsequent data transmission. The receiver responds to the enquiry signal with clear to send (CTS). If the communication between the receiver and the transmitter is established, the data information then is transmitted. Others wait for the duration indicated in the RTS and use random back-off before they start to sense the carrier again.

WiMAX is a set of WMAN standard including IEEE 802.16d and IEEE 802.16e. Their frequency band is within 2GHz to 66GHz, especially at 2.3GHz to 2.4GHz, and 2.5GHz to 2.7GHz. IEEE 802.16d is used for non-mobility communication. IEEE 802.16e is for full mobility communication in a metropolitan area. Its

maximum transmission distance is 54km. Based on IEEE 802.16 the maximum throughput can be 75Mbps. The modulation scheme can be multiple levels such as binary phase shift keying (BPSK), quadrature phase shift keying (QPSK) and 64 quadrature amplitude modulation (QAM) modulations. The convolutional code and Reed-Solomon (RS) code [41, 42] are mandatory. Block turbo code and convolution turbo code are optional. It supports time division duplex (TDD) and frequency division duplex (FDD) access mode. This technique is the most promising technique in wireless communications, and it has the potential to replace the Wi-Fi and 3G mobile communications system [43].

Bluetooth is an alias of IEEE 802.15.1a and its maximum throughput is 1Mbps and transmission range can be up to 10 meters. The channel bandwidth is 1MHz and it adopts the Gaussian frequency shift key (GFSK) modulation technique. It is one of the typical wireless personal area network (WPAN). The most common products are the Bluetooth mobile handset.

Wireless body area network (WBAN) is a very popular topic that is being developed by many researchers. There is no standard for WBAN yet. However, many developers are doing their work based on the IEEE 802.15.4a standard. WBAN transmission range is up to 3 meters. There are two ultra-wideband communications techniques used, one is the ultra-wideband ultra high speed communications such as the MB-OFDM technique [44, 45], another one is ultra- wideband low speed communications used in circumstances where high speed is not required such as in medical diagnosis.

MBOA-UWB is a multiple band OFDM ultra-wideband WPAN technique. Its peak date rate can be 640Mbps and frequency band from 3.1GHz to 10.6GHz. The maximum transmission range is 3 meters and channel bandwidth is 528 MHz. The ultra-wideband channel bandwidth is implemented by frequency hopping techniques so that the transmission signal satisfies the definition of the ultra-wideband signal made by the FCC. This technique can be applied to WPAN.

1.3 Advantages of System Coexistence

There are many distinctive advantages for multiple system coexistence. The most important advantage for wireless communications system coexistence is that the efficiency of spectrum utilization is improved. In consequence, it releases the problems of physical scarcity of spectrum and solves the air interface problems.

Another distinctive advantage for system coexistence is that it can eliminate the space problems with the layout of multiple devices in a narrow space. The typical example is the coexistence communication systems in a navy ship. In a navy ship, there are more than one hundred various antennas located in the deck. Since the space of the navy ship is very limited, the layout of the antennas must make sure that various communication systems coexist with as little interference as possible. Otherwise, the coexistence communications system would malfunction. In this case, system coexistence techniques are extremely important.

1.4 Coexistence Problems

System coexistence has brought benefits to the coexistence users and systems. However, it can also cause some severe problems. One of the biggest problems is the electromagnetic interference, which in consequence, causes the increase of bit error rate; sometimes it even causes system malfunction and collapse.

For finding out the interference problems caused by coexistence systems, let us review an experiment done by Rutgers University in the United States. This experiment is carried out when Bluetooth, multiband OFDM and microwave are collocated in the same environment. Two common interference sources are respectively generated by Bluetooth radio and microwave, and the eigenvalue of the received OFDM signal is analyzed by using computer simulation. The experiment shows that the impairment of an interfering signal on the OFDM signal depends on the power of the interference and the data rate of the transmitted OFDM signal. The

experimental results are as expected that the OFDM system bit error rate (BER) performance increases with the increasing of the interference signal power and the increasing of the OFDM transmitted signal data rate. In the presence of the Bluetooth signal interference, several eigenvalues of the received OFDM signal are proportional to the interfering signal power. In the presence of the microwave signal interference, one of 64 eigenvalues of the received OFDM signal is affected. This experiment indicates that coexistence systems interfere with each other and the influence of the interference on other coexisting systems depends on the channel parameters of the coexisting systems [46].

1.5 Interference Sources

The causes of interference among coexisitng systems come from three sources. One is because of the common frequency bands sharing among the coexisting systems. The second source is because of the same type of modulation mode of coexisting systems. The third one is from the electromagnetic propagation modes.

For the source of frequency bands sharing, since the wireless communication does not need a wire, it can implement mobile communications and share the common frequency bands by employing some kinds of access techniques. Multiple wireless access techniques such as FDMA, TDMA, CDMA and spatial division multiple access (SDMA) are designed assuming that each system is using the entire resource at the instant interval, and they can function very well independently in a single system environment [47, 48]. However, these kinds of access technologies do not work very well when multiple systems collocate in proximity to each other and share the same frequency bands. For instance, when two or more systems are coexisting in the same environment and sharing the common frequency band, the system, which transmits signals with a relatively higher power or uses certain protocols against interference, can get high throughput and achieve high speed data transmission. Others which transmit signals with a relatively lower power can not perform their functions because of the interference which is from the signal transmitted with the higher power, or at least their throughput would be reduced. With the number of the

coexisting systems increasing, the interference between the coexisting systems could be more severe, sometimes even causing the whole system to fail.

If multiple coexisting systems use the same type of modulation mode, it is similar to the situation in which multiple users of the same system work together without exchanging coordination information. In this situation, there is no doubt that interference will result.

Since electromagnetic interference is closely related to the frequency bands and electromagnetic propagations, it is necessary to observe the electromagnetic propagations characteristics. In wireless communication systems, information is transmitted by wireless electromagnetic propagation channels. By an antenna which serves as the radiator, electromagnetic energy bearing information is coupled to the propagation medium and electromagnetic wave. Different electromagnetic waves have different propagation characteristics. According to the wavelength of the electromagnetic wave, an electromagnetic wave is divided into various frequency bands which are used for different channel propagations. Figure 1.2 illustrates the various frequency bands of the electromagnetic spectrum [49].

It can be seen from Figure 1.2 that the electromagnetic propagation channels differentiate according to the electromagnetic wave frequency bands. The mode of the propagation of electromagnetic waves in the atmosphere and in free space may be subdivided into three categories. One is the ground-wave propagation which uses frequency bands from audio band 3KHz to 3MHz; the second one is sky-wave propagation which confines its frequency band from 3MHz to 30MHz; the third is line-of-sight propagation with the frequency above 30MHz.

The ground propagation mode is a kind of propagation depending on the earth and ionosphere. Frequencies between the very low frequency and audio frequency bands are primarily used to provide navigational aids from shore to ships around the world. Its channel bandwidth is usually equal to 1~10% of the carrier center frequency. The transmission speed is very slow and it is usually confined to digital transmission. The main noise source is from thunderstorms, and in tropical regions the noise from

thunderstorms is more severe. Interference to the system comes from many users of the frequency band. At frequencies above the audio band, i.e., in the medium frequency band (0.3-3MHz), the ground-wave propagation is the dominant mode of propagation. The propagation in this frequency band is used for AM broadcasting and maritime radio broadcasting. The interference is the combination of atmospheric, manmade, and thermal noise from the electronic components at the receiver.

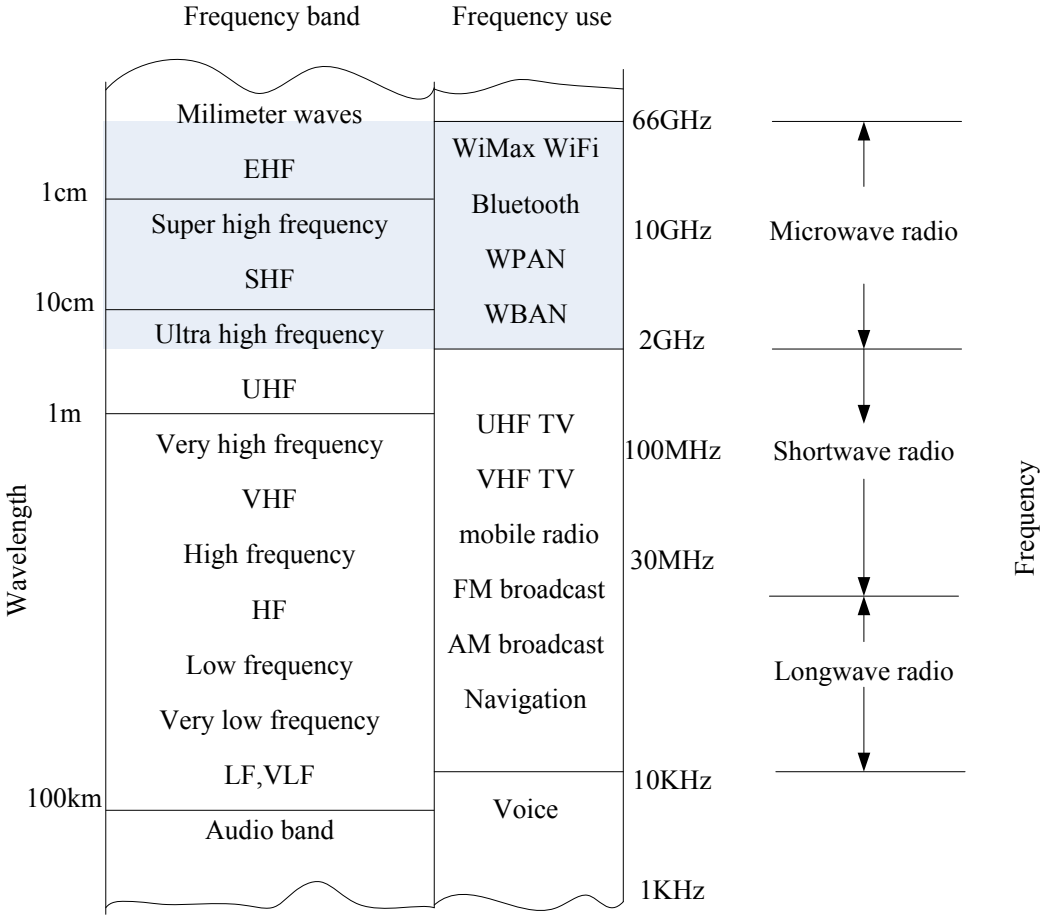

Figure 1.2 Frequency range for wireless electromagnetic channels.

Sky-wave propagation in frequency band 3MHz~30MHz results from transmitted signals being reflected from the ionosphere. Since the ionosphere comprises of many layers of charged particles which are about 50km to 400km above the surface of the earth, the sky-wave propagation yields two main problems, signal multipath and channel fading. Signal multipath results from the different paths of the signal wave propagation. Consequently, the inter-symbol interference is introduced in a digital communication system. Channel fading results because of the different propagation

delays of the same signal. Due to the different delays, received signal components with different delays add constructively. The noise in the receiver consists of the atmosphere and thermal noise.

At frequencies above 30MHz, in the frequency band from 30MHz to 66GHz, the main mode of electromagnetic propagation is line-of-sight (LOS) propagation. Frequencies in this band propagate through the ionosphere with relatively little loss and no obstructions, which makes the satellite and extraterrestrial communications possible. In very high frequency (VHF) and ultra high frequency (UHF) ranges, the main noise affecting the performance of a communication system is thermal noise generated in the receiver front end and cosmic noise picked up by the antenna. At frequencies above 10GHz, i.e., in the super high frequency band, atmospheric conditions play a major role in signal propagation. The propagation in this frequency band is easy to be interfered by the atmosphere such as heavy rain. Sometimes the systems may break down in the communications. At frequencies above 100GHz, i,e, the extremely high frequency bands, the electromagnetic spectrum belongs to the infrared and visible light regions, which can be used to provide LOS optical communications in free space. Until now some wireless products working in frequency bands 2GHz to 10GHz are seen in wireless communications markets. Most of the devices and products with frequencies higher than 5GHz are in the experimental stages.

The descriptions above introduce various electromagnetic propagation environments. In this thesis, our focus will be placed on electromagnetic propagations in atmospheric environments. The spectrum will be focused on frequency bands within 2GH to 66GHz.

1.6 Existing Solutions

The exiting solutions for overcoming the coexistence interference are different according to different coexistence environments characteristics. One Solution Is for the coexistence between the same type of wireless communication devices and

systems; the second is for the coexistence between different devices such as Wi-Fi and WiMAX; the third is for the coexistence between WiMAX and other ultra-wideband wireless communication systems.

1.6.1 Coexistence between the Same Types of Devices

The coexistence between the same type of wireless communication devices and systems are very common. For instance, in an office environment several different electronic devices, such as personal computers (PCs), printers, photocopy machines, fax machines, projectors and personal digital assistant (PDA), are deployed in a local area and serve different purposes. Some groups of them may constitute WLANs using the same OFDM-based standards such as IEEE802.11a or IEEE802.11g. As we discussed above, IEEE 802.11a and IEEE 802.11g use the same modulation mode OFDM, work with the same channel bandwidth 20MHz, the same peak data rate and the same number of subcarriers. Devices belonging to the same type of WLANs can work together without significantly impact on each other. However, coexistence interference still needs some measures to be handled.

One of the solutions for coexistence interference between the same types of devices is to use a spatial filtering technique called Virtual Subcarrier Assignment (VISA) for the OFDM signal. In this technique, the OFDM modulation subcarrers are classified into data subcarriers which are used to convey information, and virtual subcarriers which are not used for actual data transmission. Some of the virtual subcarriers are used to label different OFDM signals, based on which adaptive array antenna at the receiver can accept or reject the OFDM signal selectively [50].

1.6.2 Coexistence between the Different Types of Devices and Systems

The coexistence between different types of devices and systems such as Wi-Fi and WiMAX is implemented in both the MAC layer and physical layer. At home and in an office, WLANs are deployed and can serve different users though the connection between the office and the home still relies on the wired communications. WiMAX is expected to provide wireless backhaul connectivity to homes and offices, while WLAN offers complementary local area network capability within a home, office or campus. Thus, the coexistence between Wi-Fi and WiMAX is desirable. The challenge of the coexistence is because WiMAX operates in several frequency bands, the most common frequency bands being 2.3~2.4 and 2.5GHz and 2.7GHz. Although the frequency separation between Wi-Fi and WiMAX is greater than that between the Wi-Fi and Bluetooth, it is not enough to prevent the coexistence interference between Wi-Fi and WiMAX.

For solving the coexistence interference problem between Wi-Fi and WiMAX, the coexisting solutions are limited to the methods both in the physical layer and MAC layer. Some researcher proposed solutions in the physical layer to dynamically switch frequency channels and adaptively control the power, based on the interference detection by employing cognitive radio techniques [51]. In the MAC layer the solutions focus on rescheduling the MAC packet transmission times to ensure that the allocated frequency bands are time-multiplexed and non-concurrent. These solutions can solve the coexistence interference in a coordinated manner, but they need the supports of cognitive radio techniques.

1.6.3 Coexistence among UWB Systems

The coexistence solutions among systems such as WiMAX and ultra-wideband multiple subband OFDM are proposed by using cognitive radios. The coexistence problems between WiMAX and UWB OFDM are much more complex. In the near future, wireless UWB communication system and WiMAX devices are expected to coexist in a localized area. It is very possible that UWB systems and WiMAX will be collocated in a personal computer. In wireless UWB communications, there has been concern among many other users of the radio spectrum that UWB would

artificially boost the noise floor and degrade performance of the incumbent users as UWB signals are spread over a broad swath of spectrum at power levels near the noise floor. In 2002 the Federal Communication Commission (FCC) approved the first Report and Order, in which the FCC not only defined UWB signals, but also defined a spectrum mask that specifies the amount of power that can be radiated by UWB systems across the band. The spectral mask requires UWB to avoid emissions in a given band, even if it is not in use by any other device within the limited range of the UWB signal. If the spectral mask is satisfied, as the UWB signal is generally at or near the thermal noise floor, the UWB signal could not be perceived by devices which are more than 10 meters away unless high gain antennas are employed.

In order to satisfy the spectral mask regulated by the FCC in a given frequency band, Johann Chiang and Jim Lansford proposed the detect and avoid (DAA) solution for reducing coexistence interference between MB-OFDM UWB systems and WiMAX devices [52, 53]. The main idea for this Solution Is to sculpture the spectrum of the MB-OFDM signal based on the priori decision about restricting the emission of the UWB signal in a certain frequency bands. The tone weighting of the OFDM signal could be obtained by an environment survey done by the OFDM modem to measure the interference temperature of the environments. This Solution Is a nice idea. However, it relies only on the quality analysis and it did not offer any quantitative results.

In summary, almost all of the existing solutions for the existence interference are investigated in the physical layer or in the MAC layer. Currently, there are limited spectrum sharing rules based on listen-before-talk in the unlicensed bands, and they are considered inadequate for achieving coexistence between systems. Most of the schemes are focusing on the physical layer to allocate the system resources to separate coexisting signals from others by using time, frequency, power, space, and coding [54, 55], so that interference could be reduced, spectrum sharing efficiency could be improved and system capacity could be maximized.

1.7 Solutions in This Thesis

For improving spectrum efficiency and optimizing coexistence system performance, we propose an interleaved spread spectrum orthogonal frequency division multiplexing (ISS-OFDM) system. In this solution, the channel or the frequency band is subdivided into a number of subcarriers, each of which is modulated by its corresponding data symbol on the basis of the OFDM modulation technique. The modulated subcarrers, instead of being superimposed together like in the conventional OFDM technique, are interleaved so that the multiple versions of the transmitted signal are generated. Due to the generation of multiple versions of the transmitted signal, the transmission signal spectrum is spread greatly. At the receiver, the interference thresholds for coexisting systems are derived by using digital signal processing methods. The interference signal in the frequency band of the received signal can be adaptively avoided or ignored in terms of the interference threshold calculated based on the interference signal power and available signal power. Consequently, the system coexistence interference can be reduced, and coexistence system performance can be improved distinctively.

1.8 Objectives and Overview of This Thesis

The objectives of this thesis are to increase the efficiency of spectrum resource utilization, relax the issues of spectrum resource shortage and improve the coexistence system performance in the ISM frequency bands. These coexistence systems include WLAN, Bluetooth, WiMAX, WPAN and WBAN, and other ultra-wideband OFDM systems.

The organization of the thesis is as follows:

Chapter 2 presents two existing solutions for wireless system coexistence in the spectrum sharing environments. Our primary objectives in this chapter are to present the idea and method of solving the coexistence problems.

In Chapter 3, we introduce the most relevant basic theory and notions which will be used in the theory analysis and design of the ISS-OFDM system.

Chapter 4 is focused on the algorithm design for the generation of the spread spectrum OFDM transmitted signal.

Chapter 5 discusses the channel characteristics of the multipath fading channel and additive white Gaussian channel (AWGN).

Chapter 6 presents design of the receiver algorithms which can effectively recover the transmitted information. Included in this chapter, two receiver algorithms are introduced.

Chapter 7 analyzes and evaluates system performance including the peak-to-average power ratio (PAR) of the transmitted spread spectrum signal, frequency and time diversity of the received signal, and the system adaptive subband selection transmission and coexistence performance under different configurations.

Chapter 8 sums up the contributions of this thesis and proposes areas of future work.

The following Figure 1.3 gives the framework of the whole thesis.

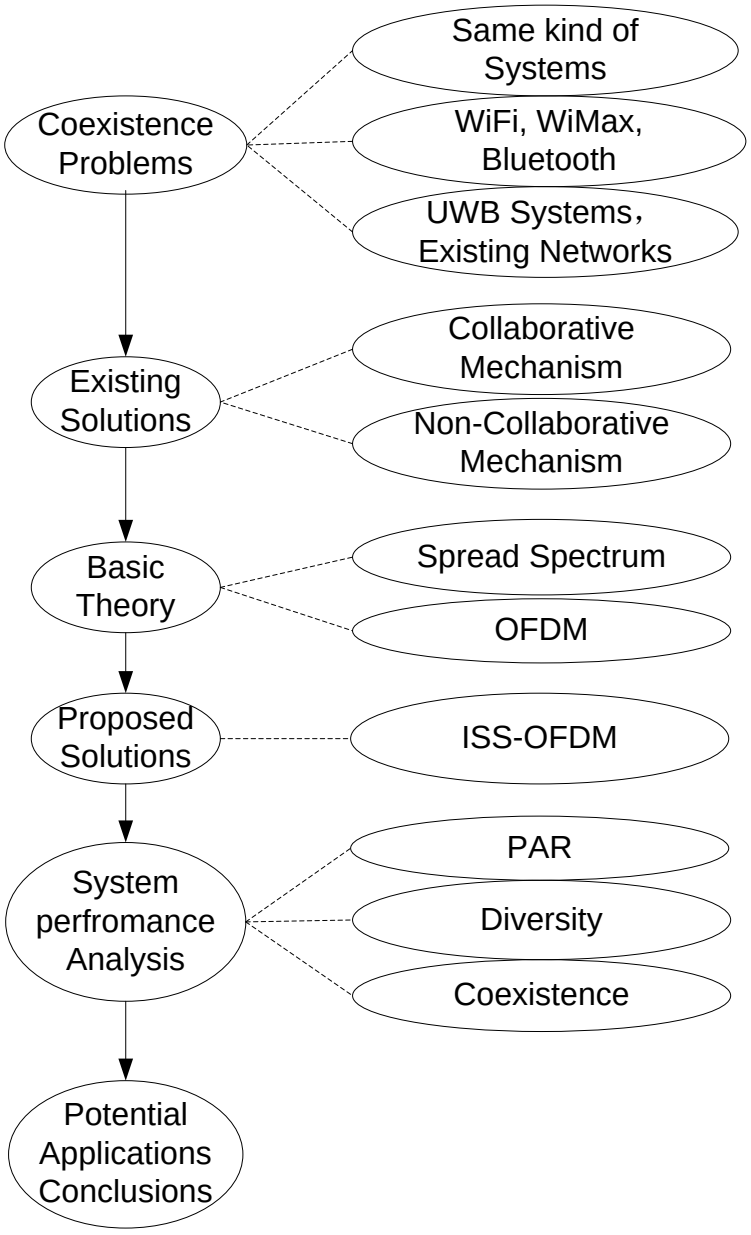

Figure 1.3 Framework of the whole thesis.

1.9 Publications

Transactions papers

[1] Pingzhou Tu, Xiaojing Huang and Eryk Dutkiewicz, “Diversity Performance of an Interleaved Spread Spectrum OFDM System over Frequency Selective

Multipath Fading Channels," *Transactions on Electrical Eng., Electronics, and Communications*, accepted for publishing on ECTI-EEC Trans. It will appear in Feb-09 issue.

[2] Pingzhou Tu, Xiaojing Huang and Eryk Dutkiewicz, "Adaptive Subband Selection in OFDM-Based Cognitive Radios for Better System Coexistence," *IEEE Transactions Letter on Wireless Communications,* under review.

International conference papers

[3] Pingzhou Tu, Xiaojing Huang and Eryk Dutkiewicz, "Adaptive Filtering for Selective subband Transmission Based on Interference Dectection," in the 1st ACM Workshop on Heterogeneous Senor and Actor Networks, May, 2008, Hongkong.

[4] Pingzhou Tu, Xiaojing Huang and Eryk Dutkiewicz, "Adaptive Subband Selection in OFDM-Based Cognitive Radios for Better System Coexistence," in the 3rd International Conference on Cognitive Radio Oriented Wireless Networks and Communications, May 2008, Singapore.

[5] Pingzhou Tu, Xiaojing Huang and Eryk Dutkiewicz, "Subband Adaptive Filtering for Efficient Utilization in Cognitive Radios," in the 3rd International Conference on Cognitive Radio Oriented Wireless Networks and Communications, May 2008, Singapore.

[6] Pingzhou Tu, Xiaojing Huang and Eryk Dutkiewicz, "Diversity Performance of Interleaved Spread spectrum OFDM Signals over Frequency Selective Multipath Fading Channels," in the 7th International Symposium on Communications and Information Technologies, Oct. 2007, Sydney, pp. 184-189 .

[7] Pingzhou Tu, Xiaojing Huang and Eryk Dutkiewicz, "Peak-to-Average Power Ratio Performance of Interleaved Spread Spectrum OFDM Signals," in the 7th

International Syposium on Communications and Information Technologies, Oct. 2007, Sydney, pp. 82-86.

[8] Pingzhou Tu, Xiaojing Huang and Eryk Dutkiewicz, "A Novel Approach of Spectrum Spreading in OFDM System," in the 6th International Syposium on Communications and Information Technologies, Sept. 2006, Bangkok, pp.487-491.

1.10 Contributions

The contributions of this thesis are made in three aspects, which are presented as follows.

1. A novel algorithm, a complex exponential spreading method (CES), is developed to generate a spreading spectrum OFDM signal with multiple subbands (Section 4.5).

2. The demodulation by using multiple fast Fourier transform (FFT) parallel operations is proposed to recover the transmitted information, which greatly reduces the receiver computational complexity and makes full use of signal diversity (Section 6.6).

3. An adaptive subband selection transmission algorithm is proposed. Based on dynamical determination of interference thresholds, system transmission band is adaptively selected to avoid coexistence interference among OFDM systems and other narrowband or ultra-wideband wireless systems (Section 7.3).

Compared to the previous solutions, the proposed ISS-OFDM system has its unique characteristics as follows.

- ISS-OFDM can adaptively implement the coexistence of systems between UWB systems and primary systems or users by adaptively calculating the interference threshold;

● Transmission system bandwidth can be adaptively adjusted by selecting a different frequency band by the receiver;

● Transmitted signal power is very low but the system performance can be maintained at acceptable levels, which is suitable for the wireless body area networks systems;

● Transmitted signal spectrum is spread by using spread spectrum OFDM modulation, rather than frequency hopping, direct sequence spread spectrum or time hopping;

● Peak-to-average power ratio of the OFDM transmitted signal is relatively low, which solves the problems of PAR in traditional OFDM systems being relatively high.

Chapter 2

Literature Review

2.1 Introduction

In Chapter 1 issues related to system coexistence including some ideas covering the existing solutions were briefly introduced. In this chapter, we will review four solutions including two examples and some ideas on spectrum sharing and system coexistence, so that we can learn how the existing solutions suppress interference and achieve better system coexistence performance. Meanwhile, we will learn the typical methods of implementing system coexistence. Also we will learn the technical knowledge and background which are applied to solve the problems of system coexistence, especially related to avoiding coexistence interference.

The interference problems severely limit coexistence system performance and they must be eliminated before systems can share public resources [56, 57]. Currently, the solutions for minimizing interference, in terms of management mechanisms, can be classified into collaborative mechanisms and non-collaborative mechanisms. Collaborative mechanisms require the coexisting systems to exchange information over a separate link between one another to minimize mutual interference. It aims at reducing the impacts of interference on the coexisitng systems and improving

spectrum efficiency by allocating spectrum resources to unique access per user at a given time instant. In this mechanism, the allocation techniques basically randomly distribute space of 3 dimensions with time, frequency and code, so that interference can be efficiently avoided if the wireless systems are capable of sharing detailed information in real-time about their desired occupancy of time, frequency, power and code [58, 59]. Non-cooperative mechanisms do not require information sharing among the coexisting systems. They need to estimate the channel according to the received signal or by sensing the radio conditions.

In terms of the protocol layers, on the other hand, the solutions can be classified into physical layer schemes and medium access (MAC) layer schemes. Physical layer collaborative coexistence mechanisms are based on the idea that frequency resources are shared by using adaptive notch filters or adaptive antenna to suppress the interference signals [60]. MAC layer collaborative coexistence mechanisms are implemented by using random access schemes such that a base station initiates transmission whenever it has data to transmit. In this way, since the bandwidth can be saved when the transmitter is idle, the system bandwidth can be used efficiently.

In the following we will discuss some solutions and ideas for system coexistence, from which we will learn some general ideas and technical knowledge on suppressing system coexistence interference using techniques in the physical layer and in the MAC layer.

2.2 Example 1: Erasure of OFDM Subcarriers

2.2.1 Scenario

In the example of the erasure of OFDM subcarriers, the scenario is the system coexistence between Bluetooth (IEEE 802.15.1) and Wi-Fi (IEEE802.11g). Bluetooth is a standard in short range (<10m) wireless communications aimed at enabling connections between portable computing and communication devices [61]. It provides short-range connectivity to headsets, laptops and peripherals such as

printers. The key characteristics of Bluetooth are low complexity, low cost and low power. It works in 2.4GHz ISM frequency band, and its channel hops at a nominal hop rate of 1600hops/s in a pseudorandom mode by using a frequency hopping spread spectrum technique. The total number of hopping channels is 79, each with bandwidth 1MHz. Bluetooth is the major member of WPAN. Wi-Fi IEEE 802.11g WLAN enables users to access internet and supports voice over Internet protocol (VoIP) [62]. It is widely deployed in campus, office and home. Wi-Fi works in the same ISM frequency band 2.4GHz and with bandwidth 20MHz as Bluetooth, and it is based on the OFDM modulation technique. Bluetooth and Wi-Fi are not competing with each other, but are complementary to each other [63].

2.2.2 Problems

When Bluetooth and Wi-Fi devices are coexisting in the same area as displayed in Figure 2.1, both the Bluetooth and IEEE 802.11g signals are overlapped in frequency and coexistence interference is unavoidable.

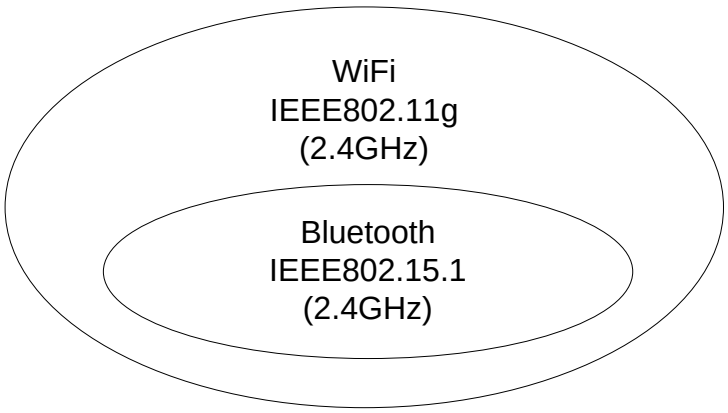

Figure 2.1 Coexistence between Bluetooth and Wi-Fi.

Coexistence interference between Bluetooth and Wi-Fi is from the collocation of antennas, the frequency proximity of the two systems and the fact that the two protocols are uncoordinated. The interference is computed according to the bandwidth occupancy, the length of the IEEE 802.11g packet and the load factor. In

coexisting systems, a Bluetooth signal appears as the narrowband interference of WLAN. The Wi-Fi signal bandwidth is much wider than that of Bluetooth. For the WLAN with bandwidth 20MHz channels, the probability of both Bluetooth and IEEE 802.11g signal being interfered is roughly 20/79 as displayed in Figure 2.2 (a). The duration of the IEEE 802.11g packets determines the probability of being interfered by a Bluetooth signal. The longer the IEEE 802.11g packets are, the more chance they have of being interfered with as indicated in Figure 2.2 (b). The interference is parameterized in terms of the signal to inference ratio.

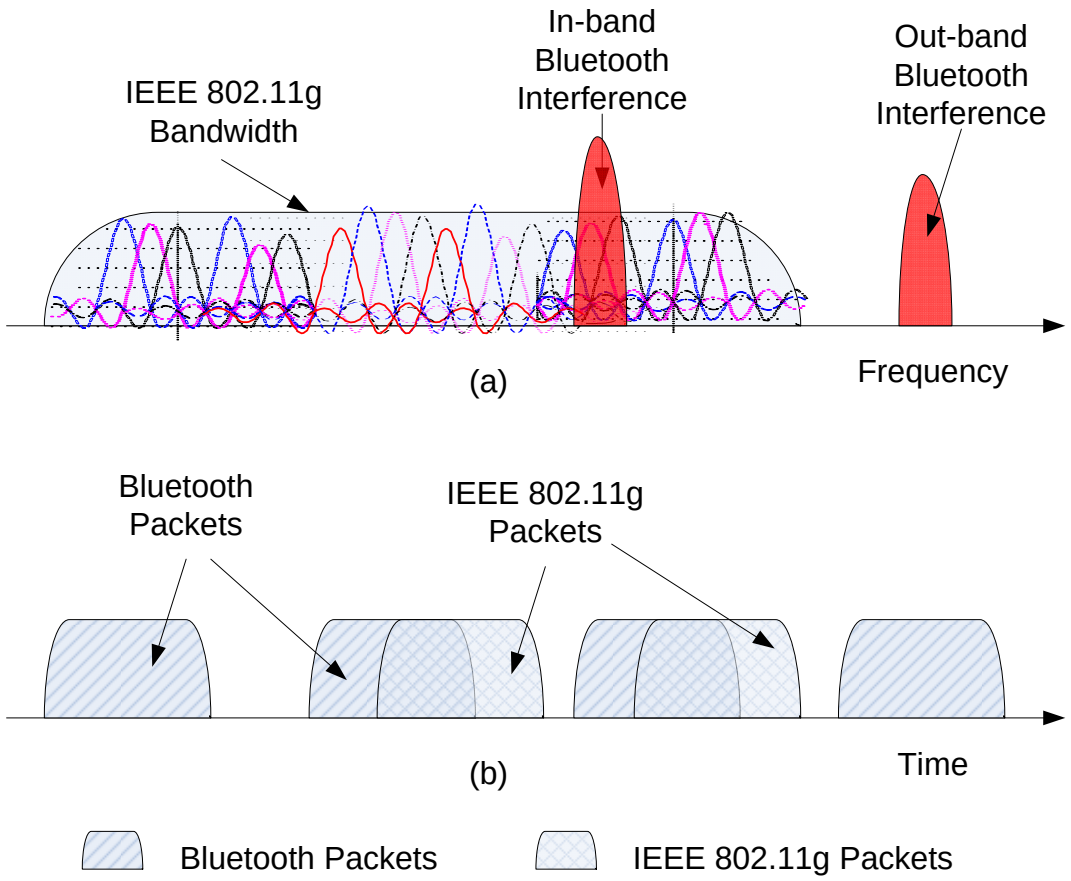

Figure 2.2 (a) Coexistence interference between IEEE 802.15.1a and IEEE 802.11g in frequency domain; (b) Coexistence interference between IEEE802.15.1a and IEEE 802.11g in the time domain.

2.2.3 Solutions

Since the WLAN receiver sees the Bluetooth signal as a narrowband interference signal predominantly affecting a small number of subcarriers which has a bandwidth of 312KHz. The signal to interference ratio (SIR) level for each independent subcarrier is decided immediately by the transmitted OFDM symbol and the power of the Bluetooth symbol transmitted over the bandwidth corresponding to that subcarrier. The solution for reducing the interference is implemented by replacing those data symbols corresponding to subcarriers with low SIR using erasures. That is, the data symbols with low SIR which include the inband Bluetooth are erased using some erasures as indicated in Figure 2.3. After the interfered data symbols are erased, the frequency band is used by the receiver to recover information.

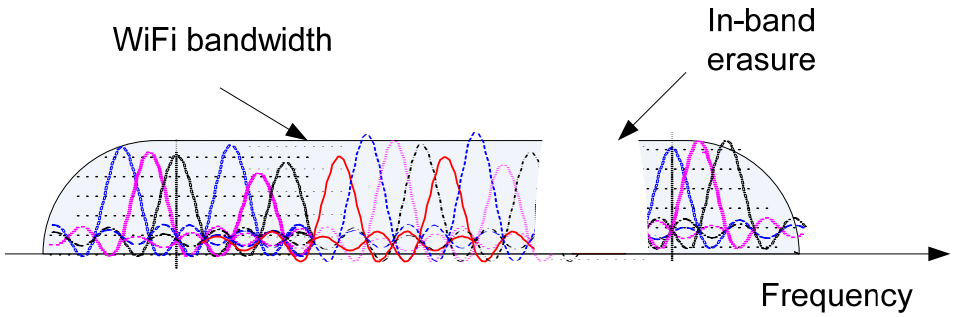

Figure 2.3 Erasure of interference signal from Bluetooth in the Wi-Fi band.

Based on the erasure idea and under the assumption that the propagation channel is a flat Rayleigh fading channel for each OFDM subcarrier, the system simulation is carried out in the frequency domain. The channel impulse response and the interfering Bluetooth signal are generated in the time domain and their frequency domain responses are obtained by using FFT. The simulation results for a subset of the data rates 24, 18 and 9Mbit/s demonstrate that their system performance is very similar in the multipath fading channels by using erasure [50, 64]. They also indicate that the erasure insertion can recover performance to satisfactory levels with a small loss in E_b / N_0 as long as the OFDM receiver can track the interference from the Bluetooth.

However, the faster data rate models combined with code puncturing and higher order modulation will require a higher signal to interference ratio (SIR) level. That means, in faster data rate models the erasure method is no longer valid for reducing coexistence interference.

2.3 Example 2: Reactive Coordination Method

2.3.1 Scenario

We take another example of the system coexistence between Wi-Fi (IEEE 802.11b) WLAN and WiMAX (IEEE 802.16a) WMAN. IEEE 802.11b is a standard of WLAN, which employs the direct sequence spread spectrum techniques to spread spectrum [65, 66]. This kind of WLAN is already widely used at home, office and campus. Since its coverage of the WLAN is less than 100 meters, the connection distance between the homes and offices is beyond the coverage of WLAN. As a complementary technique for Wi-Fi, WiMAX will be used to extend the capability of Wi-Fi with much greater robustness and range, which is designed for outdoors non line of sight and long range wireless broadband access with high throughput. It can perform the connection between homes and offices. WiMAX will coexist with WLAN to complete the wide range of mobile wireless communications as shown in Figure 2.4.

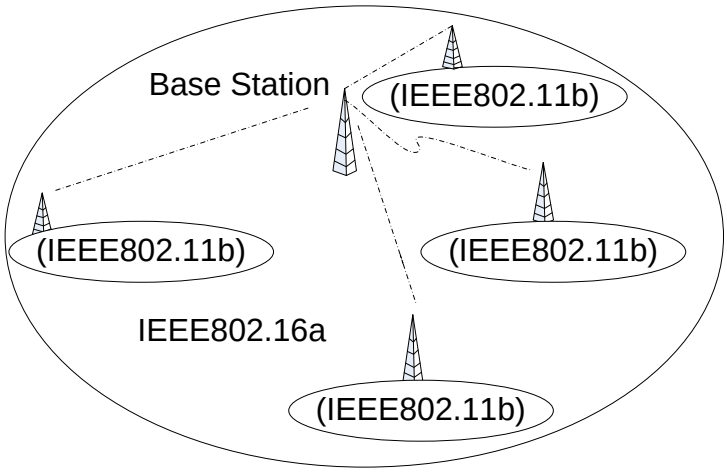

Figure 2.4 Coexistence between IEEE 802.11b and IEEE 802.16a.

Assume that the two systems Wi-Fi and WiMAX cells coexist in spectrum shared environments, which consist of one WiMAX cell with one base station (BS) and multiple subscriber station (SS). Wi-Fi hotspots are deployed inside the WiMAX cell with one access point (AP) and multiple clients. The positions of the WiMAX base station and subscriber station are independent from the access points and client locations of Wi-Fi.

For the two systems their bandwidth allocations are considered unchanged during the observation period. Wi-MAX radios employ the OFDM modulation technique and each channel has bandwidth of 20MHz. As indicated in B1, B2 and B3 in Figure 2.5 [51, 67], there are three non-overlapping channels. Wi-Fi networks use direct sequence spread spectrum (DSSS) technique and each channel has a bandwidth of 22 MHz. In the ISM band, Wi-Fi is allocated a total of 11 overlapping channels.

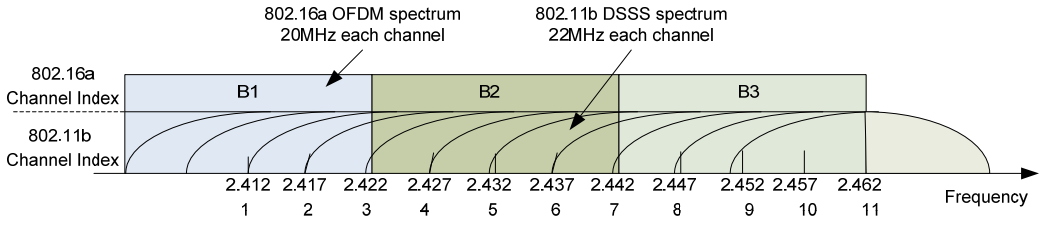

Figure 2.5 Spectrum allocations between IEEE 802.116a and IEEE 802.11b.

2.3.2 Problems

Coexistence interference between WiMAX IEEE 802.16a and Wi-Fi IEEE 802.11b is a big challenge for researchers since the WiMAX protocol operates over several frequency bands. Although the frequency separation between WiMAX and Wi-Fi is greater than that between Wi-Fi and Bluetooth, it is still not enough to prevent coexistence problems. For example, a user is conducting a cellular conversation via a Bluetooth headset, meanwhile, through the phone's WiMAX air link the user is downloading email or browsing the internet. In this circumstance, the voice quality and packet degradation will result in a poor user experience, which requires a

mechanism to guarantee the coexistence of wireless interfaces. Currently, the solution schemes in the MAC layer and physical layer for the coexistence interference between Wi-Fi and WiMAX are considered as follows.

2.3.3 Solutions

To solve coexistence interference between WiMAX and Wi-Fi, in the MAC layer the first step is to make sure that the different protocols are synchronized and ensure that bandwidth over the shared spectrum is allocated on a time multiplexed, non-concurrent fair basis. Under the premium of perfect synchronization the potential interference can be eliminated, and the inherent link performance attributes can be still maintained. After acheieving synchronization, the following task is to establish a bandwidth allocation mechanism that considers the operation of the protocols used in both systems.

In this solution, three methods for the system coexistence between the Wi-Fi and WiMAX are introduced [51]. One is dynamic frequency selection (DFS) which utilizes agility in operating frequency; the second is power control (PC) which adjust transmit power based on observed interference; and the third is time agility (TA) which schedules transmissions to avoid interference based on traffic patterns in time.

For the method of DFS, based on interference levels in available subbands, IEEE 802.11b devices can adaptively select the frequency band and switch channels. All available service bands are scanned and the channel with the lowest received signal strength indicator (RSSI) is selected for data transmission. In IEEE 802.11b systems, the network access point (AP) can do the channel selection, in which the available frequency bands are periodically scanned to obtain the channels with the lowest power level. After the channel switching all the clients in IEEE 802.11b networks are notified by broadcast messages and immediately switch to the same channel. During the period of channel switching, the current packet will be lost. The scanning time interval varies from approximately 100ms to 200ms. After rescan when the interference power level of the clearer channel is at least 10% less than of the current

channel, the RSSI values are measured and channel switching is actually carried out. In order to avoid unnecessary oscillations in channel switching, the extra 10% of channel interference power level is needed.

The second method is to eliminate interference by controlling the transmission power. Based on the feed-back information from the receiver, the two networks are allowed to dynamically select transmit powers from pre-determined 256 discrete power levels. Power control is a receiver based algorithm, in which channel scanning is performed by the receiver to achieve a target interference power level and the recommendation of minimum transmit power levels necessary to maintain adequate link quality is made. By using the MAC packet headers the recommendation information is fed back to the transmitter.

The third method is TA, which is used to reschedule the MAC packet in time to avoid interference. The basic idea of TA is to allow devices of Wi-Fi and WiMAX to adapt to each others' traffic pattern and the time varying channel conditions, so that transmit probability is controlled in time. In order to avoid transmissions between devices of Wi-Fi and WiMAX (and thus avoid retransmission) during the poor channel conditions, the transmission probability decreases when the interference power increases. The interference power levels can be calculated by using signal to interference noise ratio (SINR), and a threshold of the SINR is predetermined. If the SINR is close to the predetermined threshold, it means that there are potential interferes around. In order to avoid interference, it is preferable to make the transmit probability inversely proportional to the detected interference power. When the SINR is smaller than the threshold, it indicates that the transmitted signal is weak, or that the interference is too strong. In this circumstances, the transmit probability is controlled to be proportional to the current SINR values.

2.3.4 Summary

These solutions for the coexistence of Wi-Fi and WiMAX in the MAC layer and the physical layer are typical methods to reduce interference and improve performance

of coexisting systems. It provides us some ideas for reducing interference between coexisting systems. However, these solutions have exposed their limits in each of the algorithms. In DFS algorithms, dynamic frequency selection is based only on the Wi-Fi networks, and it can not be applied to the devices of WiMAX networks. It is not practical because it is biased and the DFS is applied to only Wi-Fi networks. In power control (PC) algorithm, the algorithm is derived under the assumption of fixed modulation. In time agility algorithms, the threshold of SINR is predetermined. In practice it is hard to use if the modulation is fixed and it is impossible to predetermine the threshold of SINR in an instantly changing radio scene.

2.4 VISA: A Solution Using Spatial Resource

VISA is the abbreviation of Virtual Subcarrier Assignment (VISA) [64], which is a spatial filtering technique. In this technique, the subcarriers of an OFDM symbol used to convey information are named data subcarriers, whereas the subcarriers which are not used for actual data transmission are named as virtual subcarriers. Different OFDM signals are colored with different virtual subcarrier positions in the spectrum of OFDM signals so that an adaptive array antenna at the receiver can identify the OFDM signals selectively. Since the cost of the array antenna is currently decreasing, each device in a WLAN can be equipped with an array antenna, so that the coexistence problem can be solved through utilizing spatial resource.

Assume that there are two types of the OFDM signal, A and B, which have different virtual subcarrier positions A and B in their spectra, respectively. When one receiver with an adaptive array antenna is receiving the OFDM signal A as a desired signal, the receiver controls the array weights so that the array antenna output of the virtual subcarrier A is forced to be zero. Hereby, the adaptive array antenna at the receiver can automatically exclude signal B through forcing nulls in the directions of signal B even if signals A and B arrive simultaneously at the receiver. If the receiver desires to receive OFDM signal B, by placing the array antenna output of the virtual subcarrier B to be zero and using the adaptive array antenna to filter out the OFDM signal A, the receiver can complete the reception of OFDM signal B. This means

that by employing an adaptive array antenna at the receiver with spatial filtering of the OFDM signal, the receiver can selectively receive the OFDM signals sharing the same channel. In this way, wireless devices can share the common frequency bands and collocate in the same wireless environments.

The algorithm, VISA, can effectively realize spectrum sharing between different WLANs. It does not care about interference by employing an adaptive array antenna. However, it can only be implemented with the support of an adaptive array antenna. If every device in multiple WLANs must install an adaptive array antenna, the cost can not be underestimated.

2.5 System Coexistence Using Cognitive Radio Techniques

Cognitive radio is a promising technique for avoiding interference between coexisting systems. It can effectively reduce interference of coexisting systems and improve system performance if the coexisting systems are aware of other radio front end signals in their environment. Cognitive radio, built on a software-defined radio (SDR) [68, 69], is defined as an intelligent wireless communication system that is aware of its environment and it uses the methodology of understanding-by-building to learn from the environment and adapt to statistical variations in the input. High reliability in communications and efficient utilization of spectrum are two main characteristics of cognitive radio systems. Cognitive radio takes an expanding view of the channel by managing time, frequency, power and code. It is a novel approach for improving utilization of a spectrum resource.

2.5.1 Problems

Cognitive radio is another access technique for the use of some frequency bands which are seldom used or unoccupied by primary users. In many frequency bands,

spectrum access is a more significant problem than physical scarcity of spectrum, in large part due to legacy command-and-control regulations that limit the ability of potential spectrum users to obtain such access. In fact, if we scan portions of the radio spectrum including the revenue-rich urban areas, we would find that some frequency bands in the spectrum are largely unoccupied most of the time; some other frequency bands are only partially occupied; and the remaining frequency bands are heavily used. The underutilization of the natural spectrum resource provides the great possibility of sharing the resource among multiple users. Spectrum utilization can be improved significantly by making it possible for a secondary user (who is not being served) to access a spectrum occupied by the primary user at the right location and the time in question.

2.5.2 Proposed Methods

Cognitive radio, inclusive of software-defined radio, has been proposed as the means to promote the efficient use of the spectrum through dynamic spectrum management. The aim of dynamic spectrum management is to develop an adaptive strategy for the efficient utilization of the spectrum resource. Dynamic spectrum management is a designed algorithm which is built on the available spectrum detected by a radio scene analyzer and output of the transmit power controller, and selects a modulation strategy to adapt to the time-varying conditions of radio environments. This algorithm can be realized in two ways. One is the dynamic modulation strategy combined with the transmit-power control; the other one is the traffic prediction technique.

Dynamic modulation strategy is a kind of flexible modulation technique used for cognitive radios. The OFDM modulation technique is suitable as a cognitive radio modulation with its flexibility and computational efficiency. It uses a set of bandwidth carrier frequencies centered on a set of corresponding channels to modulate the data bits/symbols. The most important aspect for a dynamic modulation strategy is that the transmission rate can be fed back to the transmitter

from the receiver through the use of separate feedback channels, which permits the use of the flexible bit-loading at the transmitter. Thus, the number of bits/symbols for each channel is optimized for SNR characterizing the corresponding OFDM channels. As time evolves and spectrum varies, the OFDM bandwidth frequency implementation of spectrum sharing is modified dynamically. This dynamic spectrum sharing process satisfies constraints imposed on the cognitive radios by the availability of the frequency bands at a particular location and their availability with time. Meanwhile, the transmit power controller keeps an account of the bits loading to adjust transmission power. The power manager and the dynamic modulation strategy work in concert to complete the multiple access control requirements of the cognitive radios.

The traffic prediction technique based on the OFDM multiple access mode is another dynamic spectrum management method. In order to avoid co-channel interference of OFDM systems with primary users, a traffic mode of the primary user occupying the sharing frequency bands is built on the basis of historical data. This traffic mode provides the means for predicting future traffic patterns in these frequency bands. It is possible, in turn, to predict the next vacated duration in which the frequency bands occupied by the primary user are likely to be used by cognitive radio operators. There are two classes of traffic data patterns. One is the deterministic pattern. The other one is the stochastic pattern.

The deterministic pattern is very similar to the TDMA mode. In this pattern of the traffic data, the primary users are assigned fixed time slots. When the primary users are switched off, the sharing frequency bands can be used by the secondary users, i.e., cognitive radio users.

The stochastic pattern is to obtain the statistically characteristics of the sharing channels so that the traffic data are described in statistical terms [70]. Typically, the arrival times of data packets in wireless environments are modeled as a Poisson process. Service times are modelled using the exponential distribution. In any event, the model parameters characterizing the traffic data change slowly, which provide receivers with great possibility to estimate the channels using historical data.

Furthermore, the tracking strategy combined with the design of the predictive model can further improve the accuracy of the traffic model.

Currently, a cognitive radio prototype based on OFDM techniques is being built at Rutgers University, Georgia Tech and Lucent in the United States [46, 71]. The basic design system architecture includes the following modules: a general purpose processor for implementation of spectrum etiquette policies and algorithms, a packet processing engine for routing and protocol functionality, a software designed radio modem which can support various waveforms such as OFDM and DSSS/QPSK, agile radio frequency transmitter/receiver which are operating over a number of frequency bands, and the capability of fast radio frequency scanning. The prototype of the OFDM based cognitive radio is displayed in Figure 2.6.

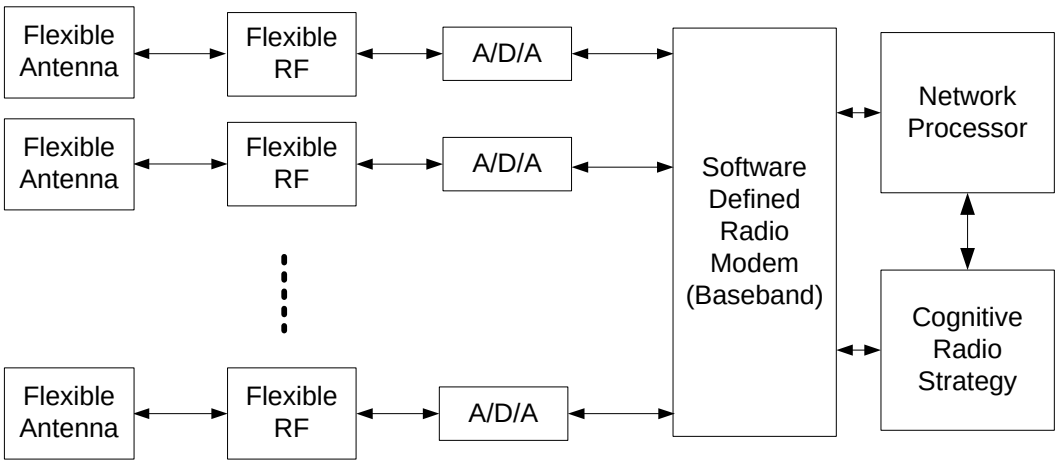

Figure 2.6 Architecture of cognitive radio.

There are two distinctive features for this architecture of the cognitive radio transceiver. One is the heterogeneous block based architecture, which helps to implement SDR base band processing in an efficient way. The second feature is that this architecture can reconfigure blocks in a few clock cycles to switch between multiple SDR physical layers. In the heterogeneous block based architecture, there is a general microprocessor which handles control intensive operations including synchronization, channel estimation, programming and interconnection of the heterogeneous blocks. Meanwhile, the heterogeneous blocks handle the data intensive operations. The heterogeneous blocks include Channelization Block, fast

Fourier transform/modified Walsh transform Block (FFT/MWT), Rake Block, Interleaver Block, Data and Channel Encoding/Decoding Block, and Detection and Estimation Block. Of all these blocks, Channelization Block is a configurable multi-rake filter used to select a subband or decimate the input signal for different standards. FFT/MWT Block is used to handle the FFT modulation operation used in OFDM and the modifier Walsh transform used in IEEE 802.11b. Rake Block is for channel estimation, and dispreading in direct sequence spread spectrum and code division multiple access. Interleaver Block is used to handle de-interleaving for different standards using a block based memory and multiplexer-based address handler and a multi-mode architecture. The Detection and Estimation Block is used to detect common interference.

This architecture of OFDM based cognitive radio transmitter/receiver has the ability to efficiently scan the spectrum usage and opportunistically use portions of the spectrum. Furthermore, it has the potential to detect and identify types of interference, even if it becomes increasingly difficult for arbitrary radio systems. Therefore, OFDM based cognitive radios are one of the most promising techniques to mitigate interference and realize system coexistence.

2.6 Summary

In this chapter, we introduced four kinds of coexistence solutions and basic ideas which include erasure of interfered OFDM subcarrier, reactive coordination method, VISA method, and OFDM based cognitive radios. They represent different kinds of ideas to implement system coexistence. Some of them are implemented in the physical layer, others are implemented in the MAC layer. According to the operation mechanism, some of them belong to the collaborative mechanism, others are non-collaborative.

After investigating the existing solutions, we propose the interleaved spread spectrum OFDM (ISS-OFDM) method, which closely associates with the existing solutions. In the following chapters, we will introduce the ISS-OFDM method.

Chapter 3

Theory of Baseband Signal Processing

3.1 Introduction

In this Chapter, some theories related to the ISS-OFDM system will be introduced. These theories include spread spectrum communication techniques, OFDM techniques, channel fading and diversity techniques, radio access technologies and some fundamental principles of digital signal processing.

3.2 Spectrum Spreading Techniques

Spread spectrum signals used for digital information transmission have the unique features that their bandwidth is much larger than the information rate. The bandwidth of a spread spectrum signal is extended much greater than unity. Since the spread spectrum signal has large redundancy, it is required to eliminate the severe interference that is encountered in the signal transmission over the wireless propagation channel.

There are many advantages for the transmission of spread spectrum signals.

1. The large redundancy inherent in the spread spectrum signal is required to suppress or combat the effects of interference produced from the wireless multipath propagation channel;

2. The spread spectrum signal has a very low power spectrum density, which makes it difficult for an unintended listener to detect the presence of the transmitted signal from the background noise. On the other hand, it reduces the possibility to interfere with other users when it shares the common frequency bands with other existing users. Thus, it helps system coexistence;

3. In the presence of other listeners, it helps to achieve message privacy.

By virtue of the advantages of spread spectrum, different types of interference, such as intentional interference, coexistence interference and self-interference, can be suppressed efficiently

Intentional interference can be overcome if the jammer who intends to interfere with the communications has very little prior knowledge of the signal features except for the transmission channel bandwidth and the type of modulation being utilized. A fine resolution jammer can imitate the signal emitted by the transmitter without difficulty, if the transmission information is only encoded by convolutional channel codes or block channel codes. To reduce the probability of the transmitted signal being interfered by other transceivers, the spread spectrum technique can be employed by the transmitter which introduces a pseudo random element in each of the transmitted coded waveforms that is known to the intended receiver but not to the jammer. Therefore, it is difficult for the jammer to analyze and track an interfering signal without the knowledge of the pseudorandom pattern.

Interference from coexisiting devices is produced in multiple-access wireless radio environments where a number of devices are sharing a common channel frequency band. At a given time instant, a group of these devices may transmit information simultaneously over the common frequency band to a destination receiver. For combating the coexistence interference, the transmitted signal may be identified

from one another by multiplying a pseudorandom sequence with each transmitted signal. Thus, the transmitted information can be recovered by a particular intended receiver by knowing the pseudorandom sequence used by the corresponding transmitter.

Another form of interference is self-interference which is resolvable multipath components caused by time delay propagation through a channel. This kind of interference can be reduced by using a spectrum spreading technique.

By using a spread spectrum technique, a message can be covered in the background noise by transmitting the resultant signal at a very low power spectrum density. Due to the very low power of the transmission signal, the transmitted signal is hidden and it has the very high probability for a casual listener to detect. On the other hand, the very low power level of the transmission signal causes little interference to the other users who are sharing the common radio channels. In addition, message privacy can be achieved by multiplying a pseudorandom sequence with a transmitted signal message.

Spectrum spreading can be implemented in many ways including using direct sequence spread spectrum, frequency hopping spread spectrum and time hopping spread spectrum techniques. For better understanding of the spread spectrum signal in the ISS-OFDM system, we will introduce two typical methods for spectrum spreading: direct sequence spread spectrum and frequency hopping spread spectrum.

3.2.1 Direct Sequence Spread Spectrum

3.2.1.1 Architecture of Direct Sequence Spread Spectrum Signal

The block diagram in Figure 3.1 illustrates the basic architecture of a direct sequence spread spectrum system. The basic elements of the system include channel encoder and decoder, pseudorandom generator, modulator and demodulator. In addition to these basic elements, it has two important elements, pseudorandom

generators, modulator that interfaces with the front end at the transmitting end, and the demodulator that interfaces with the front end at the receiving end.

Two kinds of mappings are considered, QPSK and frequency shift keying (FSK). The phase of the QPSK signal is shifted according to the pseudorandom sequence generated at the modulator. The resulting modulated signal is called a direct sequence spread spectrum (DSSS) signal [40]. When used in conjunction with binary or M-ary (M>2) FSK, the frequency of the transmitted signal is shifted according to the pseudorandom sequence pseudorandomly. The resulting signal is called a frequency-hopped spread spectrum signal (FH-SS). The FH-SS technique will be introduced in the next section [72].

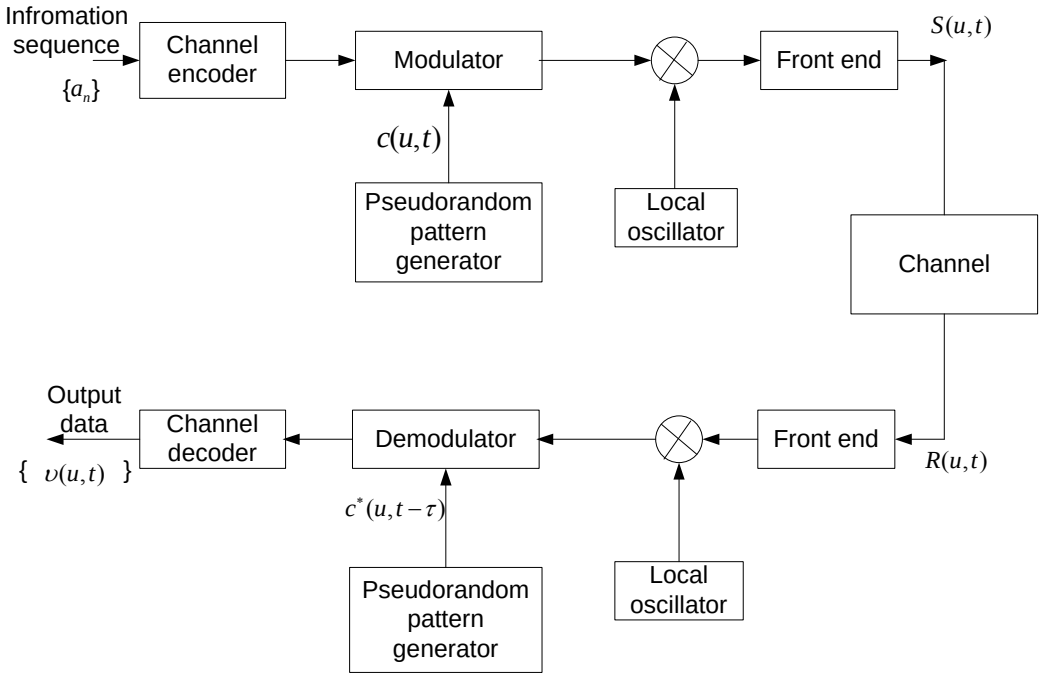

Figure 3.1 Direct sequence spread spectrum system model.

In the DSSS technique, the pseudorandom generator generates a pseudorandom binary-valued sequence which is imposed on the transmitted signal at the modulator of the transmitter and removed from the received signal at the demodulator at the receiver. In order to demodulate the received signal at the receiver, synchronization of the pseudorandom sequence generated at the receiver with the pseudorandom sequence contained in the incoming received signal is required. The synchronization

is achieved by transmitting a fixed pseudorandom sequence pattern that the receiver can recognize in the presence of interference with high probability. After time synchronization between the pseudorandom generators respectively at the receiver and transmitter is established, the information transmission starts.

3.2.1.2 Generation and Receiver of DSSS Signal

As displayed in Figure 3.1, at the transmitter, the binary information stream $\{a_n\}$ is coded by the channel encoder, and the transmitter outputs the binary code stream $d(u,t)$, in which u is a pseudorandom variable and t is the time variable. The two binary symbols in the binary code stream have the same prior probabilities and both of them are ½ and they are independent of each other. The encoded binary waveform signal $d(u,t)$ multiplies a high speed binary pseudorandom signal waveform $c(u,t)$, to obtain a complex signal $d(u,t)\cdot c(u,t)$ that greatly spreads the bandwidth of transmission information. The spread spectrum complex signal modulates the carrier, normally by using PSK in direct sequence, and then the modulated signal passes through an antenna and is sent into the wireless channel. The output from the transmitter is represented as $S(u,t)$.

At the receiver, signal demodulation is the reverse process to that at the transmitter. A local signal which synchronizes the pseudorandom codes at the transmitter conducts the coherent processing with the received signal. The coherent processing is used to multiply the received signal with the local signal which synchronizes to the pseudorandom code from the transmitter. When the two signals are completely the same, the correlation values reach the maximum, which means that the received signal approximates the local sequence. Then, the recovered signal is sent to the detector so that the original information can be recovered.

During the period of the signal transmission through the channels, the interference signals, including narrow band interference, jamming, single frequency interference and mutli-path interference and multiple division multiple access interference, enter the channel with the useful transmission signal simultaneously. Since the

narrowband noise interference and multipath interference are uncorrelated to the useful signal, these interference signals convolute with the local pseudorandom spread codes and the bandwidth of the interference signals are spread widely. The energy of the interference signal is spread over the entire spread spectrum bandwidth, and the interference signal power level is reduced greatly. After the correlation processing, only the baseband signal and the interference within the baseband filter bandwidth can be output by the baseband filter. In this way the output SNR of the system is greatly improved.

3.2.1.3 Mathematical Expression of DSSS Signal

Generally, the direct sequence spread spectrum modulation uses PSK modulation to modulate the data information, and very few of them use FSK or OOK. In the three types of modulation modes, PSK modulation can achieve the best modulated signal, which can transmit information with the least error probability. In order to save the transmission power and improve the efficiency of the radios, the Bi-phase balanced modulation mode is normally used.

We assume that r denotes the information rate at the input to the encoder and B is the transmission channel bandwidth, and PSK modulation is adopted. For spreading the spectrum of the transmission signal to the whole available channel bandwidth, the phase of the carrier is shifted pseudorandomly according to the pseudorandom sequence from the generator at a rate B. The inverse of B, defined by T_c, denotes the duration of a pulse which is called chip; T_c is called the chip interval. The chip is the basic unit in a spread spectrum transmission signal.

The duration of a chip corresponding to the transmission time of an information bit is denoted as $T_b = 1/R$, the bandwidth expansion factor or the processing gain G can be represented as

$$G = \frac{B}{R} = \frac{T_b}{T_c}.$$

We can take the integer of the bandwidth expansion factor $\frac{T_b}{T_c}$. Thus, the ratio $\frac{T_b}{T_c} = L_c$, represents the number of chips per information bit. That is, in the transmitted signal the number of phase shifts is L_c during the bit duration $1/R$. Thus, the signal spectrum expanding factor is L_c.

As we discussed above, the approach for superimposing the pseudorandom sequence on the transmitted signal can be realized by altering immediately the coded bits by modulo-2 addition with the pseudo random sequence. Thus, by addition with a bit from the pseudorandom sequence each coded bit is modified. If x_i represents the i^{th} bit of the pseudorandom sequence (PN) and y_i is the i^{th} bit from the encoder, the modulo-2 sum is:

$$z_i = x_i \oplus y_i,$$

that is:

$$z_i = \begin{cases} 0, & x_i = y_i \\ 1, & y_i \neq y_i \end{cases}.$$

The sequence $\{z_i\}$ is mapped into a binary PSK signal of the form:

$$s(t) = \pm \mathrm{Re}[f(t)e^{j2\pi f_c t}],$$

according to the rules as follows:

$$f_i(t) = \begin{cases} f(t - iT_c) & (z_i = 0) \\ -f(t - iT_c) & (z_i = 1) \end{cases}, \tag{3.1}$$

where $f(t)$ represents an arbitrary shaping pulse of duration T_c seconds.

The modulo-2 addition of the sequence $\{x_i\}$ from the pseudorandom generator and the coded sequence $\{y_i\}$ can be denoted as a multiplication of two waveforms.

To demonstrate this point, assume that the elements of the coded sequence correspond to a binary PSK signal according to the following convention:

$$y_i(t) = (2y_i - 1)\, f(t - iT_c).$$

If we denote a waveform $p_i(t)$ as $p_i(t) = (2x_i - 1)\, p(t - iT_c)$, where $p(t)$ is a rectangular pulse of duration T_c, then, the equivalent low-pass transmitted signal corresponding to the i^{th} coded bit is:

$$f_i(t) = p_i(t) y_i(t) = (2x_i - 1)(2y_i - 1)\, f(t - iT_c). \qquad (3.2)$$

We can notice that the signal agrees with the equation given by Equation (3.1) obtained from the sequence $\{z_i\}$. Thus, followed by a mapping that yields a binary PSK signal, modulo-2 addition of the coded bits with the pseudorandom sequence is equivalent to multiplying a binary PSK signal generated from the coded bits with a sequence of unit amplitude rectangular pulses, each of duration T_c, and with a polarity which is determined from the PN sequence. For the purpose of demodulation, it is easy to produce the transmitted spread spectrum signal in the multiplication form of Equation (3.2), although it is convenient to realize modulo-2 addition followed by PSK mapping instead of waveform multiplication.

The received low-pass spread spectrum signal for the i^{th} code element is

$$r_i(t) = (p_i(t) y_i(t)) + v(t), \quad iT_c \le t \le (i+1)T_c,$$
$$= (2x_i - 1)(2y_i - 1)\, f(t - iT_c) + v(t),$$

where $v(t)$ denotes the jamming or interference signal degrading the information-bearing signal. We assume that the interference is a stationary random process with zero mean.

If $v(t)$ is a sample function from a complex-valued Gaussian process, the optimum demodulator is realized as a filter matched to the waveform $f(t)$ or as a correlator. In the matched filter implementation, the output of the matched filter is multiplied by $(2x_i - 1)$ which is achieved from the PN generator at the demodulator when the pseudorandom generator is well synchronized. Since $(2x_i - 1)^2 = 1$ when $x_i = 0$ and $x_i = 1$ the effect of the pseudorandom sequence on the received coded bits is then removed.

In this section we introduced the generation of the DSSS signal, the purpose is to get to know some techniques used in the DSSS system, and have a general idea on the direct sequence spread spectrum techniques.

3.2.2 Frequency Hopping Spread Spectrum

The frequency hopping spread spectrum technique is a conventional technique where the pseudorandom sequence selects the frequency of the transmitted signal pseudorandomly to generate the spread spectrum signal [73, 74]. The available signal bandwidth is subdivided into a large number of smaller subbands. In each signal interval, the transmitted signal occupies one or more of the available subbands. The selection of the subbands is performed pseudorandomly according to a pseudorandom sequence generated from a pseudorandom generator at the transmitter as displayed in Figure 3.2 which shows the model of the transceiver for a frequency hopping spread spectrum system.

At the transmitter, the modulation is usually binary or M-ary FSK or QPSK. If we consider QPSK, the modulator selects one of four phases corresponding to the information bits 00, 01, 11, 10. The resulting QPSK signal is translated in the frequency by the amount that is determined by the output sequence from PN generator, which is, in turn, used to select the frequency that is synthesized by the synthesizer. The frequency is mixed with the output of the modulator so that the transmitted signal frequency hops according to the pseudorandom sequence. The frequency hopping signal is transmitted over the channel.

To demodulate the frequency hopping spread spectrum signal at the receiver, a corresponding pseudorandom generator, which is synchronized with the received frequency hopping spread spectrum signal, is employed to control the output of the frequency synthesizer. By performing the correlation operation, the pseudorandom frequency translation impressed at the transmitter is removed from the received signal. Then the outcome signal is achieved by means of FSK or QPSK demodulator.

In digital communication systems, a frequency hopping spread spectrum signal is preferred over a direct sequence spread spectrum signal as the direct sequence spread spectrum signal requires critical synchronization for each chip. Especially, in a direct sequence spread spectrum system, timing and synchronization must reach to within a fraction of the chip interval T_c. On the other hand, in a frequency hopping spread spectrum system the chip slot is the time spent in transmitting a signal in a particular frequency slot of bandwidth B. But this time slot is approximately 1/B, which is much larger than T_c. Thus, the synchronization in a frequency hopping spread spectrum system is not as critical as in a direct spread spectrum system.

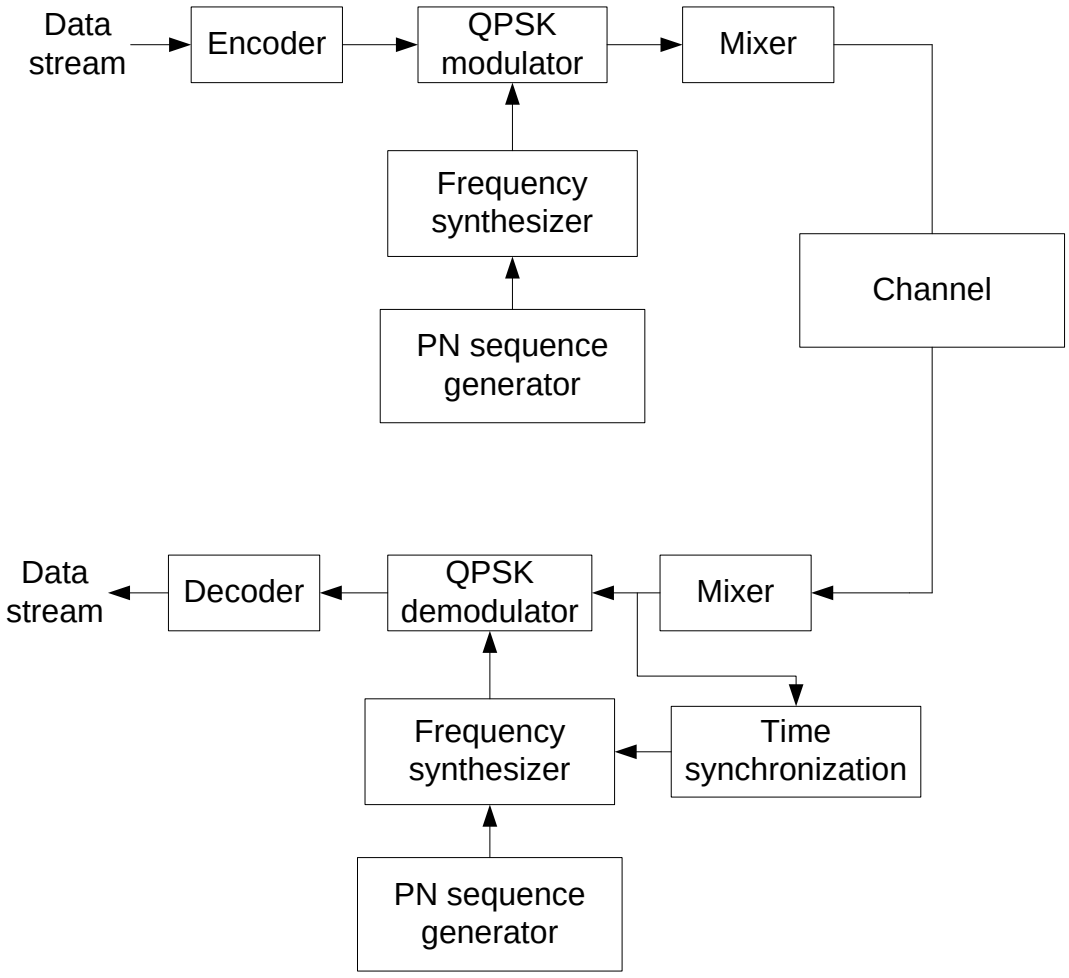

Figure 3.2 Frequency hopping spread spectrum system model.

3.3 Methods of Random Signal Processing

In this section some theories used for random signal processing are discussed. Understanding these digital signal processing techniques is helpful to better understand the analysis and design of the ISS-OFDM system.

3.3.1 Random Variables, Probability Distributions and Densities

In this section we discuss the Q function and the probability of error in Gaussian distribution [75]. Given a random variable X, consider the event $\{X \le x\}$, where x is any real number in the interval $(-\infty, \infty)$. We can denote the probability of this event as $P(X \le x)$, and the distribution of the probability can be denoted simply by $F(x)$ as:

$$F(x) = P(X \le x), \quad -\infty < x < \infty$$

Function $F(x)$ is called the probability distribution function or the cumulative distribution function (CDF) of the random variable X. Since $F(x)$ is a probability measure, its range is limited to the interval $0 \le F(x) \le 1$. Actually, if $x = -\infty$, $F(-\infty) = 0$, and if $x = \infty$, $F(\infty) = 1$.

The derivative of the cumulative distribution function $F(x)$, represented as $p(x)$, is called the probability density function (PDF) of the random variable X. Thus, the following expressions can be achieved:

$$p(x) = \frac{F(x)}{dx}, \quad -\infty \le x \le \infty,$$

or

$$F(x) = \int_{-\infty}^{x} p(u)du, \quad -\infty \le x \le \infty.$$

Since $F(x)$ is a nondecreasing function, we have the equation $p(x) \ge 0$.

3.3.2 Gaussian Distributions

The PDF of a normally or Gaussian distributed random variable is given as:

$$p(x) = \frac{1}{\sqrt{2\pi}\sigma} e^{-(x-m_x)^2/2\sigma^2}, \tag{3.3}$$

where σ^2 is the variance and m_x is the mean of the random variable X. The PDF $p(x)$ and CDF $F(x)$ are illustrated in Figure (3.3).

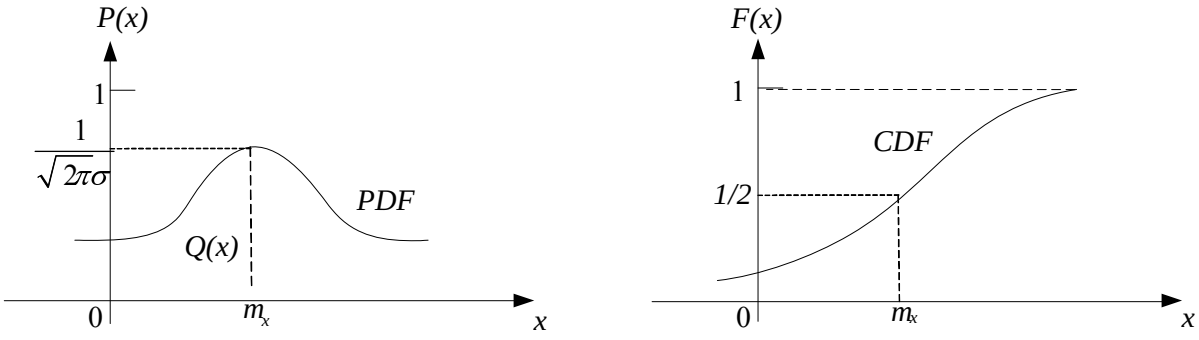

Figure 3.3 PDF and CDF.

We denote the area under the tail of the Gaussian PDF by $Q(x)$, it can be seen that the $Q(x)$ function can be defined as:

$$Q(x) = \frac{1}{\sqrt{2\pi}} \int_x^\infty e^{-t^2/2} dt, \qquad x \geq 0 \tag{3.4}$$

The meaning of the Q function represents the area under the PDF for the variable X.

3.3.3 Error Probability of Binary Modulation

Before we introduce the probability of error for an M-ary orthogonal signal which can be used to evaluate system performance, we consider the probability of error for binary modulation, pulse amplitude modulation (PAM) [49].

Firstly, we consider the simplest modulation signal, pulse amplitude modulated

(PAM) binary signals where the two signal waveforms are $s_1(t) = g(t)$ and $s_2(t) = -g(t)$, and $g(t)$ is an arbitrary pulse satisfying the conditions as follows.

$$\begin{cases} g(t) = 0 & 0 \le t \le T_b \\ g(t) \ne 0 & others \end{cases}.$$

Since $s_1(t) = -s_2(t)$, these signals are said to be antipodal. The energy in the pulse $g(t)$ is ε_g. The geometric representation of one dimensional pulse amplitude modulation (PAM) signals is simply the vector $s_1 = \sqrt{\varepsilon_b}, s_2 = -\sqrt{\varepsilon_b}$. If we assume that the two signals have equal probability and that signal $s_1(t)$ was transmitted then the output signal from the detector or the matched filter is written as:

$$r = s_1 + n = \sqrt{\varepsilon_b} + n,$$

where n denotes the AWGN noise component, which has variance $\sigma_n^2 = \frac{1}{2} N_0$ and zero mean. In this case the decision rule based on the correlation metric compares r with the threshold zero. If $r < 0$, the decision is made in favour of $s_2(t)$. If $r > 0$, the decision is made in favour of $s_1(t)$. Thus, the two conditional probability density functions (PDFs) of r are:

$$p(r / s_1) = \frac{1}{\sqrt{\pi N_0}} e^{-(r-\sqrt{\varepsilon_b})^2 / N_0} \quad , \tag{3.5}$$

and

$$p(r / s_2) = \frac{1}{\sqrt{\pi N_0}} e^{-(r+\sqrt{\varepsilon_b})^2 / N_0} .$$

If we assume that $s_1(t)$ was transmitted, the probability of error is simply the probability that $r < 0$, i.e.,

$$p(e / s_1) = \int_{-\infty}^{0} p(r / s_1) dr = \frac{1}{\sqrt{\pi N_0}} \int_{-\infty}^{0} e^{-(r-\sqrt{\varepsilon_b})^2 / N_0} dr \frac{n!}{r!(n-r)!}$$

$$= \frac{1}{\sqrt{2\pi}} \int_{-\infty}^{-\sqrt{2\varepsilon / N_0}} e^{-x^2 / 2_0} dx$$

$$= \frac{1}{\sqrt{2\pi}} \int_{\sqrt{2\varepsilon / N_0}}^{\infty} e^{-x^2 / 2_0} dx$$

$$= Q(\sqrt{\frac{2\varepsilon_b}{N_0}}) .$$

Here $Q(x)$ is the Q-function which is defined in Equation 3.4. In the same way, if we assume that $s_2(t)$ is transmitted, then, $r = s_1 + n = \sqrt{\varepsilon_b} + n$. The probability that $r > 0$ is also $p(e/s_2) = Q(\sqrt{\frac{2\varepsilon_b}{N_0}})$. Since signals $s_1(t)$ and $s_2(t)$ have equal probability to be transmitted, the average probability of error can be expressed as:

$$P_b = \frac{1}{2}P(e/s_1) + \frac{1}{2}P(e/s_2) = Q(\sqrt{\frac{2\varepsilon_b}{N_0}}).$$

From the equation for error probability above we can notice that the probability of error depends only on the ratio $\frac{\varepsilon_b}{N_0}$, and not on any detailed characteristics of the signal and the noise. That ratio is the signal bit energy to noise power density, or the signal to noise ratio per bit. We also note that $\frac{\varepsilon_b}{N_0}$ is the output SNR from the matched-filter demodulator.

In addition, it can be seen that the probability of error of the system can be represented according to the distance between the two PAM signals $s_1(t)$ and $s_2(t)$. It can also be noticed from the figure that the distance between the two pulse amplitude modulation (PAM) signals is $d_{12} = 2\sqrt{\varepsilon_b}$. By replacing $\varepsilon_b = \frac{1}{4}d_{12}^2$, we can obtain the expressions of probability of error in terms of the distance between the two signals as follows:

$$P_b = Q(\sqrt{\frac{d_{12}^2}{2N_0}}).$$

The equation above indicates how the probability of error of the binary modulation depends on the distance between the two signal points.

Similarly, according to the discussion above, we can assess the probability of error for orthogonal binary signals. Let us assume that two vector signals s_1, s_2 are orthogonal signals. They are two dimensional signals. Thus the two signals can be expressed respectively as follows:

$$s_1 = [\sqrt{\varepsilon_b} \quad 0], \qquad s_2 = [0 \quad \sqrt{\varepsilon_b}],$$

where ε_b represents the energy of each of the two waveforms, and $d_{12} = \sqrt{2\varepsilon_b}$ is the distance between the two vector signal points.

In order to assess the probability of error for the orthogonal signals, we assume that signal s_1 is transmitted. Then, the output vector of the demodulator at the receiver is:

$$r = [\sqrt{\varepsilon_b} + n_1 \quad n_2].$$

Now, if we replace r into the correlation metrics $C(r, s_1)$ and $C(r, s_2)$, we obtain:

$$C(r, s_1) = 2r \cdot s_1 - \|s_1\|^2$$

$$C(r, s_2) = 2r \cdot s_2 - \|s_2\|^2.$$

So the probability of error is the probability that $C(r, s_2) > C(r, s_1)$. That is,

$$P(e / s_1) = P[C(r, s_2) > C(r, s_1)] = P[n_2 - n_1 > \sqrt{\varepsilon_b}]$$

Because n_1 and n_2 are statistically independent Gaussian random variables each with zero-mean and variance $\frac{1}{2}N_0$, random variable $x = n_1 - n_2$ is a Gaussian random process with zero-mean and variance N_0. Hence,

$$P(n_2 - n_1 > \sqrt{\varepsilon}) = \frac{1}{\sqrt{2\pi N_0}} \int_{\sqrt{\varepsilon_b}}^{\infty} e^{-x^2/2N_0} dx$$

$$= Q\left(\sqrt{\frac{\varepsilon_b}{N_0}}\right).$$

According to the symmetry, similarly, the error probability when s_2 is transmitted is derived. Therefore, the average error probability for a binary orthogonal signal is:

$$P_b = Q\left(\sqrt{\frac{\varepsilon_b}{N_0}}\right) = Q\left(\sqrt{\gamma_b}\right),$$

where γ_b is the *SNR* per bit.

It can be found that if we want to obtain the same error probability for orthogonal signals as antipodal signals, it require a factor of 2 increase in energy, when we compare the error probability for binary antipodal signals with that for binary

orthogonal signals.

3.4 OFDM Techniques

As one of the multi-channel transmission techniques, the multicarrier technique is to subdivide the available frequency band into a number of narrow subbands, and information is transmitted on each of the subbands. The OFDM technique is a specific multicarrier technique in which the channel is subdivided into several subbands and each subband modulates the corresponding data symbol by employing the FFT [76, 77].

3.4.1 Multicarrier Transmission

In a particular given channel characteristic, it is very important for communication systems to consider how to efficiently use the given system channel frequency band for reliable information transmission in a given transmitter power and limited receiver complexity. There are two types of modes. One is to subdivide the frequency band into the non-ideal filter channels. The other one is to subdivide the frequency band into the nearly ideal filter channels. For the non-ideal filter channels, one common option is to employ a single carrier transmission system in which the information sequence is transmitted serially at some specified rate. In such a channel the time dispersion is normally much larger than the symbol rate. Thus, the inter symbol interference is caused by the non-ideal frequency response characteristics of the channel.

Another approach to improve the efficiency of channel band utilization in the presence of channel distortion is the ideal filter channel. In the ideal filter channel model, the channel is subdivided into a group of subchannels, each of which is narrow enough so that the channel is nearly ideal. To be specific, we assume the channel bandwidth is B and the channel is subdivided into several subchannels each

of which has bandwidth Δf . Furthermore, assume the frequency response of the non ideal channel is $H(f)$, and $\Phi_{nn}(f)$ is the power spectrum density of the additive Gaussian noise. Then, we divide the channel bandwidth B into $N = B/\Delta f$ subbands of widt Δf , where Δf is chosen sufficiently small that $|H(f)|^2 / \Phi_{nn}(f)$ is approximately a constant with each subband. We select $P(f)$ as the transmitted signal power to be distributed in frequency, subject to the constraint that:

$$\int_B P(f)df \le P_{av}$$

Here P_{av} is the available average power of the transmitter. Then, we transmit the data on these N subbands. In Section 3.4.2 we will learn the performance of multicarrier transmission systems. In Chapters 7, we will investigate system performance of the ISS-OFDM, which is developed based on multicarrier transmission techniques.

3.4.2 Multicarrier Transmission Characteristics

In order to learn the performance of multicarrier systems, we start from the capacity of ideal linear filter channel, and derive the capacity performance of a non ideal linear filter channel, multicarrier channel.

According to Shannon's principle, the capacity of an ideal, band limited, AWGN channel is:

$$C = B\log_2(1+\frac{\bar{P}}{N_0 B}).$$

Here, C bits/s is the channel capacity, $\bar{P}$ is the transmitted signal average power, N_0 is the power spectrum density of the AWGN noise, and B is the channel bandwidth.

In a multicarrier system, the system transmission channel is subdivided into a number of subchannels, indexed as i, each of which has channel capacity C_i, carrier

centre frequency f_i and carrier power $P(f_i)$. If the number of the subchannels is N and each subchannel bandwidth Δf is small enough, so each subchannel can be treated as an ideal, band limited AWGN channel, and each subchannel capacity of the multicarrier system is represented as follows:

$$C_i = \Delta f \log_2\left(1+\frac{|C_i(f_i)|^2 P(f_i)\Delta f}{\varphi_{nn}(f_i)\Delta f}\right),$$

where $\varphi_{nn}(\cdot)$ is the power spectrum density of the AWGN.

The system capacity C is the sum of the N subchannel capacity, which is represented as:

$$C = \sum_{i=1}^{N} C_i = \Delta f \sum_{i=1}^{N} \log_2\left(1+\frac{|C_i(f_i)|^2 P(f_i)}{\varphi_{nn}(f_i)}\right).$$

The overall channel capacity can be derived in the limit as $\Delta f \to 0$. Using the mathematical expression, the channel capacity is expressed as follows,

$$\lim_{\Delta f\to 0} C = \lim_{\Delta f\to 0} \Delta f \sum_{i=1}^{N} \log_2\left(1+\frac{|C_i(f_i)|^2 P(f_i)}{\varphi_{nn}(f_i)}\right).$$

That is, the channel capacity of a multicarrier non linear filter channel with additive Gaussian noise is:

$$C = \int_B \log_2\left(1+\frac{|C(f)|^2 P(f)}{\varphi_{nn}(f)}\right) df \ .$$

It can also be observed from the equation above that by dividing the available channel bandwidth into several subchannels, the multicarrier transmission rate can be close to the Shannon capacity. The signal in each subchannel is coded and modulated individually at a synchronous symbol rate of $1/\Delta f$. If the subcarrier bandwidth Δf is small enough, the frequency response $C(f)$ of the subcarrier channel approximate to a constant. In this case, the inter symbol interference (ISI) is negligible. Thus, neither time domain equalization nor frequency domain equalization is needed at the receiver.

On the other hand, the multicarrier modulation with optimum power distribution provides the potential for a higher transmission rate. In single carrier transmission, the attenuation distinctively increases with the increase of the signal transmission rate, which greatly limits the applications of single carrier systems in high data rate situations, because of the large ISI penalty on the transmission signal.

3.4.3 OFDM Techniques

As wireless communication systems increase their information transfer speed, the time for each transmission necessarily becomes shorter. Meanwhile, since the delay time caused by multipath remains constant, inter symbol interference becomes a limitation to high-data-rate communication [78] . The OFDM technique can effectively avoid the problem.

OFDM is a typical multicarrier system, which subdivides the available bandwidth into a large number of orthogonal, overlapping, narrowband subchannels or subcarriers. These subcarriers transmitted in parallel and the separation of the subcarriers is theoretically minimal such that there is a very compact spectral utilization.

One of the biggest attractions of the OFDM technique is mainly due to how the system handles multipath interference at the receiver. Multipath generates two effects: frequency selective fading, and ISI [79, 80]. The flatness perceived by a narrow-band channel overcomes frequency selective fading. The modulating at a very low symbol rate, which makes the symbols duration is much longer than the channel impulse response, diminishes inter-symbol interference. Using powerful error correcting codes together with time and frequency interleaving yields even more robustness against frequency selective fading, and the insertion of an extra guard interval between consecutive OFDM symbols can reduce the effects of inter-symbol interference even more. Thus, an equalizer at the receiver in OFDM systems becomes less necessary.

Another attraction of the OFDM technique becoming very popular is due to the simple implementation by employing the discrete Fourier transformation (DFT) algorithm. The modulation of OFDM is implemented by using an inverse fast Fourier transformation (IFFT) algorithm to synthesize the signal at the transmitter, and the demodulation technique is implemented by employing the FFT algorithm to demodulate the synthesized signal. The FFT is simply an efficient computational tool for implementing the discrete Fourier transform (DFT) [81, 82].

3.5 Channel Statistical Characteristics

Radio wave propagation through space is a complicated phenomenon characterized by effects of multipath and shadowing. The precise mathematical channel model is neither known nor too complicated for tractable communication systems. However, if we observe channel characteristics such as the factors of channel attenuation and channel delay dispersion at a limited space and environment for a period of time, it is very likely to obtain statistical characteristics of OFDM channels [83]. For nearly half a century, considerable efforts have been devoted to the channel statistical modeling and channel mathematical model. Until now, a range of relatively simple and accurate statistical models for channel fading has been achieved depending on the particular propagation environment and the underling communication scenario.

In this section, we will discuss briefly the principal statistical characteristics and mathematical model for channel fading. Our treatment of digital signaling over multipath fading channels will start by developing a statistical characterization of the channel. Then, system performance over such channels will be evaluated according to the received signal after the transmitted signals experiencing multipath fading channels. Due to multipath fading the penalty on SNR is severe, however, the penalty on SNR can be reduced dramatically by employing a series of modulation and demodulation, coding and decoding techniques.

Characterization of fading multipath channels can be achieved by observing the characteristics over the channels at a limited space and environment at a period of

time. If we transmit an extremely short pulse over a time varying multipath channel, the received signal may be a train of pulses. Due to the time varying characteristics of the multipath fading channels, if we repeat the extremely short pulse over and over, the received signals may change in the train of pulses. The change can be in many ways, such as the number of the pulses in the train, the duration of the individual pulse, and the delays and attenuations of each pulse. Therefore, it is reasonable to achieve the statistical characteristics of the time varying channel.

Envelope and phase are two of the main characteristics of channel fading. When a transmission signal is experiencing multipath channel fading, both the envelope and phase of the transmitted signal will fluctuate. For coherent modulation, if no corresponding measures are taken to compensate the phase distortion, the fading effects on the phase can severely reduce system performance. Generally, under the assumption that the phase distortion is completely compensated by employing channel equalization techniques, the analyses of the system performance are carried out. For non-coherent modulation, since the system performance is not affected by the phase fluctuation, system performance is only affected by the envelope of the channel fading. Thus, for both coherent demodulation and non coherent demodulation, system performance analyses require only knowledge of the channel fading envelope. Moreover, for the slow fading channel, fading is at least constant over one symbol duration.

Channel fading can be divided into two classes of fading, slow fading and fast fading, in terms of the coherent time of the channel. For better knowledge of slow fading and fast fading, it is essential to introduce two notions, the coherent time of fading channels and coherent bandwidth of the fading channels. The coherent time $(\Delta t)_c$ of the channel is the period of time over which the fading process is correlated. That is, the period of time after which the correlation function of two samples taken at same frequencies but at different time instant drops below a predetermined threshold. The coherent time is also related to the channel Doppler spread f_D by:

$$(\Delta t)_c \approx \frac{1}{f_D}$$

If the coherence time $(\Delta t)_c$ is greater than one symbol time duration T_s, i.e., $(\Delta t)_c \geq T_s$, channel fading is said to be slow fading; On the other hand, if the coherence time $(\Delta t)_c$ is smaller than the symbol time duration, i.e., $(\Delta t)_c \leq T_s$, channel fading is said to be fast fading. The slow fading and fast fading channel notation can be also viewed in the frequency domain. Corresponding to the coherence time of the fading channel is the coherence bandwidth $(\Delta f)_c$, if the coherence bandwidth is greater than the symbol bandwidth W_s, it is slow fading; otherwise, it is considered to be fast fading. The distinction between slow fading and fast fading is important for mathematical modeling of fading channels and for system performance evaluation of communication systems operating over these channels.

Frequency selectivity is also an important characteristic of fading channels. If all the spectral components of the transmitted signal in one symbol are subject to the same attenuations and phase shifts in transmission through the channel, then fading is said to be frequency non selective or equivalently, frequency flat . This is the case for narrow band systems in which the transmitted signal bandwidth W_s is much smaller than the channels' coherence bandwidth $(\Delta f)_c$, that is, $W_s \leq (\Delta f)_c$. This bandwidth measures the frequency range over which the fading process is correlated and is defined as the frequency bandwidth over which the correlation function of two samples of the channel response taken at the same time but different frequencies falls below a suitable value. In addition, the coherence bandwidth is related to the maximum delay spread $\tau_{\max}$ by:

$$(\Delta f)_c \approx \frac{1}{\tau_{\max}}.$$

On the other hand, if the spectral components of the transmitted signal are affected by different amplitude gains and phase shifts, then fading is said to be frequency selective [84, 85]. This applies to wideband systems in which the transmitted bandwidth is bigger than the channel's coherence bandwidth.

By far, frequency-non selective slow fading is the simplest to analyze. Moreover, it yields insight into the performance characteristics for digital signaling on a fading

channel and serves to suggest the type of signal waveforms that are efficient in eliminating fading resulting from the channel. When the transmission signal bandwidth W_s is smaller than the fading channel coherence bandwidth $(\Delta f)_c$, since the multipath fading components in the received signal are irresolvable, the received signal appears to come to the receiver through a single channel fading path. On the other hand, we can also choose the signal bandwidth W_s to be much greater than the coherence bandwidth of the fading channels, so that the fading channel becomes a frequency selective fading channel. Holding this condition, the multipath channel fading components can be resolvable. This frequency selective fading channel can be modeled as a tapped delay line filter channel with time-varying tap coefficients.

3.6 Summary

In this chapter, we discussed the fundamental theory including spectrum spreading techniques, OFDM techniques, and multipath channel fading and performance evaluation methods of the receiver signal and some digital signal processing methods. The framework of this chapter is illustrated in Figure 3.4. The purpose of the chapter is to make it easier to illustrate the design and analysis of the ISS-OFDM system presented from the chapter 4 to chapter 7. Another purpose is to make the thesis more systematic and complete in its content.

From the next chapter to chapter 6, we will discuss the design of the ISS-OFDM system including the transmitter or the generation of the ultra-wideband interleaved spread spectrum OFDM signal, multipath channel simulation, receiver including the single carrier (single FFT) transmission and multicarrier transmission (Parallel FFTs). After that, we will analyze the performance of the transmitted multiple subband signal such as PAR, the performance of received signal such as diversity and bit error rate, and the system coexistence systems under different system configurations.

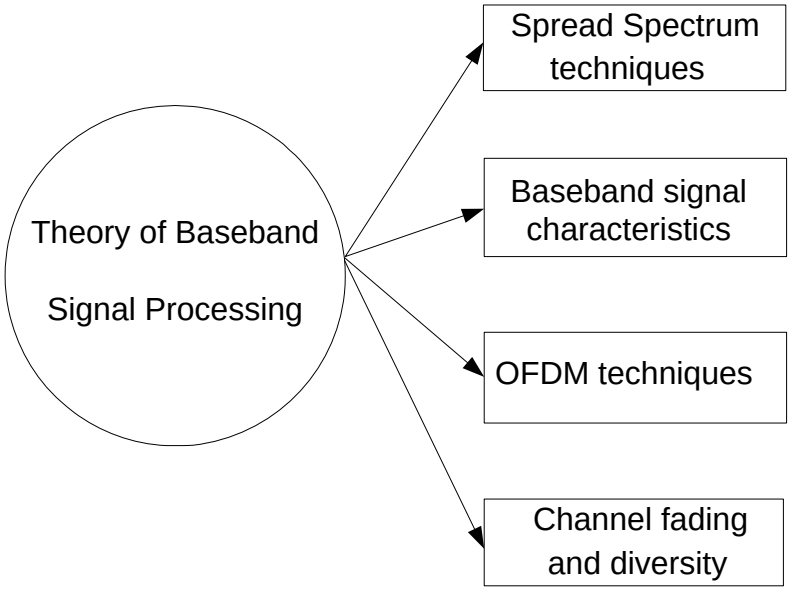

Figure 3.4 Theory of baseband signal processing.

Chapter 4

Multiple Subband Signal

4.1 Introduction

The OFDM technique as one of multi-carrier transmission techniques has been considered for a wide range of applications for many years. Since its modulation is appropriate for relatively low data rates, it has been adopted for the use in the European digital-audio broadcast (DAB) system, wireless local area network (WLAN) standards, IEEE802.11a, IEEE802.11g, and Hiperlan II. Due to its flexible modulation structure, it is considered as one of the most promising modulation techniques to be adapted in cognitive radio communications in the near future.

In recent years, OFDM has been considered for use in combinations with spread spectrum techniques. MB-OFDM is one of the applications combining spread spectrum and OFDM techniques. By using frequency hopping (FH) spread spectrum and OFDM techniques, MB-OFDM generates an ultra-wideband signal and realizes ultra-wideband communications [86]. The FH UWB system places the signal on a frequency band for a short time interval, then moves to a different frequency band, and continues hopping the signal to different frequency bands, so the signal spans a range of spectrum over a relatively long OFDM symbol duration. The long OFDM

symbol duration is of significant importance in overcoming inter-symbol interference, at the same time the overall transmission can yield high data rates . However, due to the frequency hopping in compliance with current FCC rules, it can only offer degraded range and data rate performance. In essence, FH OFDM is narrow band communication since each subcarrier used for carrying data information still works in a very narrow band. Another disadvantage is that the OFDM symbol is relatively easy to be destroyed under fading. OFDM symbols can be only partially destroyed under fading by adopting a large number of subcarriers and at cost of increasing system complexity and resulting in a poor peak-to –average power ratio [87-89].

Besides the MB-OFDM technique, some other different forms of spread spectrum OFDM systems have been proposed [90, 91], such as spread-spectrum multi-carrier multiple-access (SS-MC-MA), spread spectrum OFDM (SS-OFDM) and OFDM spread spectrum (OFDM-SS) systems to enable multipath diversity and robustify the performance of OFDM systems against channel fading. In these techniques, the spreading spectrum methods that are used, in essence, are almost the same by multiplying transmit data stream with a certain orthogonal spread code before modulation, wherein spectral spreading is accomplished by putting same data on all parallel subcarriers, producing a spreading factor equal to the number of subcarriers. After spectrum spreading, the transmission bandwidth occupied by N subcarriers is equally divided into M subbands, each containing of N/M subcarriers. Each of the M frequency subbands operates as an independent communication channel. Individual packets are assigned to each subband for transmission based on the requested data rates from the system requirements. The stream of encoded data symbols is serial to parallel converted to form N/M symbol streams. The N/M stream is spread by an orthogonal Walsh Hadmard code of length N/M , and combined with a specific pseudo noise sequence. By means of spectrum spreading techniques these systems enable full multipath diversity that can be combined at the receiver by using the maximum-ratio combining (MRC) technique. However, these spread spectrum OFDM systems only transmit one information symbol per OFDM block, and a large number of side information transmissions is needed, which causes considerable rate loss.

4.1.1 OFDM Architecture

In the following we will discuss the OFDM system architecture, its transmitter and receiver block diagram and the respective functions. Figure 4.1 displays the model of an OFDM system. This OFDM system consists of a transmitter and a receiver [92]. The transmitter consists of symbol mapping, serial to parallel converter, OFDM modulation, cyclic prefix, parallel to serial converter, and digital to analog (D/A) converter. The receiver consists of the serial to parallel converter, cyclic prefix removing, OFDM demodulation, detector and parallel to serial converter and demapping.

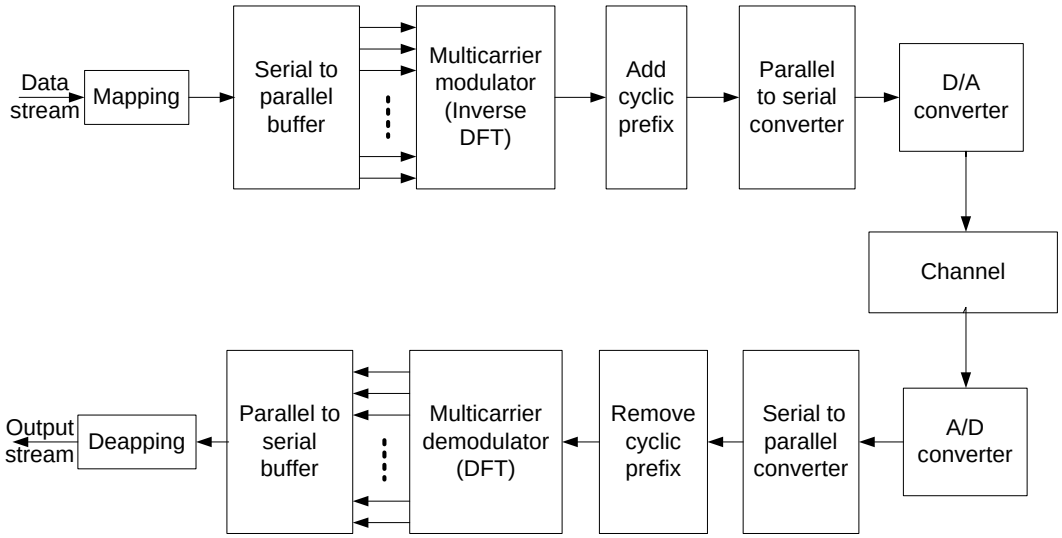

Figure 4.1 OFDM system model.

4.1.2 Mathematical Expressions of OFDM Signal

At the transmitter, the serial-to-parallel converter splits the data stream sequence into frames of M_b bits. The M_b bits in each frame are parsed into N groups. The i^{th} group is assigned n_i bits and

$$\sum_{i=1}^{N} n_i = M_b$$

Each group can be encoded individually, the number of encoder output bits from the i^{th} group is $en_i \geq n_i$. We assume the mapping is QPSK, encoded into groups of two bits en_i =2. Each group of two bits is mapped into one QPSK symbol. The N independent QPSK symbols modulate N subchannels and each operates at the same symbol rate $\frac{1}{T}$. We denote the complex-valued signal points corresponding to the data symbols on the subchannels by a_k, $k = 0,1,\cdots,N-1$. In order to modulate the N subcarriers by the data symbols $\{a_k\}$, the inverse DFT (IDFT) operation is employed, which is performed efficiently by using the FFT algorithm as indicated in Figure 4.2 [93].

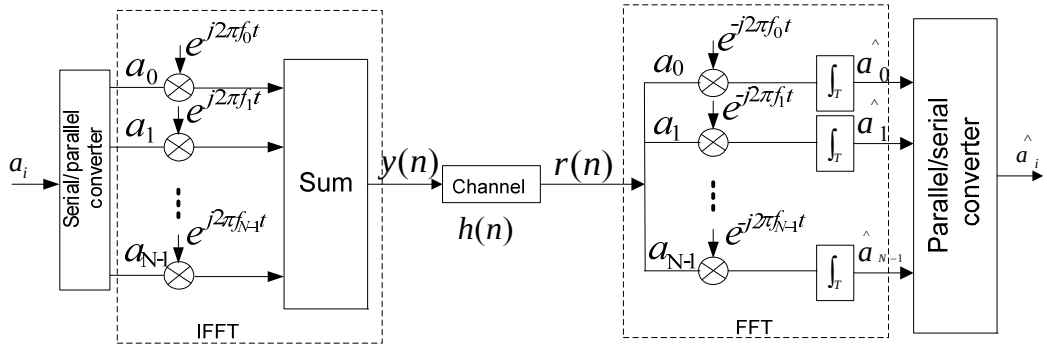

Figure 4.2 OFDM modulation and demodulation.

Then, the N -point IDFT yields the complex-valued sequence as follows:

$$y(n) = \frac{1}{N}\sum_{k=0}^{N-1} a_k e^{j2\pi nk/N}, n = 0,1,\cdots,N-1,$$

where $\frac{1}{N}$ is simply a scale factor. The sequence $\{y(n)\}$ corresponds to the samples of sum $y(t)$ of N subcarrier signals:

$$y(t) = \frac{1}{N}\sum_{k=0}^{N-1} a_k e^{j2\pi f_k t/T}, 0 \leq t \leq T,$$

where T is the symbol duration, and $f_k = k/T, k = 0,1,\cdots,N-1$. Furthermore, the discrete-time sequence $\{y(n)\}$ in the equation above represents the samples of $y(t)$

taken at time $t = nT / N$, where $n = 0,1,\cdots,N-1$.

After the computation of IDFT, the signal samples $\{y(n)\}$ pass through a D/A converter whose output, normally, should be the signal waveform $y(t)$. This signal passes through space and experiences channel fading and noise when it is propagating in the channel. At the input of the receiver, the received signals can be represented as follows:

$$r(t) = y(t) \otimes h(t) + v(t),$$

where $h(t)$ is the impulse response of the channel, "$\otimes$" is the convolution between the transmitted signal $x(t)$ and channel impulse response $h(t)$, and $v(t)$ is the noise coming from various sources.

Since OFDM symbol duration $T = \frac{1}{\Delta f}$, when the subchannel bandwidth Δf is very small, the symbol duration T is much larger than the channel time dispersion and the probability of producing ISI is reduced greatly. If we assume the channel time dispersion spans $m+1$ signal samples, where $m \ll N$, in order to avoid ISI, one common way is to insert guard intervals of duration $\frac{mT}{N}$ between transmissions of successive OFDM symbols.

The guard intervals can be implemented by adding a cyclic prefix taken from the back of the OFDM symbol samples to the beginning of each OFDM symbol with N samples $\{y(0), y(1),\cdots, y(N-1)\}$. The purpose of adding the cyclic prefix is to avoid inter-symbol interference. If we take m samples from the end of the N samples as cyclic prefix samples $\{y(N-m), y(N-m+1),\cdots, y(N-1)\}$ and append them to the beginning of the OFDM N samples. We can obtain a new sequence which can be denoted as $\{y(N-m), y(N-m+1),\cdots, y(0), y(1),\cdots, y(N-1)\}$. It is obvious that the appending of the cyclic prefix to the OFDM samples increases the length of the transmitted signal samples. The length of the transmitted signal samples increase from the original N to $N+m$, the index of the transmitted signal samples from

$N-m$ to $N-1$. As we discussed above, the input signal at the receiver can be expressed as the convolution between the transmitted signal $y(n)$ and the channel impulse response $h(n)$. The first m samples are removed since we are only interested in the useful signal $y(n)$, n=0,1,…, $N-1$.

The circular convolution operation between $h(n)$ and $y(n)$ must be performed here to get the results of the convolution. The circular convolution process can be expressed as:

$$r(m)=\sum_{m=0}^{N-1}h(m)y(n-m).$$

By employing an $N-$ point DFT operation, we can obtain the frequency representation of the received signal after the cyclic prefix is discarded. The DFT can be efficiently performed by using the FFT algorithm. Thus, the received signal in the frequency domain can be represented as:

$$\hat{R}(k)=H(k)\cdot Y(k)+V(k),\ \ k=0,1,\cdots,N-1,$$

where $\hat{R}(k)$ is the estimate value at the output of the demodulator by performing a $N-$point DFT operation, $V(k)$ is the frequency response of the noise imposed on the transmitted signal. By selecting the $M \gg m$, the rate loss due to the cyclic prefix can be rendered negligible.

4.1.3 OFDM System Performance

One of the attractions of OFDM systems is that channel equalization in OFDM systems is easy to implemente since the ISI in OFDM systems is eliminated by the long symbol duration and guard intervals. In practice, channel estimation and equalization are still employed to estimate and compensate for channel factors $\{H(k)\}$ before passing the data to the detector and decoder. A training signal consisting of either a known modulated sequence on each of the subcarriers or

unmodulated subcarriers may be used to measure $\{H(k)\}$ at the receiver. If the channel parameters vary slowly with time, it is also possible to track the time variations by using the decision at the output of the detector or the decoder, in a decision directed fashion. Thus, OFDM systems can be made adaptive.

In order to determine the capacity of each of the subchannels, it is useful to measure the SNR for each of the subchannels. The SNR for each of the subchannels can be defined as:

$$SNR_i = |H(i)|^2 T_s P_{av} / \delta_n^2 \ ,$$

where $|H(i)|^2$ is the magnitude-square of the i^{th} subchannel frequency response, δ_n^2 is the variance of the i^{th} subchannel noise and P_{av} is the average power distributed on the i^{th} subchannels and T_s is the symbol duration. Based on the measurement of the SNR, the transmission rate and the number of bits allocated to the subchannel can be optimized adaptively. By selecting the transmission power and the number of bits allocated to each subchannel, the system performance may be optimized.

The relatively large sidelobes in frequency which are inherent in DFT-type filter banks, in which the first sidelobe is only 13 dB down the peak at the desired subcarrier, limit the potential of DFT-based modulator and demodulator. As a result, if there is no full cyclic prefix, the DFT-based OFDM system can be easily affected by inter channel interference.

One of the major problems with OFDM based multicarrier modulation is the relatively large peak to average power ratio (PAR) in the transmitted signals. The PAR occurs when the modulated subcarriers add constructively in phase. The relatively high PAR in the the transmission signal results in clipping of the signal voltage when the transmission signal is passing through the Digital to Analog converter (D/A). Another impact resulting from the relatively high PAR is that it will saturate the power amplifier into the non-linear amplifier range, which causes intermodulation distortion in the transmitted signal. When the number N of the subcarriers is very large, the central limit theorem can be used to model the

combined signal on the N subchannels as a zero-mean Gaussian random process, in which the PAR is proportional to $\frac{1}{\sqrt{N}}$.

For minimizing the peak to average power ratio (PAR) of the OFDM signal, a very effective and very common method is to reduce the power in the transmitted signal and make sure the amplifier at the transmitter operate at the linear operating range. This power reduction results in inefficient operation of the communications system.

There are many kinds of methods that have been proposed to decrease PAR in OFDM based multicarrier systems. One of the simplest methods is to insert different phase shifts in each of the subcarriers, i.e., DSSS. By means of some algorithms such as pseudorandom, these phase shifts can be selected to reduce the PAR. In this way, some side information on which a set of pseudorandomly phase shifts, is transmitted to the receiver on a separate channel, i.e., one of the N subcarriers, so that the PAR performance can be satisfied to an accepted PAR level.

In addition, a small set of dummy symbols can be also used to modulate the subcarriers to reduce the PAR of the transmitted signal. The design of these sorts of dummy symbols is very flexible and does not need to satisfy the constraint of amplitude and phases from a specified constellation. The subcarriers carrying the dummy symbols may be distributed across the whole frequency band. However, the dummy symbols result in a lower throughput in the data rate. It is desirable to employ only a small percentage of the total subcarriers to modulate the dummy symbols for the PAR reduction.

Based on the OFDM techniques, from Section 4.2 we discuss the system architecture, ISS-OFDM signal generation, transmission and reception. Firstly, the generation process of interleaved spread spectrum orthogonal frequency division multiplexing (ISS-OFDM) signals is introduced. Then, they are transmitted on different time slots respectively. In this way the number of the total samples in one ISS-OFDM symbol increases greatly and the signal spectrum is spread widely, which results in the signal power spectrum density reduced but the total signal

energy remaining unchanged. Naturally, the PAR is reduced significantly. At the receiver, the receiver can be supplied several replicas of the baseband signal transmitted over independently fading channels. After frequency domain equalization, the diversity of the signal can be collected by using maximal ratio combination (MRC) techniques. Thus, the probability that all the signal components fade simultaneously is reduced considerably. Except for retaining the merits of conventional OFDM systems, the proposed ISS-OFDM system has some distinctive features, such as good BER performance, very lower peak to average power ratio (PAR), flexible system bandwidth, lower power spectrum density, and good coexistence with other system [94].

4.2 System Architecture

In this section, we describe the baseband system model. Then the generation of ISS-OFDM signals is introduced in Section 4.3, where the ISS-OFDM signal characteristics in the frequency domain and time domain are analyzed.

We assume that the data bit to symbol mapping scheme in Figure 4.1 on the ISS-OFDM baseband system model is QPSK, the channel is frequency selective with slow fading, and the noise is AWGN with zero mean. At the transmitter, each data symbol modulates its corresponding subcarrier multiple times, and several different samples bearing the same data information can be generated. The replicas of the same data information are interleaved and then transmitted in different time slots, instead of adding the modulated samples together. Assume N data symbols in parallel modulate N subcarriers to produce N samples at each time slot, and each symbol modulates the corresponding subcarrier N times to produce N data samples in one ISS-OFDM symbol time duration, and if one ISS-OFDM symbol duration is divided into N time slots, after the spread spectrum modulation a $N \times N$ matrix of data samples is generated in an ISS-OFDM symbol duration. The resulting N samples in the column of this matrix are not added together, instead, they are interleaved according to a certain pseudorandom code. A cyclic prefix (CP) is also

added to preserve the orthogonality of the subcarriers and eliminate ISI between consecutive ISS-OFDM symbols.

Under the above assumptions we now describe the function of each module shown in Figure 4.3. The function of the transmitter is to generate an ISS-OFDM signal with time and frequency diversities. The complex QPSK data symbols to be transmitted are first divided into an N by 1 vector, where N is the number of subcarriers. This vector modulate N subcarries in parallel by using a spread spectrum modulation technique, which we call complex exponential spreading (CES), and then the spread signals are interleaved to form an ISS-OFDM symbol of N^2 samples. After a CP insertion and filtering, the ISS-OFDM signal $y(m)$ (also represented by $Y(k)$ in the frequency domain) with spectrum spreading is transmitted into the frequency selective multipath fading channel with impulse response $h(m)$ (denoted as $H(k)$ in the frequency domain). Meanwhile, the AWGN noise $v(m)$ (denoted as $V(k)$ in the frequency domain) is added to the signal. After being distorted by the fading channel, the signal is filtered, CP is removed, and then the signal is demodulated. The output of the demodulator is equalized and combined to form a decision variable U_k by employing a maximal ratio combining (MRC) technique.

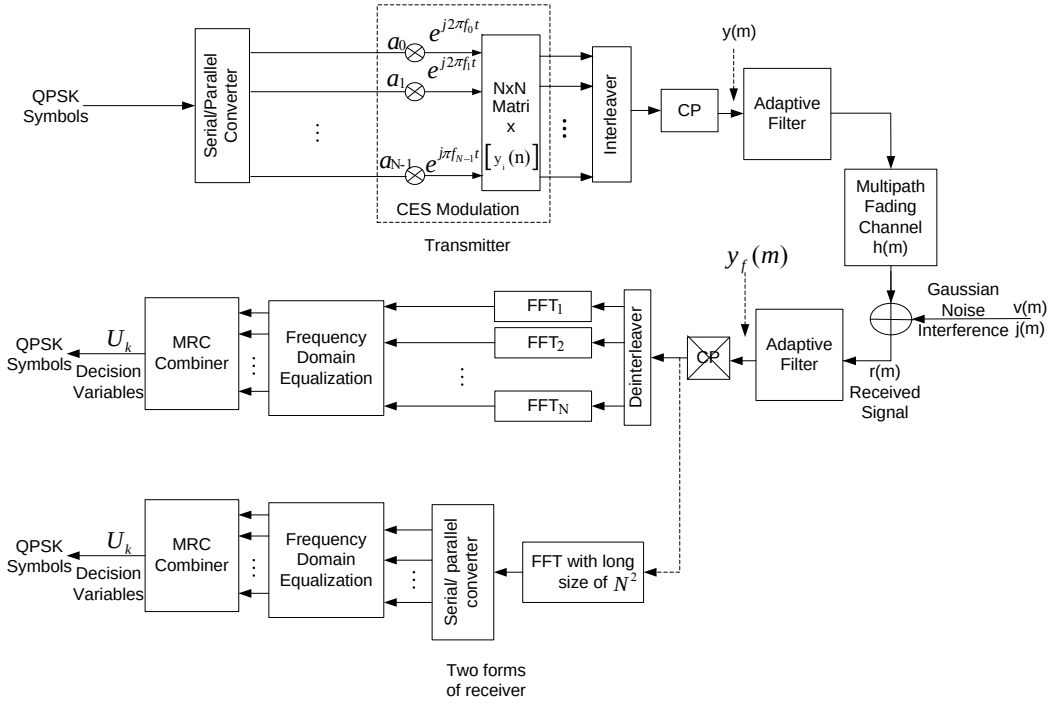

Figure 4.3 Baseband system model.

As is well known, when signals are propagated in a frequency selective multipath fading channel, the presence of reflecting objects and scatters in the channel creates a constantly changing environment that dissipates the signal energy in amplitude, phases and time. These effects result in multiple versions of the transmitted signal, which are received by the receiver at different times from different multipaths, displaced with respect to one another in time and spatial orientation. We may assume that the transmitted ISS-OFDM signal bandwidth $B_{ISS-OFDM}$ is greater than the coherence bandwidth $(\triangle f)_c$, $B_{ISS-OFDM} \gg (\triangle f)_c$, thus the channel can be considered as a frequency-selective fading channel. The channel model can be expressed in the form:

$$h(m) = \sum_{i=0}^{N^2-1} \alpha_i(m)\delta(m-m_i),$$

where $\alpha_i(m)$ is the multipath fading channel attenuation factor on the m^{th} path and m_i is the propagation delay for the m^{th} path. Correspondingly, the channel frequency response is written as:

$$H(k) = \sum_{m=0}^{N^2-1} h(m) e^{-j\frac{2\pi}{N^2}km} .$$

After the transmitted signal, denoted as $y(m)$, passes through the fading channel, the received equivalent low-pass signal is viewed as the convolution between $h(m)$ and $y(m)$ plus noise as follows:

$$r(m) = h(m) \otimes y(m) + v(m),$$

where $v(m)$ represents the complex-valued white Gaussian noise process corrupting the signal and "$\otimes$" denotes convolution. In the frequency domain, the equation above is equivalent to the output of the FFT demodulator:

$$R(k) = H(k) \cdot Y(k) + V(k),$$

where $R(k), Y(k), H(k), V(k)$ denote the frequency representations of the received signal $r(m)$, the transmitted signal $y(m)$, the channel impulse response $h(m)$ and the noise $v(m)$, respectively.

4.3 Transmitter Architecture

Figure 4.4 shows the transmitter model for the ISS-OFDM system, which consists of the QPSK mapper, spread spectrum modulation module, interleaver and filter. The function of the transmitter is to generate a transmitted signal with multiple subbands, which is called an ISS-OFDM signal. In the transmitter, the complex QPSK data symbol sequence is first divided into an N by 1 vector, where N is the number of subcarriers. Then, the vector with N data symbols modulates N subcarries in parallel by using the CES operation, by which each data symbol modulates its corresponding subcarrier. After the modulation, an $N \times N$ matrix is formed, and the modulated subcarriers in the matrix are interleaved and placed on different time slots to form a serial sequence. The sequence is pulse shaped by passing through a root raised cosine filter and thus an ISS-OFDM signal $y(t)$ is generated.

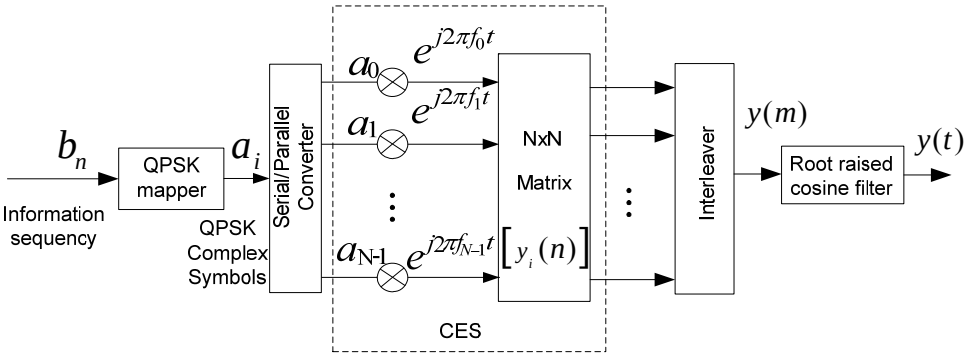

Figure 4.4 Transmitter model.

4.3.1 QPSK Mapping

Mapping is to match digital information into different symbols. The mapping is performed by taking blocks of binary information $k = \log_2{}^M$ from the information sequence $\{b_n\}$ at a time and selecting one of the $M = 2^k$ symbol - deterministic energy waveforms for transmission over the channel.

Since the information sequence is mapped into a set of waveforms, the waveforms may differ either in amplitude or in frequency or in phase, or in the combinations of two or more parameters. In the following, the signal representation of the phase shift keying (PSK) modulation will be briefly introduced, in which the waveform differs in phase, then the characteristics of the PSK signal, in particular, the characteristic of 4 PSK (quadrature phase shift keying, QPSK) signal when M =4 and BPSK (k =2) is introduced.

In digital phase modulation, the M signal waveforms are represented as

$$a_i(t) = \mathrm{Re}\left[g(t) e^{j2\pi \frac{i-1}{M}} e^{j2\pi f_c t} \right] = g(t)\cos\left[2\pi f_c t + \frac{2\pi}{M}(i-1) \right]$$

$$= g(t)\cos\left[\frac{2\pi}{M}(i-1) \right]\cos[2\pi f_c t] + g(t)\sin\left[\frac{2\pi}{M}(i-1) \right]\sin[2\pi f_c t],$$

where $\theta_i = \frac{2\pi}{M}(i-1)$, $i = 0,1,\cdots,M$, are the M possible phases of the carrier that convey the transmitted information, and g(t) ($0 \le t \le T$) is the signal pulse shape. It is noted that these signal waveform have equal energy, i.e.

$$\varepsilon = \int_0^T a_i^2(t)dt = \frac{1}{2}\int_0^T g^2(t)dt = \frac{1}{2}\varepsilon_g .$$

We can note that the signal waveform can be expressed as a linear combination of two orthonormal signal waveforms, $f_1(t)$, $f_2(t)$:

$$a_i(t) = a_{i1} f_1(t) a_{i2} f_2(t),$$

where $f_1(t) = \sqrt{\frac{2}{\varepsilon_g}} g(t)\cos(2\pi f_c t)$, $f_2(t) = -\sqrt{\frac{2}{\varepsilon_g}} g(t)\sin(2\pi f_c t)$,

and the two dimensional vectors can be expressed as:

$$a_i = \left[\sqrt{\frac{\varepsilon_g}{2}}\cos\left(\frac{2\pi}{M}(i-1)\right) \quad \sqrt{\frac{\varepsilon_g}{2}}\sin\left(\frac{2\pi}{M}(i-1)\right)\right], \quad i = 0,1,\cdots,M .$$

A signal space diagram for $M = 4$ are shown in Figure 4.5 (a).

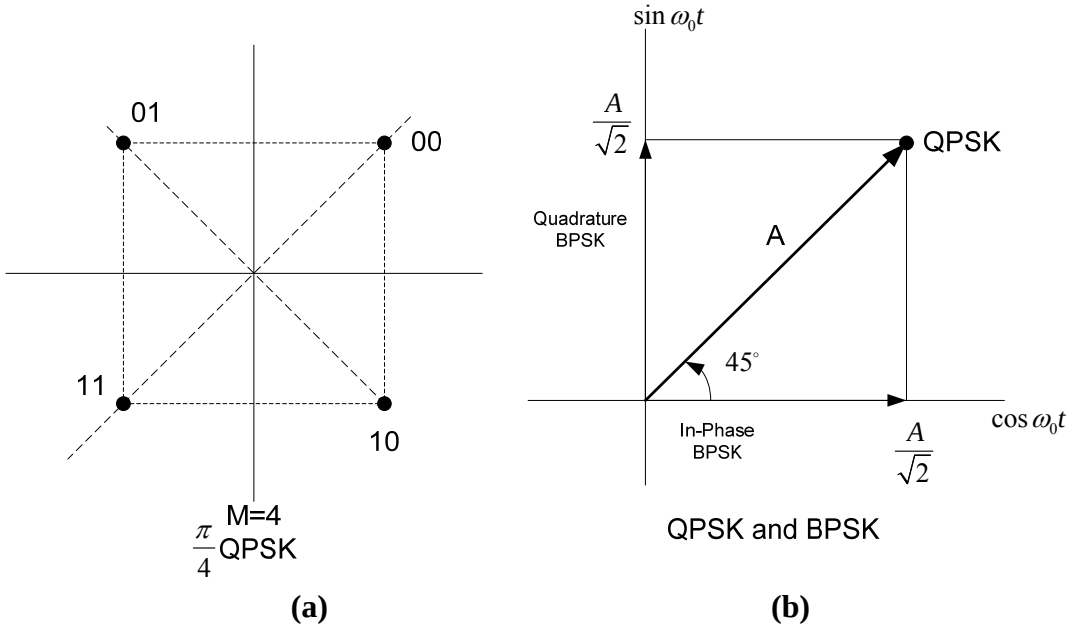

Figure 4.5 (a) Mapping of QPSK; (b) Relation between QPSK and BPSK.

A QPSK signal can be characterized as two BPSK channels as shown in Figure 4.5 (b). The QPSK signal is usually partitioned into two even and odd (or inphase and quadrature (I and Q)) streams; each new stream modulates an orthonormal component of the carrier at half the bit rate of the original stream. The I stream modulates the $\cos\omega_0 t$ term and the Q stream modulates the $\sin\omega_0 t$ term. If the magnitude of the QPSK signal is A, then each of the quadrature BPSK signals has half of the average power of the original QPSK signal. Hence if the original QPSK waveform has a bit rate of R and signal power P watts, the quadrature partitioning results in each of the BPSK waveforms having a bit rate $\frac{R}{2}$ bits/s and an average power of $\frac{P}{2}$ watts.

4.3.2 Serial/Parallel Converter and Modified OFDM Modulation

After QPSK mapping, serial to parallel conversion is performed. The QPSK complex-valued sequence is taken in blocks of N (assume N is the number of subcarriers for OFDM modulation) and each block of N complex-valued QPSK symbols is converted into a vector $N \times 1$, which will be used to modulate N subcarriers in OFDM spread spectrum modulation.

In this system OFDM spread spectrum modulation, which we call complex exponential spreading (CES), is implemented by modifying OFDM modulation.

For convenience of description, we will discuss the modulation process of only one OFDM symbol. After serial to parallel converter each of the QPSK symbols modulates the corresponding subcarrier of the N subcarriers. If the ISS-OFDM symbol period is T_s, $f_i = \frac{i}{T_s}$ denotes the i^{th} subcarrier frequency of the N orthogonal

subcarriers, and a_i modulates the i^{th} subcarrier at time $t = \frac{n}{N}T_s$, $n = 0,1,\cdots,N-1.$, where n is the sampling interval. The modulated symbol on i^{th} subcarrier and n^{th} time is written as:

$$y_i(n) = a_i e^{j2\pi f_i t} = a_i e^{j2\pi ni/N}. \tag{4.1}$$

In ISS-OFDM symbol duration T_s, each element of the $N \times 1$ data symbol vector modulates the same corresponding subcarrier N times. N elements in the vector generate $N \times N$ matrix samples after modulation. Mathematically, the matrix can be expressed as:

$$\begin{aligned}\left[y_i(n)\right] &= \begin{pmatrix} y_0(0), y_0(1), \cdots, y_0(N-1) \\ y_1(0), y_1(1), \cdots, y_1(N-1) \\ \cdots \\ y_{N-1}(0), y_{N-1}(1), \cdots, y_{N-1}(N-1) \end{pmatrix} \\ &= \begin{pmatrix} a_0 e^{j2\pi 0\frac{0}{N}}, a_0 e^{j2\pi 0\frac{1}{N}}, \cdots, a_0 e^{j2\pi 0\frac{N-1}{N}} \\ a_1 e^{j2\pi 1\frac{0}{N}}, a_1 e^{j2\pi 1\frac{1}{N}}, \cdots, a_1 e^{j2\pi 1\frac{N-1}{N}} \\ \cdots\cdots\cdots \\ a_{N-1} e^{j2\pi (N-1)\frac{0}{N}}, a_{N-1} e^{j2\pi (N-1)\frac{1}{N}}, \cdots, a_{N-1} e^{j2\pi (N-1)\frac{N-1}{N}} \end{pmatrix}. \end{aligned} \tag{4.2}$$

Let W_N denote the modulation factor, $W_N = e^{-j\frac{2\pi}{N}}$, and $\left[W_N^{-ni}\right] = \left[e^{j\frac{2\pi}{N}ni}\right]$, W_N^{-ni} denote the i^{th} sub-carrier at the $\frac{n}{N}T_s$ time instant.

$$Diag(a_i) = \begin{pmatrix} a_0, 0, ...0 \\ 0, a_1, 0...0 \\ ..... \\ 0, 0, ...a_{N-1} \end{pmatrix}.$$

Thus, Equation (4.2) can be rewritten as:

$$[y_i(n)] = \begin{pmatrix} a_0 W_N^{-0\cdot 0}, a_0 W_N^{-0\cdot 1}, ..., a_0 W_N^{-0\cdot (N-1)} \\ a_1 W_N^{-1\cdot 0}, a_1 W_N^{-1\cdot 1}, ..., a_1 W_N^{-1\cdot (N-1)} \\ ..... \\ a_{N-1} W_N^{-(N-1)\cdot 0}, a_{N-1} W_N^{-(N-1)\cdot 1}, ..., a_{N-1} W_N^{-(N-1)\cdot (N-1)} \end{pmatrix}$$

$$= Diag(a_i) \times \left[W_N^{-ni} \right]. \qquad (4.3)$$

Equation (4.3) indicates the method of the realization of the CES modulation, in which the N transmitted data symbols at the input of the modulator must be reorganized into the diagonal elements of a diagonal matrix, then, by using the CES technique the data symbols are modulated.

4.4 Interleaving

Interleaving is used to obtain time diversity in a digital communications system without adding much overhead. Interleaving has become an extremely useful technique in all second and third generation wireless systems. The function of the interleaver is to spread the OFDM modulated signal samples out in time so that if there is deep fading or a noise burst, the signal samples from the modulated signal are not corrupted at the same time.

There are many forms of interleaving methods to implement the permutation of the signal samples in the matrix, which is derived from the output of OFDM modulation. These interleaving techniques include pseudorandom interleaving, convolutional interleaving (CI), periodic interleaving (PI) and odd-even symmetric interleaver (OESI) and spread interleaving (SI) techniques. In the following, we introduce these interleaving methods.

4.4.1 Pseudorandom Interleaving

A pseudorandom interleaver is a special form of the block interleaver that accepts the input symbols in blocks, and rearranges symbols in the other forms to the output of the interelaver. If the symbols are rearranged in a pseudorandom order, this kind of interleaving is called pseudorandom interleaving. For example, samples of $I \times N$ matrix $\left[y_i(n) \right]$ are interleaved to become serial $y(m)$,

$$m = R(i, n),$$

where R is a one to one mapping implemented by employing a pseudorandom function. The transmitter stores the permutation information and transmits them into the receiver with the available data information. Thus, the pseudorandom permutation function can be obtained from a linear, or a specific algorithm to generate each permutation.

4.4.2 Convolution Interleaving

Figure 4.6 shows an instance of a convolutional interleaver with M registers and J storage for M =4 and J =1. D denotes one symbol delay unit. The code symbols are shifted sequentially into the bank of M registers, each register provides J symbols more storage than does the preceding one, where the m^{th} register delays the input symbol by $m \times j$ time units. Here $m \in [0, M-1]$ and $j \in J$. The zeroth register provides no storage or no delay and the symbol is passed through immediately. With each new code symbol coming, the commutator switches to the next register. After the $(M-1)^{th}$ register, the commutator returns to the zeroth register and restarts again. If we put the input sequence as $1,2,3,4,5,6,7,8,9,10,11,12,13,14,15,16$, after the convolutional interleaving, the resultant output is $1,\times,\times,\times,5,2,\times,\times,9,6,3,\times,13,10,7,4\cdots$. Here "$\times$" denotes the empty element at the time instant.

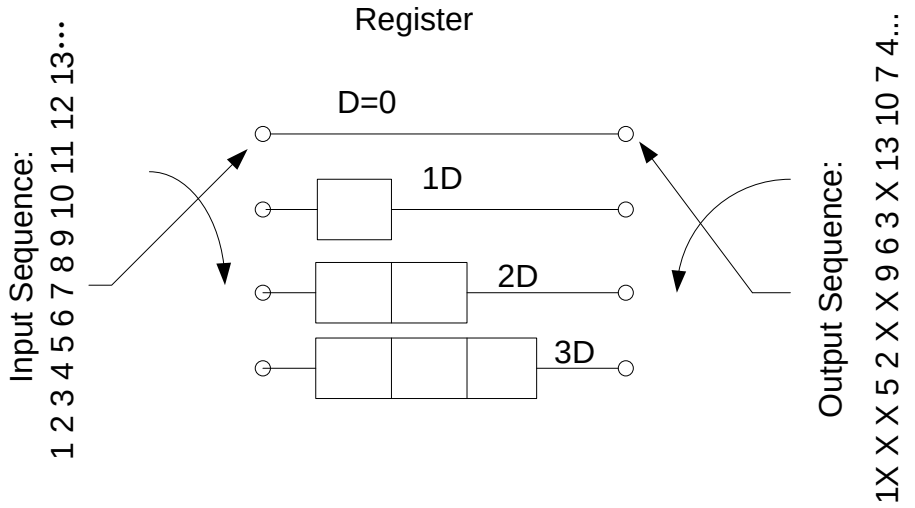

Figure 4.6 Convolutional interleaving with register number $M = 4$ and symbol storage $J = 1$.

4.4.3 Odd-Even Symmetric Interleaver

This kind of interleaver can reduce the side information transmission. As a result of this kind of interleaving, the information transmission rate increases relatively. This interleaver needs only half of the interleaver rules as it swaps the pairs of positions symmetrically. An odd-even symmetry interleaver swaps every odd position with an even position and vice versa, which can be achieved by employing the following two restrictions:

(1) $\text{i mod } 2 \neq \Re(i) \quad \forall i$ (odd to even),

(2) $\Re(i) = j \rightarrow \Re(i) = i$ (symmetry).

By utilizing these two rules, if the rules of all the odd positions are stored, it is adequate for the deinterleaver to recover the information. By performing swap, the even positioned bits are automatically interleaved. By using this interleaving algorithm, storing the full interleaver rules needs only less than 50 percent memory storage.

4.4.4 Periodical Interleaving

A periodical interleaver is the simplest method to permute the transmission sequence. For example, for the $I \times N$ matrix for one OFDM symbol, the interleaver writes the modulated samples for each of the same subcarrier row by row to form the $I \times N$ matrix and reads the samples from the matrix column by column and places the samples on a time axis, which is displayed in Figure 4.7.

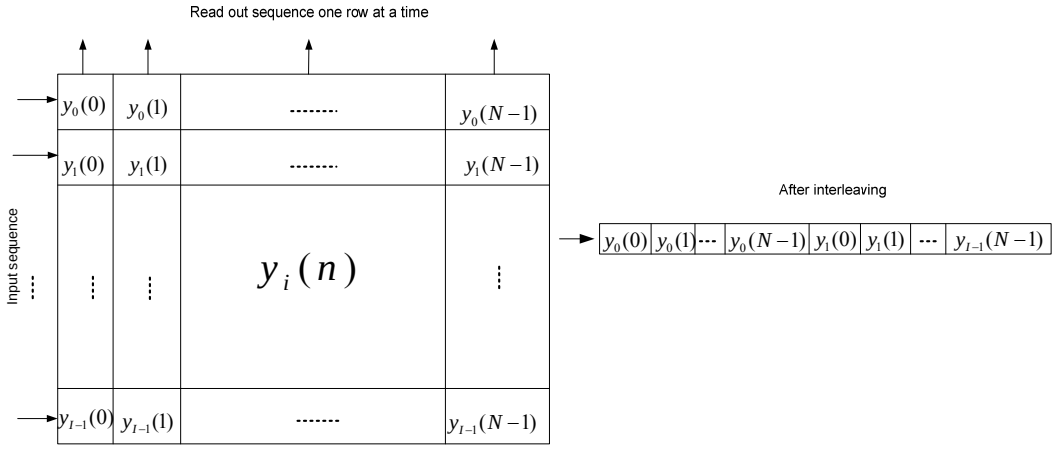

Figure 4.7 Periodical interleaving.

The de-interleaver inverts this permutation by writing the received samples into a matrix column by column. Mathematically, if the $I \times N$ matrix is denoted as $[y_i(n)]$, $i = 0,1,\cdots,I-1, n = 0,1,\cdots,N-1.$, then, let the period of the interleaving be N, after periodically interleaving, the interleaved serial sequence can be written as follows:

$$\begin{aligned} y(m) &= y(nN+i) \\ &= y_i(n) \\ &= a_i e^{j2\pi f_i t} = a_i e^{j2\pi ni/N}, \end{aligned} \tag{4.4}$$

where $i = 0,1,\cdots,I-1, n = 0,1,\cdots,N-1.$

4.5 Generation of ISS-OFDM Symbol

In section 4.4 we discussed various forms of interleaving methods. According to any kinds of these interleaving methods, we can interleave the OFDM modulated samples and generate the interleaved OFDM symbol. Let us take the periodically interleaving methods as an example to generate the ISS-OFDM symbol.

After CES modulation, the $N \times N$ matrix samples are interleaved. Different interleaving algorithms can be employed. However, for the simplicity of description, we adopt the periodic interleaving algorithm. In the following, we discuss interleaved results by using the periodic interleaving alogrithm. The periodic interleaving can be realized by shifting N modulated subcarriers on a different time slots and adding them together. For instance, the i^{th} subcarrier of the N subcarriers is shifted by $i \cdot \tau$, where τ is the sampling interval, $\tau = \frac{T_s}{N}$. Then, the N shifted subcarriers are added together to form one ISS-OFDM symbol with N^2 samples. The m^{th} sample in the ISS-OFDM symbol, denoted by $y(m)$, $m = nN + i = 0,1,\cdots,N^2 - 1.$, can be mathematically written as follows:

$$y(m) = \sum_{i=1}^{N} \sum_{n}^{N} y_i(n) \delta\left[m - i - nN\right], \tag{4.5}$$

where $\delta\left[m - nN - i\right] = \begin{cases} 1, & \text{for } m = nN + i \\ 0, & \text{for } m \neq nN + i. \end{cases}$ is the unit impulse. If periodical interleaving is performed, taking out $y(m)$ for every $m = nN + i$, $y(m)$ can be simplified in the form:

$$y(m) = y(nN + i) = y_i(n), \; m = nN + i, \text{ and } n, i = 0,1,\cdots,N-1.$$

Thus, N^2 samples are produced in the same symbol period T_s, and the number of samples is spread N times. The sampling rate is N^2 / T. Therefore, an ISS-OFDM symbol is generated.

Figure 4.8 shows the signal modulation and periodical interleaving process for generating an ISS-OFDM symbol in the case of subcarriers number $N = 4$. It is seen that the modulated samples on the i^{th} ($i = 0,1,2,3$) subcarrier are shifted i time intervals, and then they are added on the time axis, and the number of samples increases to N^2 from the original number N .

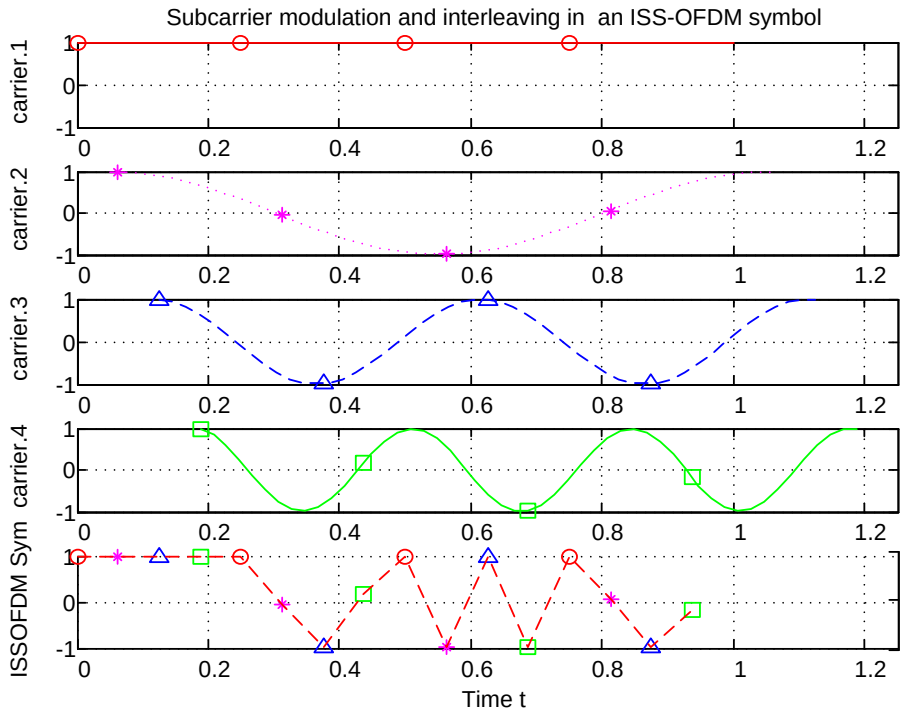

Figure 4.8 Modulation and interleaving process with subcarrier number $N = 4$.

Furthermore, we can have a look into the ISS-OFDM signal from the view of the frequency domain. The frequency domain transmitted signal can be written as:

$$Y(k) = FFT(y(m)) = FFT(y(nN+i))$$

$$= \sum_{nN+i=0}^{N^2-1} y(nN+i)e^{-j\frac{2\pi}{N^2}(nN+i)k} .$$

That is,

$$Y(k) = \sum_{n=0}^{N-1}\sum_{i=0}^{N-1} y(nN+i)e^{-j\frac{2\pi}{N^2}(nN+i)k} . \qquad (4.6)$$

Substituting $y(nN+i)$ by $y_i(n)$ from Equation (4.5) into Equation (4.6), $Y(k)$ has the form as:

$$Y(k) = \sum_{n=0}^{N-1}\sum_{i=0}^{N-1} y_i(n) e^{-j\frac{2\pi}{N^2}(nN+i)k}$$

$$= N\sum_{i=0}^{N-1} a_i e^{-j\frac{2\pi}{N^2}ki} \underbrace{\frac{1}{N}\sum_{n=0}^{N-1} e^{-j\frac{2\pi}{N}(k-i)n}}_{\delta((k-i)_N)} \quad . \tag{4.7}$$

Replacing $\frac{1}{N}\sum_{n=0}^{N-1} e^{-j\frac{2\pi}{N}(k-i)n}$ by $\delta((k-i)_N)$ in Equation (4.7), we have the equation as:

$$Y(k) = N\sum_{i=0}^{N-1} a_i e^{-j\frac{2\pi}{N^2}ki}\delta((k-i)_N), \tag{4.8}$$

where $\delta((k-i)_N) = \begin{cases} 0, & k \neq pN+i \\ 1, & k = pN+i \end{cases}$, that means:

$$Y(pN+i) = Y_p(i)$$

$$= \begin{cases} 0, & k \neq pN+i \\ N\sum_{i=0}^{N-1} a_i e^{-j\frac{2\pi}{N^2}(pN+i)i}, & k = pN+i \end{cases} \quad i, p = 0,1,\cdots,N-1. \tag{4.9}$$

Equation (4.9) indicates that each data symbol a_i is modulated on $p = N$ subcarriers, and the total spectrum of the signal is spread N times. Figure 4.9 shows the spectrum of the ISS-OFDM signal with subcarrier number $N = 4$. In this case, the signal spectrum of ISS-OFDM is spread 4 times and contains 4 subbands. Each of the subbands contains the whole data information of the baseband signal.

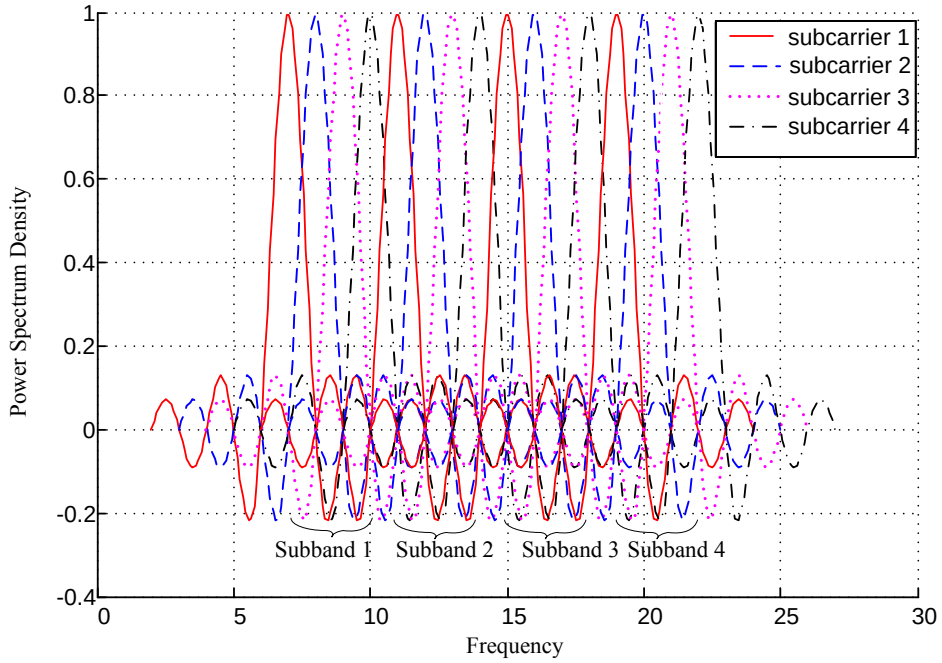

Figure 4.9 Spectrum of ISS-OFDM symbol with subcarrier number $N = 4$.

4.6 Cyclic Prefix and ISI

After generation of each ISS-OFDM symbol, the cyclic prefix is inserted to the ISS-OFDM symbol. The cyclic prefix is a very crucial part which is used to combat the ISI and inter channel interference (ICI) introduced by multipath fading channels through which the signal is propagated.

4.6.1 Cyclic Prefix Insertion

As we discussed above, the main problem of ISI is from the energy leaking from one symbol to the other neighbor symbol. Our objective is to confine one symbol energy from leaking. Cyclic prefix insertion can effectively solve the problem.

Similar to the other normal OFDM systems, cyclic prefix (CP) is inserted in front of the OFDM symbols to reduce ISI. The basic idea of the cyclic prefix is to replicate

the part of the OFDM symbol in the time domain from the back to the front to create the guard period. The purpose of the CP insertion is to confine the energy of one symbol in its own range, without or with less leaking into others. The simplest way to control the leaking energy into others is to slow down the symbol rate so that a symbol time is bigger than the delay spread time. The CP insertion is another way to extend the symbol duration (the OFDM technique has already extended the symbol duration by using IFFT). The duration of the cyclic prefix T_g is selected longer than the worst-case channel delay spread $\tau_{\max}$ of the target multipath environment, i.e.,

$$\tau_{\max} \le T_g .$$

In order to guard the OFDM symbols and make sure the receiving end receives the OFDM symbols with the lowest error probability, the selection of the guard period T_g must consider the sampling starting position T_x, so that the sampling starting position must be chose within the cyclic prefix. That is:

$$\tau_{\max} \le T_x \le T_g .$$

The selection of the guard period T_g in the ISS-OFDM design is chosen as ¼ of the length of the ISS-OFDM symbol. Since the length of the ISS-OFDM symbol is N^2, the length of the cyclic prefix is $\frac{N^2}{4}$. After cyclic prefix insertion, the length of the ISS-OFDM symbol increases to $N^2 + \frac{N^2}{4}$. In the computer simulation on the length of the cyclic prefix, we tried several different values for the length of the cyclic prefix. We found that when the length of the cyclic prefix is chosen as $\frac{1}{4}$ of the ISS-OFDM symbol length, the previous symbols will only have effect over samples within $[0, \tau_{\max}]$, and the ISI effects can be effectively overcome.

It is seen from Figure 4.10 that the sampling period starting from T_x will encompass the contribution from all the multipath components. Due to the insertion of cyclic prefix, the symbol rate is slowed down and the symbol energy is confined in its own range. Therefore, ISI is released greatly.

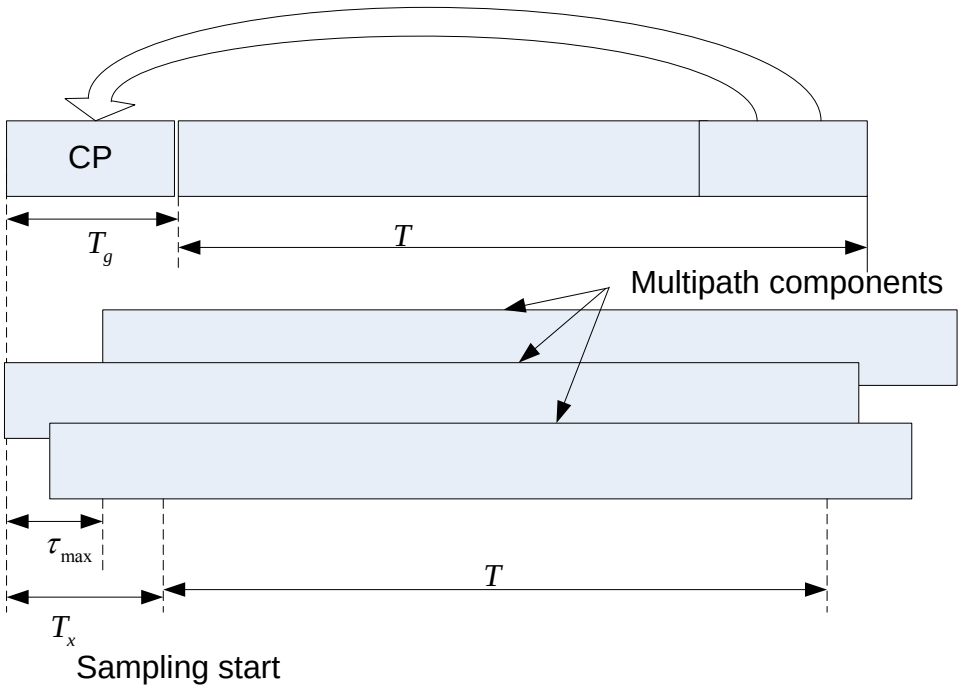

Figure 4.10 Cyclic prefix insertion.

4.6.2 Pulse Shaping

A pulse shaping technique is employed to further reduce ISI. In the simulation of the ISS-OFDM transmitted signal, pulse shaping is implemented by using a pulse that is shaped like a Sinc function. We employ a pair of square root raised cosine filters to produce a cosine signal. This signal waveform shape can keep the symbol from interfering in such a way that they do not affect the amplitude at the sampling slots (slicing instant), and it is suitable for channel transmission and reception. The secret lies in the digital demodulation process used. At the receiver, when the timing pulse slices the received signal into samples to determine the value of the signal at an instant, the sample values only depend on the values of the sampling instant. It does not matter what the signal looks like before or after the sampling instant. To satisfy the requirements of the signal waveform, the best choice is to adopt the Sinc function which can be realized by employing a square root raised cosine filter.

We adopt the cosine roll-off transfer function which is achieved by using identical square root raised cosine filters at the transmitter and the receiver [95]

$$p(n)=\begin{cases}\dfrac{\sin(\pi\dfrac{n}{T_c}(1-\beta))+4\beta\dfrac{n}{T_c}\cos\left(\pi\dfrac{n}{T_c}(1+\beta)\right)}{\pi\dfrac{n}{T_c}\left(1-(4\beta\dfrac{n}{T_c})^2\right)}, & n\neq 0\\ 1-\beta+\dfrac{4\beta}{\pi}, & n=0\end{cases} \tag{4.10}$$

where T_c is the inverse of the sampling rate and β is the roll-off coefficient which is set to be 0.22. The impulse response of the filter in Equation (4.10) is shown in Figure 4.14. This figure displays the impulse response of the adaptive filter with a breakpoint at the peak of the waveform of the Sinc function. The breakpoint is indicated with a circle at the peak of the waveform.

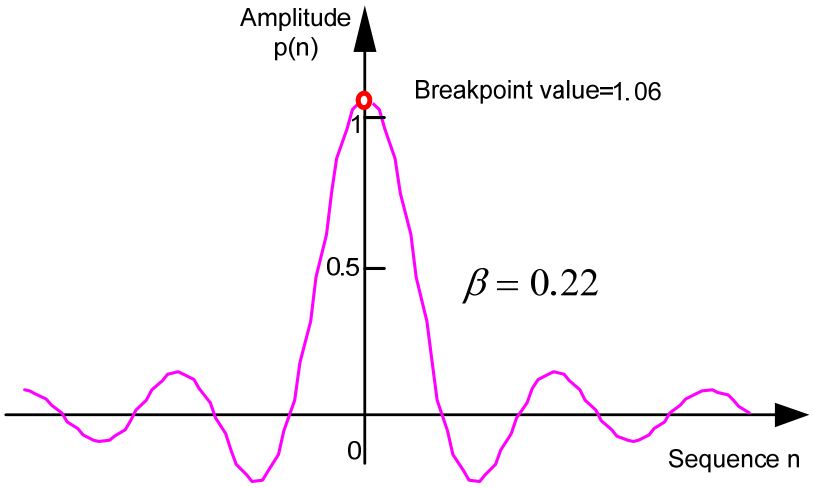

Figure 4.11 Impulse response of the adaptive filter with a breakpoint.

After pulse shaping, the output signal of the shaping filter is the convolution between the signal and the impulse response of the filter, and can be expressed as follows:

$$y_o(n)=y(n)\otimes p(n), \tag{4.11}$$

where $y_o(n)$ denotes the pulse shaping filtered signal, $y(n)$ is the interleaved multiple subband signal and $p(n)$ is the impulse response of the pulse shaping filter.

Substituting $y(n)$ from Equation (4.5) and $p(n)$ from Equation (4.10) into Equation (4.11), we have:

$$y_o(n) = y(n) \otimes p(n)$$

$$= \frac{\sin(\pi \frac{n}{T_c}(1-\beta)) + 4\beta \frac{n}{T_c} \cos\left(\pi \frac{n}{T_c}(1+\beta)\right)}{\pi \frac{n}{T_c}\left(1-(4\beta \frac{n}{T_c})^2\right)} \otimes y(n). \qquad (4.12)$$

According to Equation (4.12), if the transmit signal sequence is 1 1 0 0 1 0 1 1, we can draw the impulse response of the pulse shaping filter as indicated in Figure 4.15. In this figure, the thick black curve denotes the actual transmitted signal, which is the sum of all the pulses. We can see that each signal bit is transformed into a sinc like pulse. Each of the pulses is centered within its respective bit period.

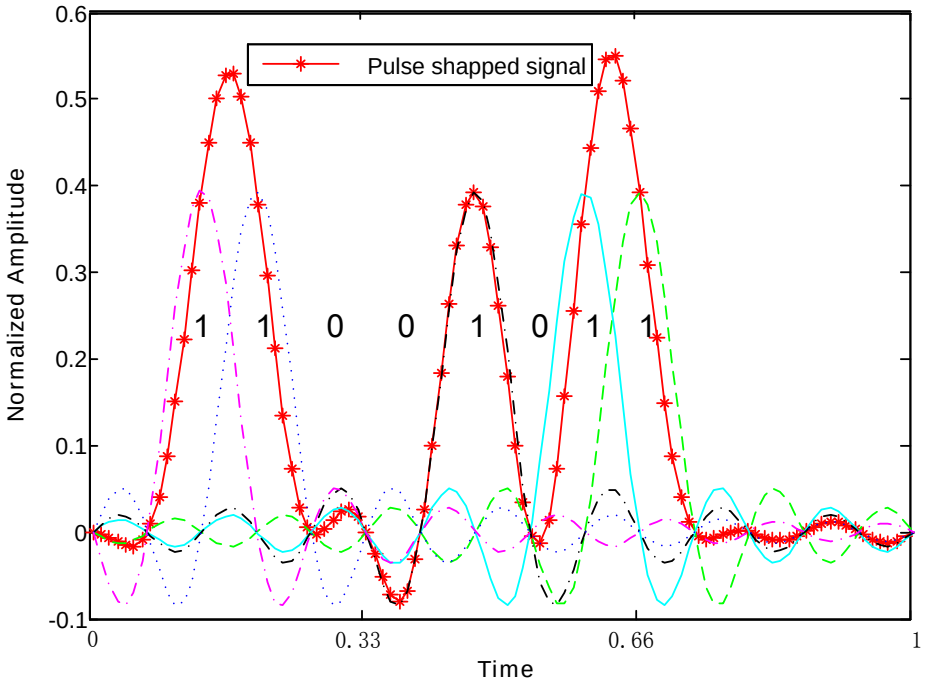

Figure 4.12 Pulse shaping signal.

In the ISS-OFDM system, the transmitter filter and receiver filter are used in a pair of root raised cosine filters, so that the total filtering effect is that of a raised cosine filter. The advantage is that if the transmit side filter is stimulated by an impulse, then the receive side filter is forced to filter an impulse shape that is identical to its own impulse response, thereby setting up a matched filter and maximizing the signal to noise ratio while at the same time minimizing ISI. Transmitted signal spectrum bandwidth can be adjusted by designing the filter pass band according to different system requirements.

4.7 Multiple Subband Signal

After pulse shaping, the transmitted ISS-OFDM signal has a wide bandwidth. If the bandwidth of the pulse shaping filter is designed to equal to the bandwidth of the ISS-OFDM signal frequency band, the transmitted signal has N subbands and each of the subbands consists of N subcarriers.

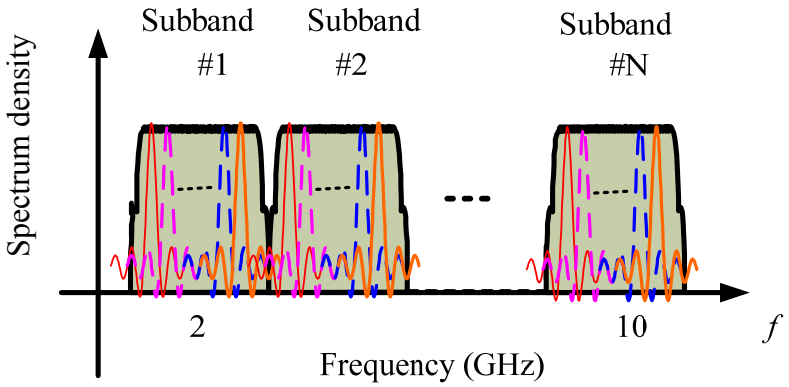

Figure 4.13 Spectrum of ISS-OFDM signal.

If the bandwidth of the filter is designed to be equivalent to M out of N ($M \le N, N$ is the number of subcarriers of the base band signal) subbands of the ISS-OFDM spread spectrum signal, only M subbands of the ISS-OFDM signal are transmitted, or only M subbands of the N subband ISS-OFDM signal are received, and the transmitted information will be recovered according to the M subbands. In

the extreme case, if the filter pass band is equal to one subband of the ISS-OFDM signal, the ISS-OFDM system is equivalent to the conventional OFDM system.

The transmitted ISS-OFDM signal in the time domain is the sum of all individual root raised cosine signals for each sample. The transmitted ISS-OFDM signal in the time domain is presented in Figure 4.14 as follows.

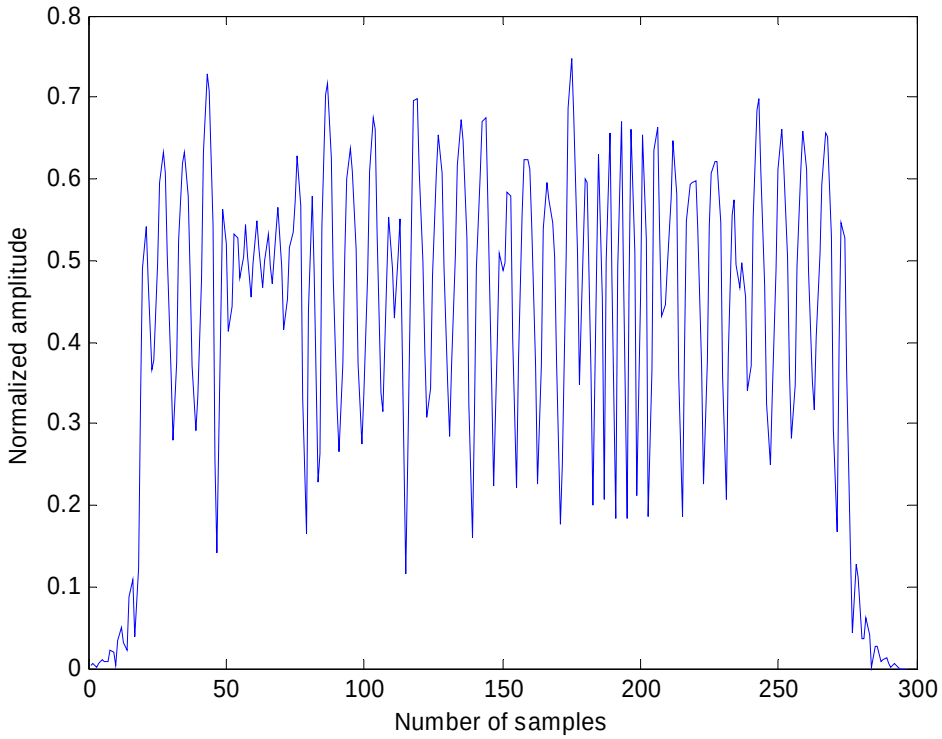

Figure 4.14 Transmitted ISS-OFDM signal in one symbol with $N = 8$ in the time domain.

4.8 Summary

In this chapter, we have described the generation process of multiple subband ISS-OFDM signals. This novel multiple subband signal has many unique characteristics. It has frequency diversity and time diversity characteristics. Its signal bandwidth is very flexible, and can be tailored according to different channel bandwidths of different transmission channel environments. In the following sections we will

introduce the algorithms for receiving this kind of multiple subband ISS-OFDM signals by employing a single FFT operation with a long size and by employing parallel multiple FFT operations. Before we talk about the receiver algorithms, we need discuss how the channel impacts on the transmitted ISS-OFDM signal.

Chapter 5

Channel Characterization

5.1 Introduction

In Chapter 3, we have briefly reviewed the channel models commonly used in wireless communication networks. In this chapter, we will discuss the channel characterization and its impacts on the transmitted ISS-OFDM signal.

Signal distortions from the transmission primarily come from two resources. The first is the impacts from the filtering effects of the transmitter, channel and receiver. The second is caused by noise that is produced by a variety of sources, such as galaxy noise, terrestrial noise, amplifier noise and other coexisting users [96, 97]. An unavoidable noise is the thermal motion of electrons in any conducting media. This motion of the electrons causes the noise in amplifiers and circuits which corrupt the transmitted signal. The primary characteristic of thermal noise is Gaussian distribution. That is, its noise amplitudes are distributed according to a normal or Gaussian distribution. The other primary characteristic is that it is white. That is, its power spectral density is flat from frequency zero to 10^{12} Hz. Since thermal noise is the predominant noise in radio communication system, its characteristics of additive,

white and Gaussian distribution (AWGN), are most often used to model the noise in the detection process and in the design of the optimum receiver.

In communications, the AWGN channel model is one in which the only impairment is the linear addition of wideband or white noise with a constant spectral density (expressed as watts per hertz of bandwidth) and a Gaussian distribution of amplitude [98]. The model does not account for the phenomena of fading, frequency selectivity, interference, nonlinearity or dispersion. However, it produces simple, tractable mathematical models which are useful for gaining insight into the underlying behaviour of a system before these other phenomena are considered.

In this chapter, we will discuss the channel characterization including AWGN channels and multipath fading channels, and their impacts on the ISS-OFDM multiple subband signal. Firstly, we discuss the impacts of the AWGN channel on the ISS-OFDM system. Then, the impairments of the multipath fading channel on the transmitted ISS-OFDM signal are analysed. Due to multipath channel fading, transmitted signals are distorted in amplitude and phase, which some times causes severely errors in the received signals. The mutipath fading channel includes the Nakagami-m channel fading model, Lognormal channel model and Rayleigh fading channels.

5.2 AWGN Channel

We assume that there are no attenuations from multipath channel fading and no interference. The signal is propagated only through the AWGN channel. Since the AWGN imposes on the transmitted signals, the received signal after experiencing an AWGN propagation channel can be expressed as:

$$r(t) = y(t) + v(t), \tag{5.1}$$

where $y(t)$ is the transmitted signal and $v(t)$ is the AWGN noise with mean zero and variance σ^2.

AWGN noise, when the signal is transmitted through channels, is imposed on the transmitted signal as denoted in Figure 5.1.

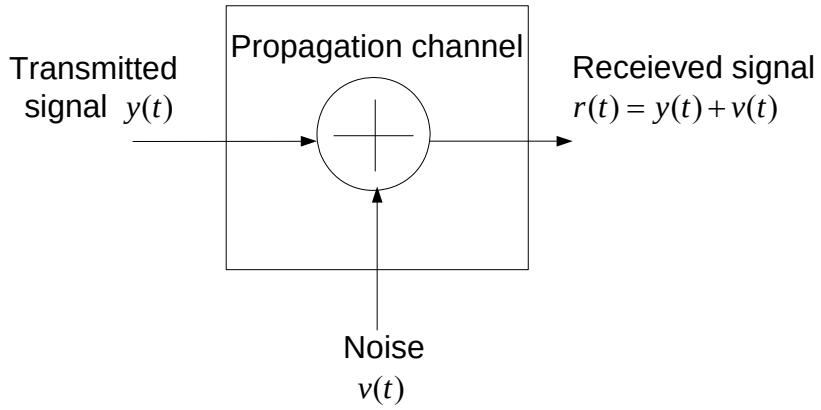

Figure 5.1 Propagation channel model for AWGN noise.

5.3 Fading Channel

5.3.1 Statistical Characteristics

All the changes of channel fading on transmitted signals are unpredictable. It is desirable to get the statistically characteristics of the fading channels. Generally, the transmitted signal can be expressed in the following form:

$$y(t) = \mathrm{Re}[y_l(t)e^{j2\pi f_c t}] \ . \tag{5.2}$$

Since channel fading varies with time, the transmitted signal may have fluctuations in both attenuation and propagation delays with time. After the transmitted signal experiences channel fading, the received signal at the input of the receiver can be expressed as:

$$x(t) = \sum_n \alpha_n(t) y(t - \tau_n(t)), \tag{5.3}$$

where $\tau_n(t)$ is the propagation delay of the transmitted signal for the n^{th} path, t is a time instant, and $\alpha_n(t)$ the attenuation factor for the received signal on the path n^{th}. Substituting the transmitted signal $y(t)$ from Equation (5.2) into Equation (5.3), we can obtained the received signal in the form:

$$\begin{aligned} x(t) &= \sum_n \alpha_n(t) \operatorname{Re}[y_l(t - \tau_n(t)) e^{j2\pi f_c (t - \tau_n(t))}] \\ &= \operatorname{Re}\left(\left[\sum_n \alpha_n(t) e^{-j2\pi f_c \tau_n(t)} y_l(t - \tau_n(t)) \right] e^{j2\pi f_c t} \right). \end{aligned} \tag{5.4}$$

It can be seen from the equation above that the received equivalent low-pass signal is as follows:

$$r_l(t) = \sum_n \alpha_n(t) e^{-j2\pi f_c \tau_n(t)} y_l(t - \tau_n(t)) \ . \tag{5.5}$$

The $r_l(t)$ is the response of the fading channel corresponding to the equivalent low-pass signal $y_l(t - \tau_n(t))$ in the time domain, so the channel response can be written as:

$$h(\tau; t) = \sum_n \alpha_n(t) e^{-j2\pi f_c \tau_n(t)} \delta(\tau - \tau_n(t)).$$

According to Equation (5.5), and letting $y_l(t - \tau_n(t)) = 1$ for all t, we can consider the transmission of the unmodulated carrier. Thus, signal $r_l(t)$ in Equation (5.5) can be simplified as:

$$\begin{aligned} r_l(t) &= \sum_n \alpha_n(t) e^{-j2\pi f_c \tau_n(t)} \\ &= \sum_n \alpha_n(t) e^{-j\theta_n(t)} \ . \end{aligned} \tag{5.6}$$

It can be seen from Equation (5.6) that the received signal $r_l(t)$ changes randomly with the variation of the random variables $\alpha_n(t)$ and $\theta_n(t)$. That is, the received signal $r_l(t)$ can be modeled as a random process. When there are a large number of paths, the central limit theorem can be applied. That is, $r_l(t)$ may be modeled as a complex-valued Gaussian random process. This means that the time-variant impulse response of $h(\tau; t)$ is a complex-valued Gaussian random process in the time

variable t.

Due to the multipath propagation with the channel model embodied in the received signal $r_l(t)$, given in Equation (5.6), signal fading is generated. Channel fading is mainly related to the time variations of the phase factor $\theta_n(t)$. Since the received signal is the sum of the number of mulitpath signals with different phases, the multipath signals with different phases add destructively. In this case, the received fading signal is very small or close to zero. On the other hand, when the multipath signals have the same phases, they add constructively. In consequence the received fading signal is very large. Thus, the amplitude of the received signal varies in a great range due to the time varying multipath characteristics of the channel.

If the impulse response $h(\tau;t)$ of the multipath fading channel is modeled as a zero-mean complex-valued Gaussian process, the envelope $|h(\tau;t)|$ at any time interval t has a Rayleigh distribution, and the channel is a Rayleigh fading channel.

5.3.2 Channel Models

There are many kinds of channel models, including Nakagami-m distribution, Lognormal distribution and Rayleigh distribution [67, 99].

The Nakagmi-m distribution, one of the channel models, is a two-parameter distribution, involving parameter m and the second moment $\Omega = E\left(R^2\right)$. This distribution provides more accuracy and flexibility in matching the signal statistics. The Nakagami-m distribution can be used to model fading channel conditions that are either more or less severe than the Rayleigh distribution. It has been shown that the Nakagami-m distribution is the best fit for data signals received in urban radio multipath channels. Together with the lognormal channel model, Nakagami-m channel model can be also used to model the body area propagation channel, and it can model energy fluctuations due to the movements of some parts of the body. As a special case of Nakagmi-m when m =1, the Rayleigh distribution is the most

common used fading channel model. It can be used in modeling non line-of-sight channel propagations. In the following, we discuss the impacts of the Rayleigh distribution model on the ISS-OFDM signal.

We assume that the ISS-OFDM signal $y(t)$ is transmitted over a fading channel, and let $Y(f)$ denote its frequency components. If the channel impulse response is $h(\tau,t)$, after the channel propagation, the received signal $r(t)$ in Equation (5.1) can be expressed as:

$$r(t) = y(t) \otimes h(\tau,t) + v(t). \tag{5.7}$$

If we exclude the noise effect, Equation (5.7) can be simplified as:

$$r(t) = y(t) \otimes h(\tau;t) = \int_{-\infty}^{\infty} h(\tau;t) y(t-\tau) d\tau$$

$$= \int_{-\infty}^{\infty} H(f;t) Y(f) e^{j2\pi ft} df \tag{5.8}$$

where $H(f;t)$ is the frequency response of the channel impulse response. According to the channel fading characteristics, by choosing different parameters in Equation (5.8), we can derive the expressions for a frequency non-selective fading channel and for a frequency selective fading channel.

5.3.3 Frequency Non-Selective Fading Channels

We assume that the ISS-OFDM signal is transmitted over a frequency non-selective fading channel. In this case, bandwidth B of the transmitted signal is much smaller than the channel coherence bandwidth Δf. That is, all the frequency components in the transmitted ISS-OFDM signal suffer from the same attenuations and phase shifts. It implies that within the bandwidth occupied by transmitted signal $Y(f)$, the time variant variable transfer function $H(f;t)$ is a constant since the frequency content

of the transmitted signal $Y(f)$ concentrates in the vicinity of $f = 0$, $Y(0)$, and $H(f;t) = H(0;t)$. Therefore, for a frequency non selective fading channel Equation (5.8) can be simplified as follows:

$$r(t) = \int_{-\infty}^{\infty} H(0;t)Y(0)e^{j2\pi ft}df = H(0;t)y(t). \quad (5.9)$$

Equation (5.9) indicates that the faded signal is simply the multiplication between the transmitted signal and a complex-valued random process $H(0;t)$ where $H(0;t)$ is expressed as:

$$H(0;t) = \alpha(t)\,\mathrm{e}^{-j\phi(t)}. \quad (5.10)$$

When there are a large number of scatters in a multipath fading channel that contribute to the received signal, according to the central limit theorem, the channel fading impulse response $H(0;t)$ can be viewed as zero mean and complex-valued Gaussian random process and it has the following form . In this case, the envelope $\alpha(t)$ of the channel impulse response has a Rayleigh probability distribution at any time instant t and the phase is uniformly distributed in the interval $(-\pi, \pi)$.

5.3.4 Frequency Selective Channels

In ISS-OFDM systems, the transmitted ISS-OFDM signal spectrum is spread greatly by using spread modulation and the interleaver as discussed in Chapter 4. Then the signal is transmitted over frequency selective fading channels. The probability that the signal bandwidth W is greater than the coherence bandwidth $(\Delta f)_c$ is greatly increased. That is,

$$W \geq (\Delta f)_c. \quad (5.11)$$

In this case, the channel is a frequency selective fading channel. The received signal is the signal as expressed in Equation (5.11).

From Equation (5.11) we can see that when the signal is transmitted over the multipath fading channel at the rate $\frac{1}{T}$, where T is the signaling interval, the transmitted signal is distorted by the fading channel which is characterized by $H(f;t)$. Since the bandwidth of the transmitted signal is greater than the channel coherence bandwidth as denoted in Equation (5.11), $W \geq (\Delta f)_c$, signal $Y(f)$ is subject to the different gains and phase shifts across the whole band. That is to say, the signal spectrum is selectively distorted due to channel attenuations at different frequency intervals. Under this condition, the multipath components in the received signal are resolvable with a reSolution In time delay of $\frac{1}{W}$. Thus, the frequency selectivity can be modeled as a tapped delay line filter with time variant tap coefficients. In Chapter 6 and 7 we will illustrate that the resolvable components can be combined by using a maximal ratio combiner after the components are equalized.

5.4 Faded Multiple Subband Signal

The channel fading profile obeys the Rayleigh distribution at different time instants. According to the Rayleigh channel model in Equation (5.9), we can draw the multiple subband signal after Rayleigh channel fading as shown in Figure (5.2).

Due to the effects of frequency selective channel fading on the multiple subband signal, some of the subcarriers or subchannels are faded and each of the subchannels has different attenuation at different time instants.

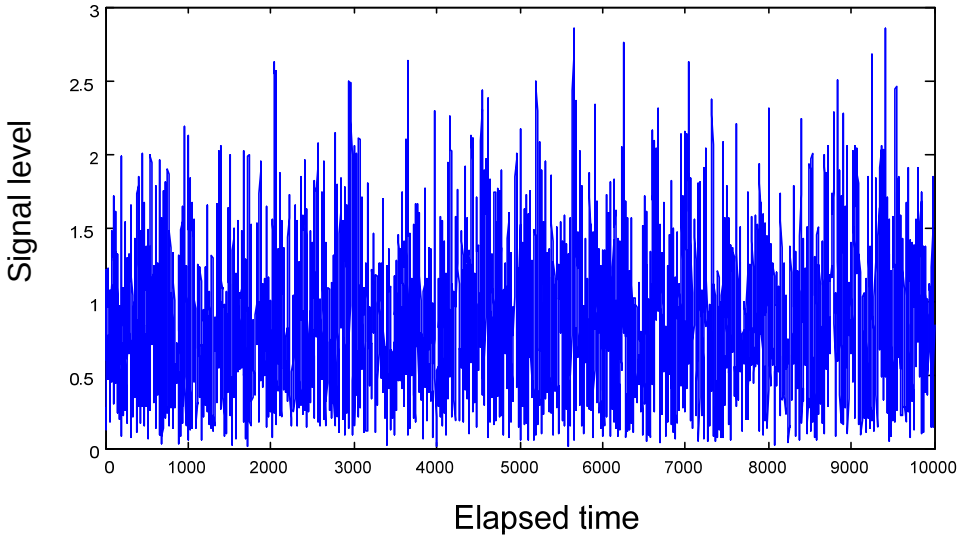

Figure 5.2 Multiple subband signal after Rayleigh fading.

Let the number of subcarriers $N = 4$. The received signal after channel fading is illustrated in Figure 5.3. It can be seen from Figure 5.3 that due to frequency-selective channel fading, different subcarriers of the received ISS-OFDM multiple subband signal have different attenuations.

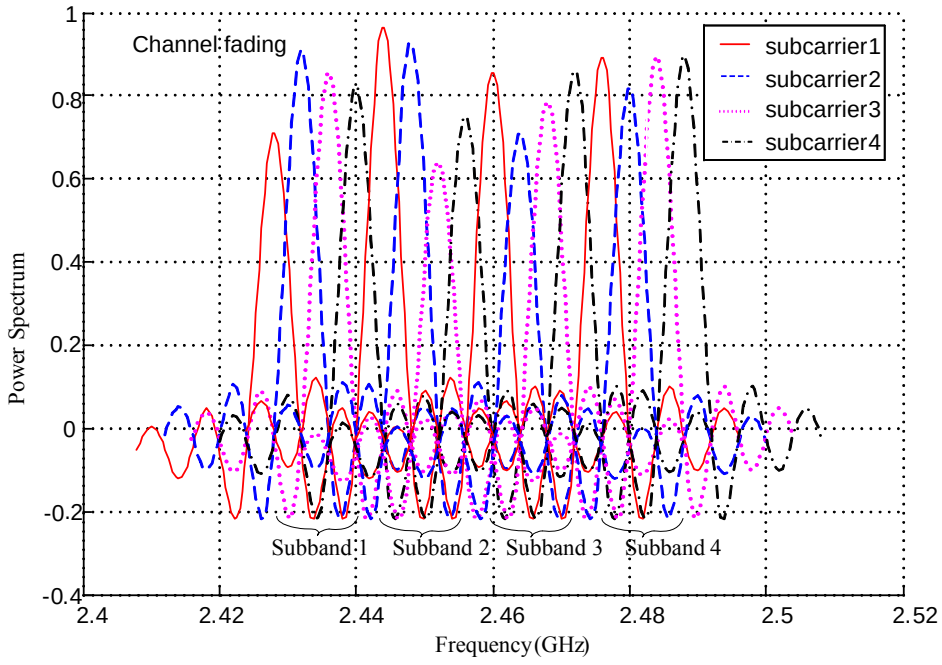

Figure 5.3 Channel fading effects on subbands when subcarrier number $N = 4$.

For finding out the statistical characteristics of the Rayleigh channel, we use a probing pulse which approximates a delta function at the transmitter to experience the Rayleigh channel over a relatively long period of time. We observe that the power delay profile of the Rayleigh channel over a long period of time is approximately flat. Thus, for simplicity of the simulation process of channel fading in our channel simulation, we set the power delay profile of the channel as flat.

In order to realize the frequency domain analysis and computation of the received multiple subband ISS-OFDM signal, the corresponding frequency response of the fading channel (excluding noise and interference) can be achieved by performing the DFT operations with ISS-OFDM of length N^2. That is:

$$H(k) = DFT(h(n)).$$

This frequency domain response $H(k)$ is significant for the theoretical operation of demodulation of the received signal, which will be discussed in the next chapter on receiver algorithms.

5.5 Interference

Interference can be caused by many sources such as another device from a different system in the same area, other devices in the neighboring systems, or other base stations working in the same frequency band. Interference is a major limiting factor to coexistence between multiple systems in wireless communication. Different interference from different sources may cause different impairments. On a voice channel, interference may cause crosstalk. On a control channel, interference may lead to missed calls or blocked calls. In urban areas, interference may be more severe due to the raised RF noise floor caused by the overload of subscribers. Many based stations from different providers may be in close proximity to each other and try to cover as many customers as possible.

There are two types of interference sources, one is co-channel interference or coexistence interference. Another one is from the adjacent channels. Controlling the effects generated from an interfering signal within the co-channels is difficult due to the random propagation effects. It is more difficult to control the effects from out of band users. In our system design, we do not consider interference from the adjacent channels. It is assumed that there is only co-channel interference. Our purpose is to avoid the effects of co-channel interference.

Unlike thermal noise which can be overcome by increasing the SNR of the transmitted signal, co-channel interference can not be combated by simply increasing the carrier power of a transmitter. This is because increasing the transmitter carrier power means that the interference to neighboring co-channel systems will also be increased. Thus, one way to minimize interference is that the co-channel systems and devices must be physically separated by a minimum distance to provide sufficient isolation, however this method limits the location range of coexisting systems. To suppress interference and maintain system coexistence, the best way, we think, is to avoid interference from outside of the system. In the design of our ISS-OFDM system, we propose a multiple subband selection transmission method which can efficiently avoid interference from the co-channels of the different systems, and improve system performance of coexisting systems. This multiple subband selection transmission method will be discussed in Chapter 7 on system coexistence performance.

5.6 Summary

In this chapter, we discussed the models of the AWGN channel and fading channels, and their impairments on the ISS-OFDM signal.

The AWGN channel and multipath fading channels are discussed respectively. The purpose is to learn the potential performance of ISS-OFDM by comparing the system performance in both channel types. System performance of ISS-OFDM

experiencing the AWGN channel will be regarded as a reference, when the system performance under multipath fading channels is evaluated.

We also discussed the types, sources, and effects of interference on the ISS-OFDM signal and control methods which may be used for achieving interference thresholds to be used to select multiple subbands according to the interference level.

Chapter 6

Reception of Multiple Subband Signal

6.1 Introduction

The reception of the ISS-OFDM multiple subband signal is a reversed process to the generation process of the ISS-OFDM signal, and it demodulates the received signal and recovers the information bit stream. The receiver constitutes of receiver filter, A/D converter, synchronization, demodulation, channel estimation, frequency domain equalization and combining and de-mapping.

In the receiving process, we assume the system between the receiver and transmitter is perfectly synchronized including frame synchronization, carrier synchronization and sample synchronization. Under this assumption, we discuss signal reception and receiver performance.

In this chapter we propose two receiver solutions for signal demodulation according to the received multiple subband signals at the receiver. One Solution Is the algorithm using a single FFT with a long size of N^2; the other is to use several parallel FFTs each with a size of N to demodulate the received signal. For the two

solutions, we produce the mathematical expressions for the demodulated signal respectively. Then we derive the mathematical formulas for calculating the SNR at the output of the detectors. As a result, we can calculate the theoretical values for the system bit error rate (BER) performance. Later, we will consider practical system to obtain the simulated system performance. By comparing theoretical system performance with simulated system performance we can verify the correctness and validity of the proposed algorithms.

6.2 Receiver Signal Filtering

At the receiving end, the received signal is firstly filtered by using a root raised cosine filter, which has been discussed in Chapter 4. The receiver filter in a conventional system is used in pairs with the transmitter filter, so that the total effect of filtering is that of a raised cosine filter [100]. In our system, the receiver filter is designed to be reconfigurable. Since the transmitted signal consists of multiple subbands, each of which has the whole transmitted information of the baseband signal, the receiver can obtain the received signal with a different number of subbands by filtering the received signal using a filter with different parameters. By adjusting the parameters of the filter according to the different radio scenarios, the bandwidth of the signal used for demodulation can have different number of subbands.

Figure 6.1 shows the adaptive filter impulse response and frequency response under different filter parameters reconfigured according to the channel environments.

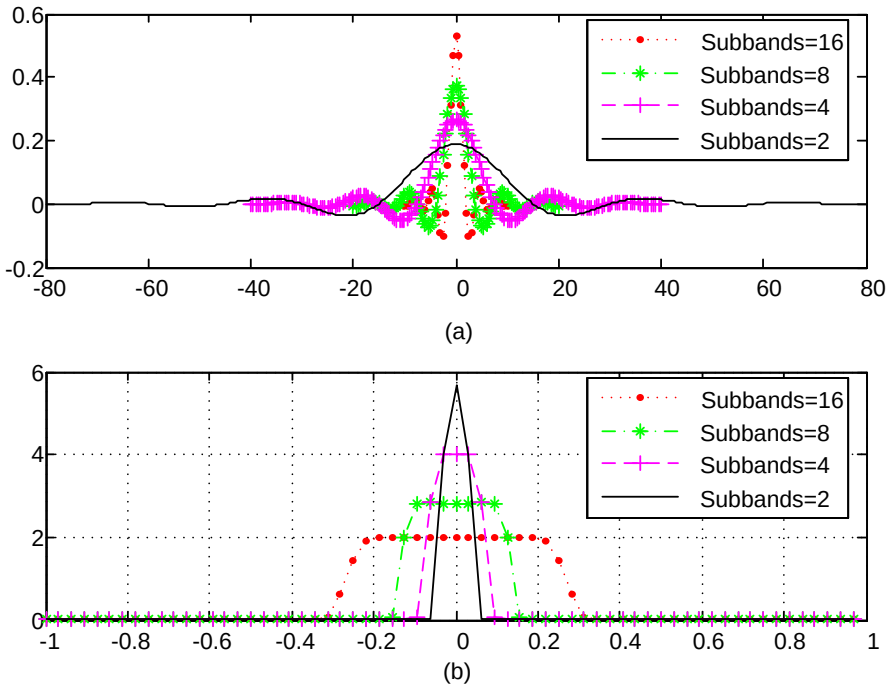

Figure 6.1 (a) Filter impulse responses with different subband configurations; (b) Filter passbands with different subband configurations.

After filtering, we can see that the received signals can be in different forms with a different number of subbands. Each subband contains the whole transmission information. Figure 6.2 indicates the signal spectrum before the receiver filter and after the receiver filter. The received signal contains N subbands, where N is the number of the subbands of the transmitted signal. If the pass band filter is configured to be equivalent to the bandwidth of 6 subbands of the transmitted signal as displayed in the green shadow, the signal used for demodulation has 6 subbands. The others will be filtered because of interference on the other subands, or because of channel bandwidth limitations. The filtered signal can be used to recover transmitted information, and receiver performance can satisfy different requirements in practical application scenarios.

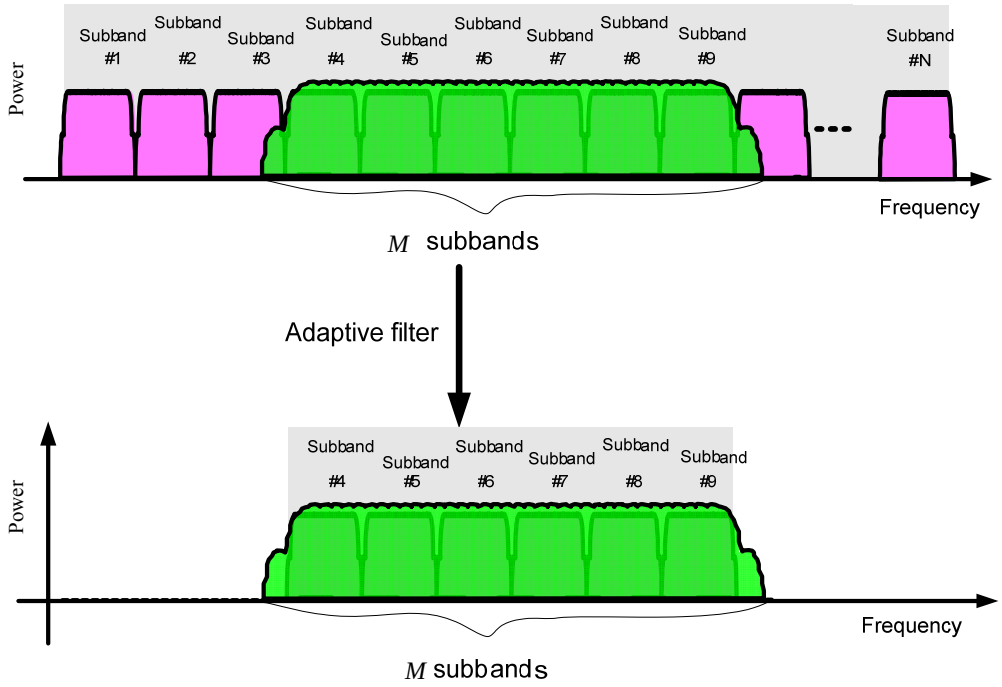

Figure 6.2 Adaptive filtering at receiver.

In the process of filtering, since the received signal used for recovering the information contains a smaller number of the subbands than the transmitted signal, this leads to a problem of signal energy loss. Some portions of signal energy are lost. In consequence, it causes the reduction in power efficiency. Thus, this problem requires that we must take some trade-off in the selection of the subband number. In chapter 10 on system coexistence we will discuss the trade-off strategy by which the subband selection algorithm is more practical and efficient.

After filtering, A/D conversion and synchronization will be performed. Since synchronization is not the focus of this thesis, as discussed above, we assume that synchronization between the transmitter and receiver is perfect. Now the next step is to remove the cyclic prefix and perform demodulation.

6.3 Cyclic Prefix Removal

The cyclic prefix removal is exactly the inverse process to the cyclic prefix insertion at the transmitter as shown in Figure 6.3. In this figure the terms T_g , T_x and T have the same meanings as in Figure 4.11. Since ¼ samples from the back of the ISS-OFDM symbol is added to each ISS-OFDM symbol at the transmitter, at the receiver the cyclic prefix of the same length in front of the ISS-OFDM symbol is removed, so that the ISS-OFDM symbol at the receiver has the same samples as the symbol before the cyclic prefix addition.

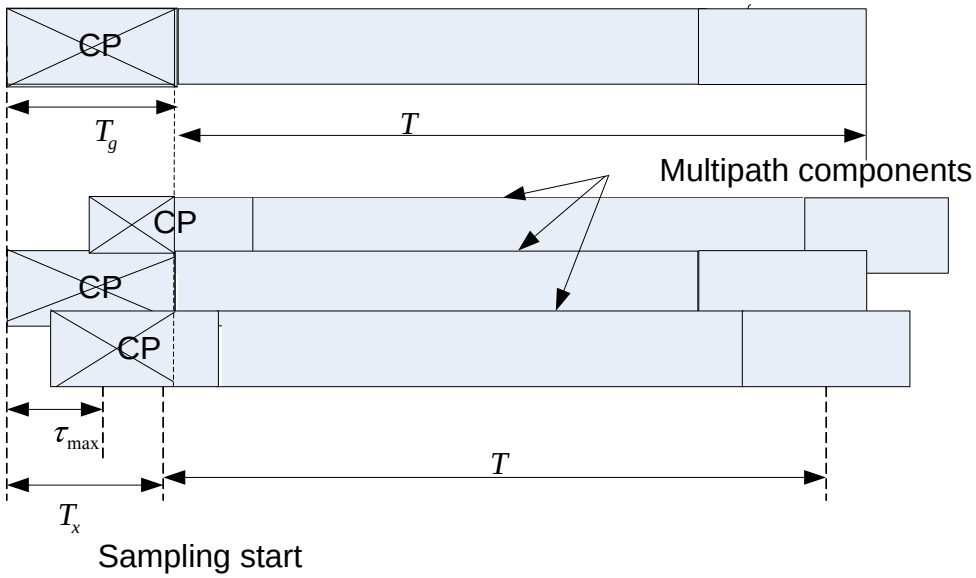

Figure 6.3 Cyclic prefix removal.

Since synchronization between the transmitter and receiver is perfectly implemented, the sampling starts from the first sample of the received signal. If one ISS-OFDM symbol time duration is T , for the recover information without loss of information, the sampling interval is $t = \frac{1}{T}$ according to the Nyquist theorem.

6.4 Deinterleaver

Deinterleaver is to retrieve the order of the data sequence before the interleaving at the transmitter. As we discussed in Chapter 4 on the multiple subband selection at

the transmitter, the interleaver algorithms can be pseudo random interleaving, convolutional interleaving, and periodical interleaving. Corresponding to the periodical interleaving algorithms used at the transmitter end, the deinterlever must be implemented by using the corresponding periodical algorithms [101, 102]. For example, assume there is a periodically interleaved data sequence as follows: $a_0 b_0 \cdots c_0 a_1 b_1 \cdots c_1 a_{N-1} b_{N-1} \cdots c_{N-1}$. The deinterleaver is to retrieve the periodical order of the serial sequence as $a_0 a_1 \cdots a_{N-1} b_0 b_1 \cdots b_{N-1} c_0 c_1 \cdots c_{N-1}$, which is shown in Figure 6.4.

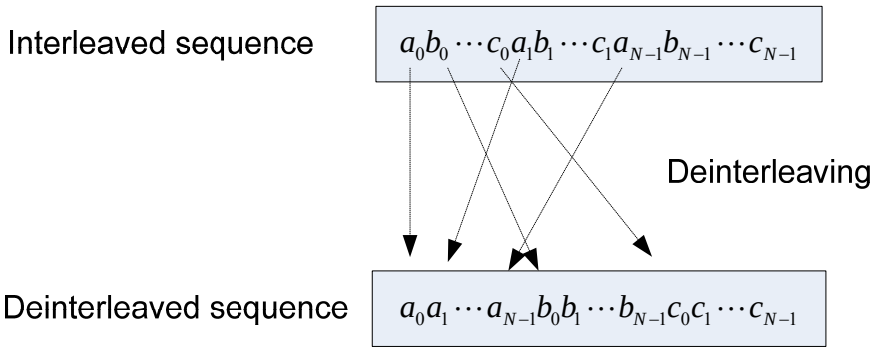

Figure 6.4 The principle of deinterleaver.

In the deinterleaving of ISS-OFDM, the de-interleaver is implemented by using a shift register. No matter what kind of interleaving algorithm is employed, the deinterleaving algorithm must be exactly identical to the algorithm used by the interleaving algorithm. The information on the interleaving process, which is called side information, is stored and transmitted to the receiver with the data information. The side information is decoded and used for deinterleaving. The periodically de-interleaving process corresponding to the interleaving can be illustrated as in Figure 6.5.

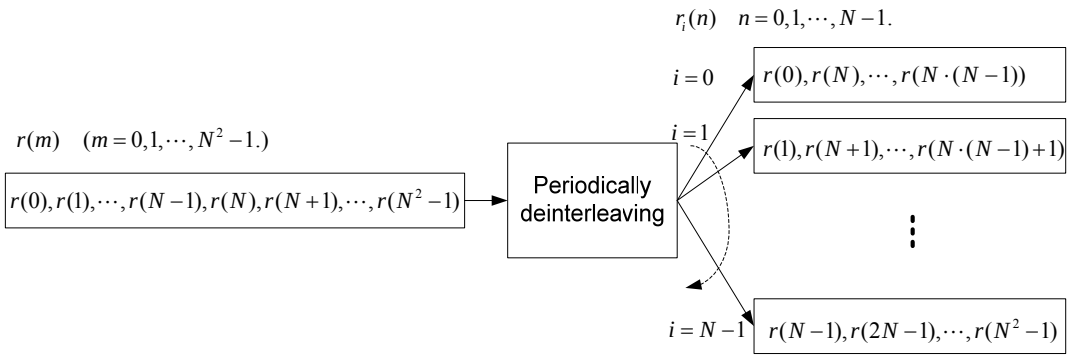

Figure 6.5 Implementation of periodical deinterleaver.

It can be seen that the received time domain signal sequence $r(m)$, $m = 0,1,\cdots,N^2-1$, at the input of the de-interleaver, has N^2 data samples, and they are deinterleaved into N streams each of which has N samples. The N streams samples can be represented as one $N \times N$ matrix with element $r_i(n)$. Each row of the matrix is simply constituted by taking one of every N samples in the signal sequence $r(m)$. Thus, the N data streams can be expressed from $r(m)$ as follows:

$$\begin{pmatrix} r(0) & r(N),\cdots,r(N\cdot(N-1)) \\ r(1) & r(N+1),\cdots,r(N\cdot(N-1)+1) \\ & \cdots \\ r(N-1), & r(2N-1),\cdots,r(N^2-1) \end{pmatrix}.$$

That is,

$$r_i(n) = r(nN+i) = r(m), \tag{6.1}$$

where $m = nN+i, \quad i = 0,1,\cdots N-1, \ n = 0,1,\cdots,N-1.$

6.5 Solution I: Serial Demodulation Using One FFT

After the cyclic prefix removal and deinterleaving, the following steps are to design the demodulation algorithms. In the ISS-OFDM system, two demodulation solutions are proposed. One Solution Is the serial demodulation which uses one single FFT operation of size N^2 to demodulate the signal. We call this serial demodulation. The second Solution Is parallel demodulation by employing a multiple FFTs operation. In this section, we will consider the design of the serial demodulation solution.

6.5.1 Receiver Structure of Serial Demodulation

Figure 6.6 shows the receiver structure for serial demodulation, which is realized by using one FFT operation of size N^2. After CP removal, the serial data stream in the block of N^2 is demodulated by using a single FFT operation. The output signal of the demodulator is equalized in parallel in the frequency domain, and then combined by using a maximal ratio combining (MRC) technique. The combined results are the decision variables which can be used for data detection, BER system performance computation and system performance analysis.

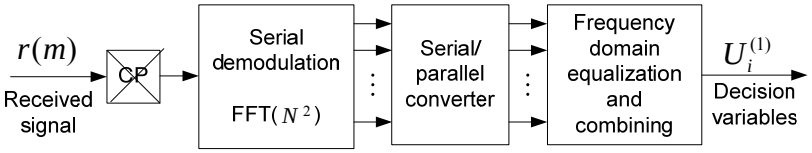

Figure 6.6 Serial demodulation and equalization.

6.5.2 Demodulation

The demodulation using a single FFT at the receiver is the inverse process of IFFT modulation at the transmitter. The signal at the input of FFT demodulation is a time domain signal which has N^2 samples. By performing the FFT operation, we can

obtain the demodulated signal. If the received signal at the input of the FFT demodulator is denoted as $r(m)$, the output of the demodulator is expressed as:

$$R(k) = FFT(r(m))$$

where $r(m) = y(m) \otimes h(m) + v(m) + j(m)$.

We start the derivation process from Equation 4.5, which shows the expression for the transmitted signal $y(m)$. Recall $y(m)$ from Equation 4.5, the m^{th} sample in the ISS-OFDM symbol, denoted by $y(m)$, $m = 0,1,\cdots,N^2-1$, can be mathematically written as follows:

$$y(m) = \sum_{i=1}^{N}\sum_{n}^{N} y_i(n)\delta\left[m - i - nN\right], \qquad n,i = 0,1,\cdots,N-1.$$

where $\delta\left[m-nN-i\right] = \begin{cases} 1, & \text{for } m = nN+i \\ 0, & \text{for } m \neq nN+i. \end{cases}$ is the unit impulse. If periodical interleaving is performed, that is, taking out $y(m)$ for every $m = nN+i$, $y(m)$ can be simplified in the form:

$$y(m) = y(nN+i) = y_i(n), \qquad m = nN+i. \tag{6.2}$$

Recall Equation (4.4), $y(m)$ has the form:

$$y(m) = y_i(n) = a_i e^{j2\pi f_i t} = a_i e^{j2\pi ni/N}, \tag{6.3}$$

where $y_i(n)$ is the modulated symbol on the i^{th} subcarrier and n^{th} time.

By using the FFT operation, the frequency domain transmitted signal can be written as:

$$Y(k) = FFT(y(m)) = FFT(y(nN+i))$$

$$= \sum_{nN+i=0}^{N^2-1} y_i(n) e^{-j\frac{2\pi}{N^2}(nN+i)k}. \tag{6.4}$$

Substituting $y_i(n)$ in Equation (6.3) into Equation (6.4), $Y(k)$ is further derived as follows,

$$Y(k) = N\sum_{i=0}^{N-1} a_i e^{-j\frac{2\pi}{N^2}ki} \underbrace{\frac{1}{N}\sum_{n=0}^{N-1} e^{-j\frac{2\pi}{N}(k-i)n}}_{\delta((k-i)_N)} \quad .$$

That is

$$Y(k) = N\sum_{i=0}^{N-1} a_i e^{-j\frac{2\pi}{N^2}ki} \cdot \delta((k-i)_N) . \tag{6.5}$$

Substituting $Y(k)$ from Equation (6.5) into Equation (4.5) ($R(k) = H(k)\cdot Y(k) + V(k)$), the output of the demodulator can be rewritten as follows:

$$R(k) = N\sum_{i=0}^{N-1} a_i e^{-j\frac{2\pi}{N^2}ki} H(k)\cdot\delta((k-i)_N) + V(k), \qquad k = 0,1,\cdots,N^2-1. \tag{6.6}$$

It can be observed from Equation (6.6) that the sample at the i^{th} position is repeated in every N samples of the N^2 samples of $R(k)$. Equation (6.5) also indicates that the energy of each data symbol a_i is distributed on the $\left(pN+i\right)^{\text{th}}$, $p = 0,1,\cdots,N-1$, subcarriers. That means that the energy of a_i is distributed at the position i of each subband with N subcarriers. Each subcarrier has a phase shift, which must be compensated by the equalization in the frequency domain before the signal can be combined. The effect of the equalization and combining is to compensate for the phase shift in the channel and to weight the signal by a factor that is proportional to the signal strength.

6.5.3 Channel Compensation

Based on the analysis above, we can observe that the channel introduces distortion on the transmitted signal. The distortion must be compensated before the transmitted date bits can be recovered.

6.5.3.1 Frequency Domain Equalization

To compensate for the channel distortion, the frequency domain equalizer is used as Figure 6.7.

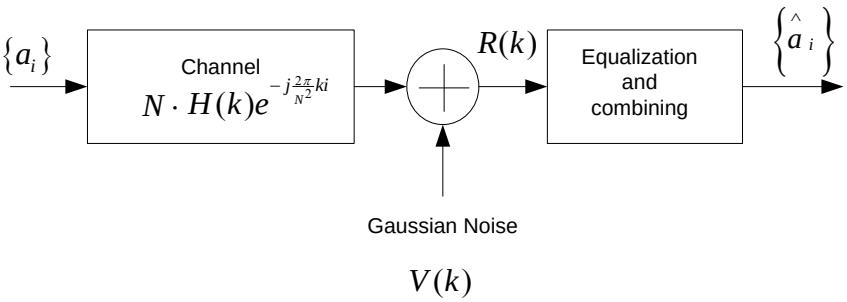

Figure 6.7 Frequency domain equalizer.

According to the received signal and channel models, we can derive the algorithms for computing the estimate $\{\hat{a}_i\}$ at the output of the frequency domain equalizer.

We start the derivation from the output of the demodulator. After demodulation the demodulator output signal in the frequency domain with multipath distortions is given as in Equation (6.6), which is rewritten as follows:

$$R(pN+i) = Na_i C_{i,p}^{(1)} + V(pN+i), \tag{6.7}$$

where

$$C_{i,p}^{(1)} = e^{-j\frac{2\pi}{N^2}(pN+i)i} H(pN+i), \quad p = 0,1,\cdots,N-1 \ , \ i = 0,1,\cdots,N-1. \tag{6.8}$$

From the equation above, it can be seen that $R(pN+i)$ composites of N groups, each group forms one subband which consists of N subcarriers, and each subcarrier consists of the corresponding weighted signal and noise. Generally, we assume that the received signal contains M subbands, $M \le N$, and use the M subbands to demodulate the transmitted signal. The structure of $R(pN+i)$ can be illustrated in Figure 6.8.

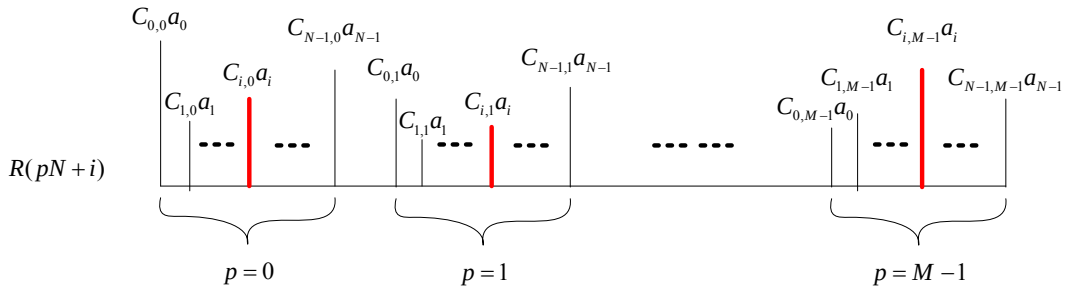

Figure 6.8 The structure of $R(k)$.

The transmitted data symbol a_i, $i=0,1,\cdots,N-1$, can be recovered from $R(pN+i)$, $p=0,1,\cdots,M-1$, which can be expressed in matrix form as follows:

$$\begin{pmatrix} R(i) \\ R(N+i) \\ \vdots \\ R((M-1)N+i) \end{pmatrix} = N \begin{pmatrix} C_{i,0}^{(1)} \\ C_{i,1}^{(1)} \\ \vdots \\ C_{i,M-1}^{(1)} \end{pmatrix} a_i + \begin{pmatrix} V(i) \\ V(N+i) \\ \vdots \\ V((M-1)N+i) \end{pmatrix}.$$

According to the above matrix equation, a minimum mean squared error (MMSE) estimate of a_i can be obtained as follows:

$$\hat{a}_i = \frac{1}{N} \left(C_{i,0}^{(1)*} \quad C_{i,1}^{(1)*} \quad \cdots \quad C_{i,M-1}^{(1)*} \right) \begin{pmatrix} C_{i,0}^{(1)} \\ C_{i,1}^{(1)} \\ \vdots \\ C_{i,M-1}^{(1)} \end{pmatrix} + \frac{1}{SNR} \Bigg)^{-1} \cdot$$

$$\left(C_{i,0}^{(1)*} \quad C_{i,1}^{(1)*} \quad \cdots \quad C_{i,M-1}^{(1)*} \right) \begin{pmatrix} R(i) \\ R(N+i) \\ \vdots \\ R((M-1)N+i) \end{pmatrix}$$

$$= \frac{1}{N} \sum_{q=0}^{M-1} \frac{C_{i,q}^{(1)*}}{\sum_{p=0}^{M-1} \left| C_{i,p}^{(1)} \right|^2 + \frac{1}{SNR}} R(qN+i),$$

where SNR is the signal-to-noise ratio before the MMSE equalization.

To analyze the system BER performance, the normalized MMSE can be expressed as

$$\varepsilon_{\min}^2 = \left(SNR\begin{pmatrix} C_{i,0}^{(1)*} & C_{i,1}^{(1)*} & \cdots & C_{i,M-1}^{(1)*} \end{pmatrix} \begin{pmatrix} C_{i,0}^{(1)} \\ C_{i,1}^{(1)} \\ \vdots \\ C_{i,M-1}^{(1)} \end{pmatrix} + 1 \right)^{-1}$$

$$= \frac{1}{SNR\sum_{p=0}^{M-1}\left|C_{i,p}^{(1)}\right|^2 + 1}.$$

Therefore, the output signal-to-noise ratio after MMSE equalization is

$$\gamma_{out} = \frac{1-\varepsilon_{\min}^2}{\varepsilon_{\min}^2} = \frac{1}{\varepsilon_{\min}^2} - 1 = SNR\sum_{p=0}^{M-1}\left|C_{i,p}^{(1)}\right|^2 .$$

Assuming QPSK modulation for data symbols and making a Gaussian distribution approximation for the intersymbol interference after MMSE equalization, we finally obtain the expression for the average BER using the Q function

$$P_e^{(MMSE)} = E\left(Q\left(\sqrt{\gamma_{out}}\right)\right), \tag{6.9}$$

where $E(\cdot)$ denotes ensemble average over channel coefficients.

6.5.3.2 Maximal Ratio Combining

From Equation (6.7) we see that a data symbol a_i is transmitted on different subcarriers and experiences independent fading. Thus, another effective way to gain frequency diversity is to directly use the maximal ration combining (MRC) technique to collect signal energy from all information bearing subcariers. In this way the system diversity can be made full use of and the best system performance can be achieved.

Similar to the above MMSE equalization, we assume that only M subbands, $M \le N$, are used to recover the transmitted data symbols. The MRC process proceeds as follows. First, we multiply the conjugated channel coefficient $C_{i,p}^{(1)*}$ with the received $R(pN+i)$ to compensate the channel phase shift and weight the

information bearing subcarrier with a gain proportional to the signal strength. Then, all the weighted subcarriers corresponding to the same data symbol a_i are combined to produce the decision variable $U_i^{(1)}$ for the detection of a_i. That is,

$$U_i^{(1)} = \sum_{p=0}^{M-1} C_{i,p}^{(1)*} R(pN+i).$$

To analyze the BER performance of the MRC technique, we substitute $R(pN+i)$ in the above equation with Equation (6.7) and have

$$U_i^{(1)} = N\sum_{p=0}^{M-1}\left|C_{i,p}^{(1)}\right|^2 a_i + \sum_{p=0}^{M-1} C_{i,p}^{(1)*} V(pN+i).$$

The output signal-to-noise ratio after MRC can be obtained as

$$\gamma^{(1)} = \frac{\left(N\sum_{p=0}^{M-1}\left|C_{i,p}^{(1)}\right|^2\right)^2 E\left(\left|a_i\right|^2\right)}{E\left(\left|\sum_{p=0}^{M-1} C_{i,p}^{(1)*} V(pN+i)\right|^2\right)}$$

$$= \frac{\left(\sum_{p=0}^{M-1}\left|C_{i,p}^{(1)}\right|^2\right)^2 N^2 E\left(\left|a_i\right|^2\right)}{\sum_{p=0}^{M-1}\left|C_{i,p}^{(1)}\right|^2 E\left(\left|V(pN+i)\right|^2\right)}$$

$$= \sum_{p=0}^{M-1}\left|C_{i,p}^{(1)}\right|^2 SNR,$$

where $SNR = \frac{N^2 E\left(\left|a_i\right|^2\right)}{E\left(\left|V(pN+i)\right|^2\right)}$ is the signal-to-noise ratio before MRC.

For QPSK modulated data symbols, the average error probability can be therefore written as:

$$P_e^{(MRC)} = E\left(Q\sqrt{\gamma^{(1)}}\right). \qquad (6.10)$$

From Equation (6.9) and Equation (6.10) we see that the MMSE equation and the MRC have the same performance for the serial demodulation.

6.5.3.3 BER Performance Normalization

For diversity performance comparison, the normalized signal-to-noise ratio E_b/N_0 is more often used than SNR. In this section, we briefly discuss the normalization method in our system.

E_b/N_0 is the ratio of bit energy to noise power spectral density, which is used to evaluate the BER performance. Thus, it is desirable to obtain the relation between SNR and E_b/N_0, so that we can obtain the system BER performance as a function of E_b/N_0.

In Figure 6.9, let σ_x^2 and σ_v^2 denote the signal variance, or average signal power, and average noise power, respectively. N is the number of subcarriers used to modulate data symbols. E_s, E_b, N_0 denote QPKS symbol energy, bit energy and noise power spectral density, respectively. M ($M \le N$) denotes the number of subbands of the received signal after the receiver filter. $M = N$ means that all the subbands of the transmitted signal are used to recover the transmission information. Thus, the relation between SNR and E_b/N_0 can be expressed as:

$$SNR = \frac{\sigma_x^2}{\sigma_v^2} = \frac{MN\sigma_x^2}{MN\sigma_v^2} = \frac{MN\sigma_x^2 \cdot T \cdot MN}{MN\sigma_v^2 \cdot T \cdot MN} = \frac{E_s \cdot N}{MN\sigma_v^2 \cdot T \cdot MN}$$

$$= \frac{E_s \cdot N}{N_0 \cdot \frac{1}{T} \cdot T \cdot MN} = \frac{E_s}{N_0 \cdot M} \cdot = \frac{2}{M}\frac{E_b}{N_0} \cdot$$

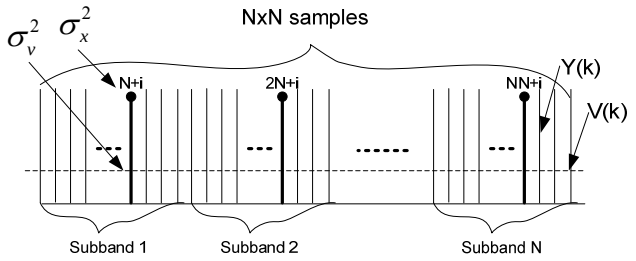

Figure 6.9 SNR normalization.

According to the above relationship between SNR and E_b/N_0, the system BER performance expression in Equation (6.10) can be rewritten as:

$$P_e^{(MRC)} = E\left(Q\left(\sqrt{\sum_{p=0}^{M-1} \left| C_{i,p}^{(1)} \right|^2 \frac{2}{M} \frac{E_b}{N_0}} \right) \right). \tag{6.11}$$

6.6 Solution II: Reception Using Parallel FFTs

The demodulation in Solution I using single FFT is straightforward to realize. However, the computational complexity in Solution I is relatively high.

In order to reduce the complexity, we propose Solution II, a parallel demodulation method by employing multiple FFTs. The parallel demodulation method consists of cyclic prefix removal, deinterleaver, demodulation, and maximum ratio combining. Compared with the serial demodulation, the difference is the number of FFTs employed. In the parallel FFT solution, the demodulation is realized by employing N FFTs operations, rather than a single FFT operation.

6.6.1 Receiver Input Signal

Figure 6.10 shows the receiver structure for Solution II using parallel demodulation, which is realized by using N parallel FFTs, each of which is of size N. We assume that the signal in the time domain at the receiver input is known. To obtain the data vector for each FFT operation, the time domain signal is split into N groups, each group is demodulated by using an FFT operation with the size N.

In order to compensate the channel distortion using frequency domain equalization, we must find out the relationship among each parallel FFT output, the channel coefficient, and the transmitted data symbol. For doing that, the first step is to express the received signal in the time domain at the input of the receiver in terms of the channel frequency response and the transmitted data symbol.

The signal in the time domain at the input of the receiver can be obtained by conducting the IFFT operation of size N^2 on $R(k)$, i.e.,

$$r(m) = IFFT(R(k)) = \frac{1}{N^2}\sum_{k=0}^{N^2-1} R(k)e^{j\frac{2\pi}{N^2}km} . \tag{6.12}$$

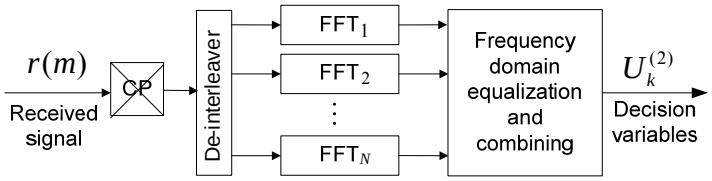

Figure 6.10 Parallel demodulation and combination.

Substituting $R(k)$ from Equation (6.6) into Equation (6.12), the received signal in the time domain $r(m)$ can be rewritten as:

$$r(m) = \frac{1}{N}\sum_{k=0}^{N^2-1}\sum_{i=0}^{N-1} a_i e^{-j\frac{2\pi}{N^2}k(i-m)}\delta((i-k)_N)H(k) + \frac{1}{N^2}\sum_{k=0}^{N^2-1} V(k)e^{j\frac{2\pi}{N^2}km} . \tag{6.13}$$

6.6.2 Parallel Demodulation FFTs

After the time domain signal is received, it is then deinterleaved. The deinterleaved process is exactly the same as the method discussed in Section 6.4.

After the deinterleaver, the signal in the time domain is split into N data streams, each of which can be demodulated using one FFT operation. Thus, to demodulate the $N \times N$ data samples simultaneously, N parallel FFTs, each of size N, are needed. In this way, the demodulation of the received signal is completed by employing N parallel FFT operations. The deinterleaved signals can be written as:

$$r_i(n) = r(nN+i) = r(m), \quad i = 0,1,\cdots N-1,\ n = 0,1,\cdots,N-1.$$

To derive the frequency domain representation of $r_i(n)$, we can perform the FFT operation on $r_i(n)$. The output of the demodulation can be obtained as follows:

$$R_i(k) = \sum_{n=0}^{N-1} r_i(n) e^{-j\frac{2\pi}{N}kn}$$

$$= \sum_{n=0}^{N-1} r(nN+i) e^{-j\frac{2\pi}{N}kn} \quad .$$

Where $k = 0,1,\cdots,N-1$. It must be noted that the definition of k in the above equation is a different variable from that of $R(k)$ in Solution I, in which $k = 0,1,\cdots,N^2-1$.

Substituting $r(m)$ in Equation (6.13) in to the above equation, $R_i(k)$ can be written as follows:

$$R_i(k) = \frac{1}{N}\sum_{n=0}^{N-1}\left[\sum_{k'=0}^{NN-1}\sum_{i'=0}^{N-1} a_{i'} e^{-j\frac{2\pi}{NN}k'(i'-nN-i)}\delta((k'-i')_N)H(k') + \frac{1}{N}\sum_{k'=0}^{NN-1} V(k') e^{j\frac{2\pi}{NN}k'(nN+i)}\right] e^{-j\frac{2\pi}{N}kn}$$

$$= \sum_{k'=0}^{N-1}\sum_{i'=0}^{N-1} a_{i'} e^{j\frac{2\pi}{NN}k'(i-i')}\delta((i'-k')_N)H(k')\underbrace{\frac{1}{N}\sum_{n=0}^{N-1} e^{j\frac{2\pi}{N}(k'-k)n}}_{\delta((k'-k)_N)}$$

$$+ \frac{1}{NN}\sum_{k'=0}^{NN-1} V(k') e^{j\frac{2\pi}{NN}k'i}\underbrace{\frac{1}{N}\sum_{n=0}^{N-1} e^{j\frac{2\pi}{N}(k'-k)n}}_{\delta((k'-k)_N)} .$$

Since $k'-k$ must be integer multiples of N, i.e., $k'-k = qN$, we express $k' = qN+k$, and $R_i(k)$ becomes

$$R_i(k) = \sum_{i'=0}^{N-1} a_{i'} \sum_{k'=0}^{NN-1} H(k') e^{j\frac{2\pi}{NN}k'(i-i')}\delta((i'-k')_N)\underbrace{\delta((k'-k)_N)}_{k'=qN+k}$$

$$+ \frac{1}{N}\sum_{k'=0}^{NN-1} V(k')\underbrace{\delta((k'-k)_N)}_{k'=qN+k} e^{j\frac{2\pi}{NN}k'i}$$

$$= \sum_{i'=0}^{N-1} a_{i'} \sum_{q=0}^{N-1} H(qN+k) e^{-j\frac{2\pi}{NN}(qN+i)(i'-i)}\underbrace{\delta((qN+k-i')_N)}_{i'=k}$$

$$+ \frac{1}{N}\sum_{q=0}^{N-1} V(qN+k) e^{j\frac{2\pi}{NN}(qN+i)i} .$$

Again, since $qN+k-i'$ must be integer multiples of N, we have $i' = k$ and $R_i(k)$ is finally expressed as

$$R_i(k) = a_k \sum_{q=0}^{N-1} H(qN+k) e^{-j\frac{2\pi}{NN}(qN+i)(k-i)} + \frac{1}{N}\sum_{q=0}^{N-1} V(qN+k) e^{j\frac{2\pi}{NN}(qN+k)i}$$

$$= a_k \underbrace{\sum_{q=0}^{N-1} e^{j\frac{2\pi}{N}q(i-k)} H(qN+k) e^{-j\frac{2\pi}{NN}i(k-i)}}_{C_{k,i}^{(2)}} + \underbrace{\frac{1}{N}\sum_{q=0}^{N-1} V(qN+k) e^{j\frac{2\pi}{NN}(qN+k)i}}_{v_{k,i}}$$

$$= a_k C_{k,i}^{(2)} + v_{k,i}. \qquad (6.14)$$

Where $C_{k,i}^{(2)} = \sum_{q=0}^{N-1} e^{j\frac{2\pi}{N}q(i-k)} H(qN+k) e^{-j\frac{2\pi}{NN}i(k-i)}$ is an equivalent channel coefficient and $v_{k,i} = \frac{1}{N}\sum_{q=0}^{N-1} V(qN+k) e^{j\frac{2\pi}{NN}(qN+k)i}$ is the independent additive noise.

Now the relationship among each demodulated output $R_i(k)$, the equivalent channel coefficient $C_{k,i}^{(2)}$, transmitted signal a_k, and noise $v_{k,i}$ is clearly shown in Equation (6.14).

6.6.3 MRC Equalization

The MRC technique for Solution II is very similar to the one used in Solution I. After the parallel FFTs, the decision variable $U_k^{(2)}$ for the detection of a_k is calculated by

$$U_k^{(2)} = \sum_{i=0}^{N-1} C_{k,i}^{(2)*} R_i(k).$$

To analyze the BER performance of the MRC technique, we substitute $R_i(k)$ in the above equation with Equation (6.14) and have

$$U_k^{(2)} = \sum_{i=0}^{N-1} \left|C_{k,i}^{(2)}\right|^2 a_k + \sum_{i=0}^{N-1} C_{k,i}^{(2)*} v_{k,i}.$$

The output signal-to-noise ratio after MRC can be obtained as

$$\gamma^{(2)} = \frac{\left(\sum_{i=0}^{N-1} \left|C_{k,i}^{(21)}\right|^2\right)^2 E\left(\left|a_k\right|^2\right)}{E\left(\left|\sum_{i=0}^{N-1} C_{k,i}^{(2)*} v_{k,i}\right|^2\right)}$$

$$= \frac{\left(\sum_{i=0}^{N-1}\left|C_{k,i}^{(2)}\right|^2\right)^2 E\left(\left|a_k\right|^2\right)}{\sum_{i=0}^{N-1}\left|C_{k,i}^{(2)}\right|^2 E\left(\left|v_{k,i}\right|^2\right)}$$

$$= \sum_{i=0}^{N-1}\left|C_{k,i}^{(2)}\right|^2 SNR, \tag{6.15}$$

where $SNR = \frac{E\left(\left|a_k\right|^2\right)}{E\left(\left|v_{k,i}\right|^2\right)}$ is the signal-to-noise ratio before MRC.

Similarly, the average error probability can be written as:

$$P_e^{(MRC)} = E\left(Q\sqrt{\gamma^{(2)}}\right). \tag{6.16}$$

6.7 Summary

In this chapter, we have introduced the design of the receiver algorithms including deinterleaver, demodulation, channel equalization, and maximal ratio combining. For demodulation, two solutions using a single FFT operation and multiple FFT operations are discussed. Based on the theoretical analysis we derived the theoretical expressions for the system BER performance.

The theoretical analysis of the system BER has produced a method to evaluate system performance, which will provide a very good reference for the practical system simulation. In the following chapters, we will discuss the system performance by simulating the practical system, which will be compared with that of the theoretical analysis. In consequence, we can determine if the theoretical analysis is correct and reliable. Meanwhile, the practical system simulation process can be optimized according to the theoretical analysis results.

In Chapter 7 we will investigate the system performance including the transmitted signal peak-to-average power ratio, transmitted signal time diversity and frequency

diversity, and system coexistence. After that, it will be easy for us to observe the advantages of the ISS-OFDM system over the conventional OFDM systems.

Chapter 7

Performance Analysis

7.1 Peak to Average Power Ratio

7.1.1 Introduction

The OFDM technique has attracted significant attention due to its simple implementation by employing the IFFT operation and its extended symbol duration to combat ISI. It has found wide applications in digital audio/video broadcasting (DAB/DVB), WLAN (e.g., IEEE802.11a/g and Hiperlan II), and WPAN (e.g., MB-OFDM). More recently, OFDM has been considered as one of the most promising techniques to be applied to adaptive frequency sharing management systems in prospective cognitive radio communications.

However, OFDM has some drawbacks which prevent it from being used for low power and low cost applications. One of the major disadvantages is the large peak-to-average power ratio (PAR) of the transmitted signal, which renders a straightforward implementation very costly and inefficient. Especially, when the number of subcarriers becomes large, the PAR of the transmitted signal is sometimes unacceptable. The cause of a large PAR in conventional OFDM systems

is partially related to how the OFDM signal is formed. Consider the case when the signal frequency band is divided into N subcarriers and the frequency separation between subcarriers is $1/T$, where T is the OFDM symbol time duration. The data to be transmitted are split into N streams, each of which modulates a corresponding subcarrier. The N streams are modulated in parallel on closely-spaced subcarriers. The practical implementation of this process is performed using IFFT to generate a sampled version of the composite time signal. When the large number of signals from different subcarriers is added together, the signals with the same phases at the same time instants will produce high amplitude peaks. Compared with the average signal power, the instantaneous power of these peaks is very high, making the amplifier of the transmitter work in the non-linear range, which significantly degrades system performance.

In order to reduce the PAR and improve OFDM system performance, different algorithms have been proposed, such as selected mapping (SLM), partial transmit sequences (PTS), interleaved OFDM (IOFDM) [101], and block coding and clipping with filtering. For the SLM method, the basic idea is to have N statistically independent vectors representing the same information before modulation. After modulation and filtering, the time domain symbol with the lowest PAR is selected for transmission. PTS is based on the same principle as that of SLM, except that the transformation vectors have a different structure [88]. The clipping technique is the most straightforward way to deal with the PAR problems, by just clipping the signal with amplitudes over a certain threshold, but it results in a large amount of noise [87, 89]. These methods, except for clipping, are the same in principle, i.e., they generate some redundant signals bearing the same information and then select the best vector with the lowest PAR. A common problem for these algorithms is that they need to transmit side information so that the receiver can recover the original information. This causes transmission data rate loss. Another main drawback is the high computational complexity for choosing a good vector with the lowest PAR.

In this section, we analyze ISS-OFDM signal PAR characteristics. As we introduced in Chapter 4, the ISS-OFDM signal is generated by two steps. The first step is to modulate the data information by complex exponential spreading and the second is

to spread the signal spectrum by interleaving. At the transmitter, each data symbol modulates the corresponding subcarriers multiple times, and several different samples bearing the same data information can be obtained. The replicas of the same data information are interleaved into a serial sequence and then transmitted in different time slots. Assume that N data symbols in parallel modulate N subcarriers to produce N samples at each time slot. The produced N samples are not added together. Instead, they are interleaved pseudo randomly according to a certain pseudorandom code. Then, they are transmitted on different time slots respectively. After this spread spectrum modulation, an $N \times N$ matrix of data samples is generated, and then interleaved. In this way, the number of the total samples in one ISS-OFDM symbol increases greatly, which results in reduced signal power spectrum density if the total signal energy remains unchanged. At the same time, the PAR is reduced significantly. At the receiver, the received signal replicas in different subbands can be used to recover the data information by employing FFT without using any side information.

7.1.2 PAR Calculation

At the transmitter of the ISS-OFDM system, the transmitted signal is generated by using spectrum spreading and interleaving techniques. The transceiver model is presented in Figure 4.2 and the generation process of the transmitted signal $y(t)$ is clearly illustrated in Section 4.5.

Time domain samples of the transmitted signal $y(t)$ in the equivalent complex valued low-pass domain are approximately Gaussian distributed due to the statistical independence of carriers. Resulting PAR of $y(t)$ can be written as:

$$\xi = \frac{\max |y(t)|^2}{E[|y(t)|^2]}, \tag{7.1}$$

where $\max |y(t)|^2$ is the maximum instantaneous power of the ISS-OFDM signal and $E[|y(t)|^2]$ is the expected value of $|y(t)|^2$.

Note that the actual PAR of the continuous-time ISS-OFDM signal can not be determined by using the Nyquist sampling rate. Otherwise, the signal peaks are often missed and PAR reduction estimates are unduly optimistic. In order to evaluate the PAR performance of the transmitted signal, we over-sample the signal by a factor of four, which is sufficient to produce accurate PAR.

7.1.3 Phase Shifting and Interleaving

In order to spread the signal spectrum and at the same time reduce the probability of occurrence of large signal peaks in the transmitted signal, the samples in the $N \times N$ matrix are interleaved to form a serial sequence of length N^2 in the time domain. Each of the samples is placed in a certain time slot. Here, different interleaving algorithms can be employed such as pseudo random interleaving, periodic interleaving and convolutional interleaving. In this section, we discuss the periodic interleaving only. The periodic interleaving is realized by taking out the N samples in columns of the matrix and then placing the N modulated samples on different time slots respectively.

It can be seen from Figure 4.8 in Chapter 4 that instead of being superimposed together, the N modulated samples are interleaved periodically and then added together at different time instants. Thus, one ISS-OFDM symbol with N^2 samples is produced in the symbol duration T_s, and the number of samples is increased by N times. The sampling rate is increased to N^2 / T_s. Consequently, the signal spectrum is spread N times and the power spectrum density decreases to $1/N$ for the same transmitted signal energy.

Also Figure 4.8 in Chapter 4 shows the subcarrier shift in the time domain for the ISS-OFDM transmitted signal when the number of subcarriers N is equal to 4. It can be seen clearly that the modulated samples on the i^{th} ($i = 1, 2, 3, 4$) subcarrier are shifted i time intervals, so that the number of samples increases to N^2 from the

original number N after interleaving. We can observe that the maximum power of the ISS-OFDM transmitted signal is 1, and there is no increase in the maximum power compared to the individual subcarrier.

Figure 4.9 in Chapter 4 shows the four subcarriers and their spectrum expansion in the frequency domain. The subcarrier spectrum expansion is due to the subcarrier shifting and interleaving in the time domain. It is expected that after filtering the probability of the peak signal power above a certain threshold will be decreased greatly compared with the conventional OFDM system. The higher the number of subcarrriers is, the wider the subcarrier spectrum expands.

7.1.4 PAR Comparison

If we compare the transmitted signal power of the ISS-OFDM with that of conventional OFDM systems, the difference is obvious. Assume that the total power of the transmitted signal is P and N subcarriers are modulated by N QPSK symbols. In conventional OFDM systems, there are N modulated samples produced within one OFDM symbol duration, and the power on each sample is $\frac{P}{N}$. At some time instants the subcarriers are combined constructively and the maximum power of the transmitted signal is N times larger than average. It is expected that the probability of the occurrence of large signal peaks increases greatly after pulse shaping by the transmitter filter. In the ISS-OFDM system, due to the signal spectrum spreading, there are $N \times N$ samples produced within one ISS-OFDM symbol duration, and the power on each sample is $\frac{P}{N \times N}$. It is observed that the power on each individual subcarrier in the ISS-OFDM transmitted signal is reduced to $\frac{1}{N}$ of the conventional OFDM signal.

7.1.5 PAR Simulation and Analysis

Assume that the data symbol mapping scheme uses QPSK and the number of subcarriers $N = 32$. The generated ISS-OFDM signal has N^2 samples and contains N subbands, each of which contains N subcarriers and carries the same data information. The transmitter is designed so that M subbands are selected, $M = 1, \cdots, N$, respectively, and thus the transmitted signal contains M subbands. This means that the spectrum spreading factor is M.

Figure 7.1 shows the transmitted ISS-OFDM signal waveforms with various spectrum spreading factors $M = 1, 2, 4, 8, 16$ and 32 respectively. We assume that the data symbol has the same energy for different spreading factors. It can be observed from Figure 7.1 that with the increase of the spreading factor the signal amplitude (power) necessary for achieving the same bit error performance decreases.

Under the same assumptions as above, we select the signal bandwidth to contain $M = 1, 2, 4, 8, 16$ and 32 subbands respectively (M is the spreading factor), and the filtered signal is oversampled by a factor of four, which is commonly used to estimate the PAR of an analog signal from its samples. When $M = 1$, there is only one signal subband to be allowed to pass through the filter, resulting in a conventional OFDM signal. When $M = 2, 4, 8, 16$ and 32, respectively, i.e., the spreading factor is $2, 4, 8, 16$ and 32, the signal contains $2, 4, 8, 16$ and 32 subbands respectively.

According to Equation (7.1) we can compute the PAR performance curves. Figure 7.2 shows the PAR performance of the ISS-OFDM transmitted signal when PAR exceeds a certain threshold PAR0 with the increase of the spectrum spreading factor M from 1 to 32.

It can be seen from Figure 7.2 that with the increase of the number of subbands passing through the filter, the PAR performance is improved considerably. The most right-hand-side curve shows the PAR performance of the ISS-OFDM signal when

M is equal to 1, which is the same as that of the conventional OFDM signal. As M increases to 2, 4, 8, 16, and 32 respectively, the PAR gains are 0.5dB, 1.5 dB, 3.5 dB, 5 dB and 7 dB respectively.

Computational complexity for both Solution I and Solution II can be compared. Assumed the number of subcarriers is N and M subbands of the ISS-OFDM signal are received at receiver. For Solution I, if we ignore the complex addition, one FFT operation in long size of $N \cdot M$ performs the demodulation, the total complex multiply is $\frac{1}{2} N \times M \log_2{}^{NM}$. For Solution II, $N \cdot M$ FFT operations are employed to complete demodulation, the total complex multiply is $\frac{1}{2} N \times M \log_2{}^{N}$. The computational complexity in Solution II is reduced $\frac{\log_2{}^{MN}}{\log_2{}^{N}}$ times.

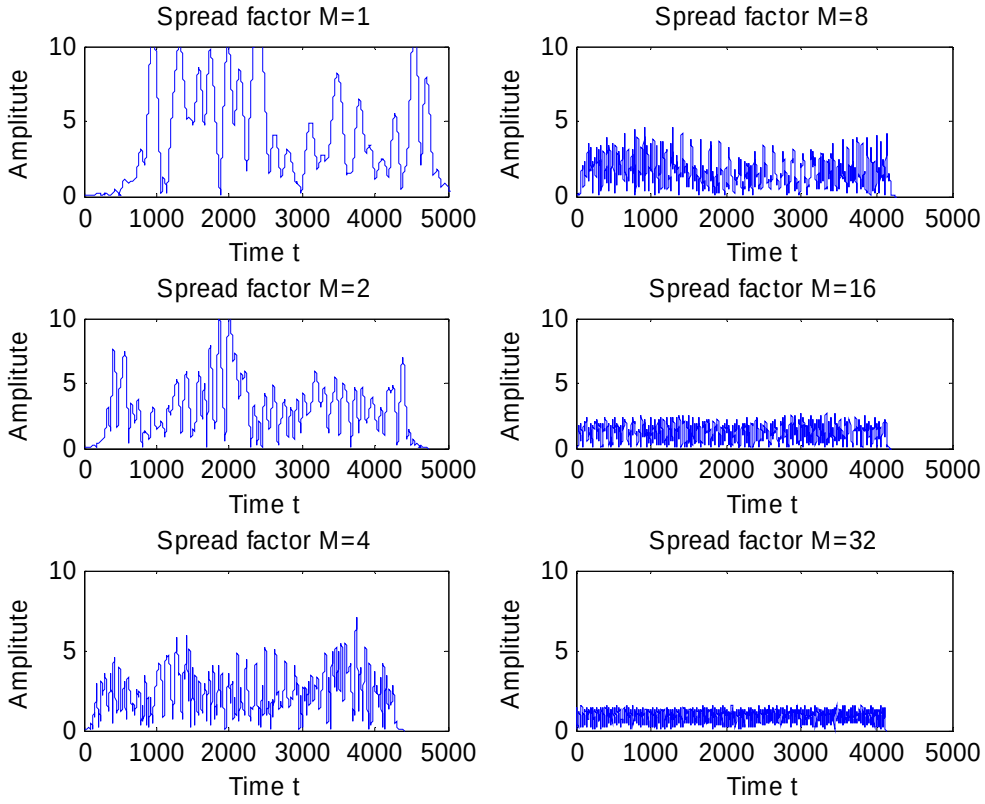

Figure 7.1 Transmitted signals waveforms with different spreading factors.

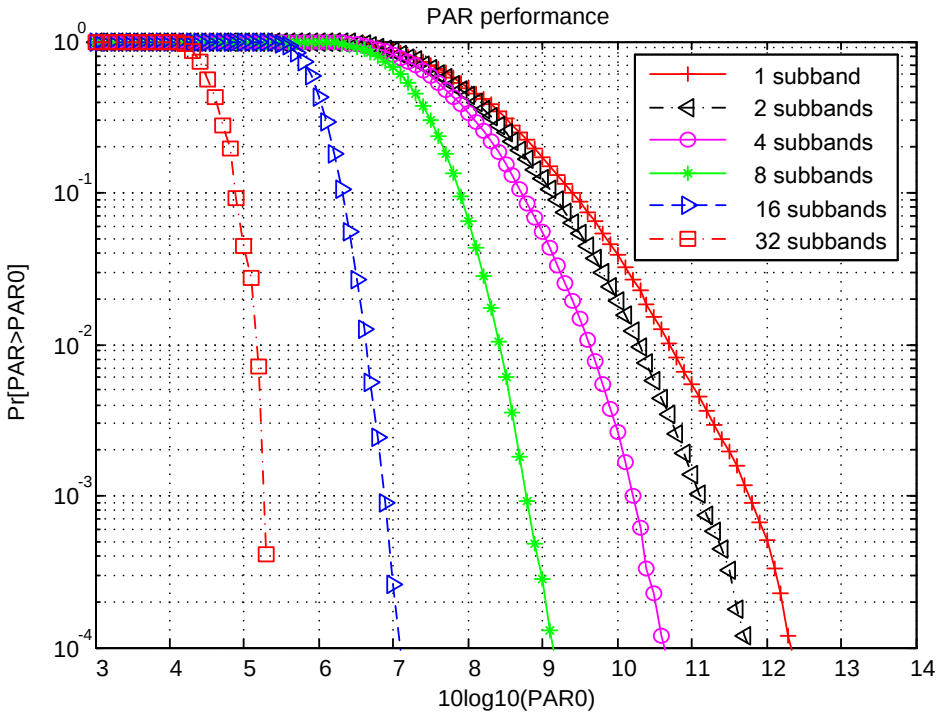

Figure 7.2 PAR performance for ISS-OFDM signals with different number of subbands.

7.1.6 PAR Improvement

In this section, we have investigated the PAR performance of the ISS-OFDM system. It has been shown that the combination of complex exponential spreading and interleaving not only spreads the signal spectrum but also significantly reduces the PAR of the resulting ISS-OFDM signal. It has been also shown that the PAR performance can be improved up to 2 dB once an additional subband is added to the signal spectrum. Compared with other previous PAR reduction algorithms, ISS-OFDM also effectively realizes a spread spectrum so that it does not degrade the range of communications or need to transmit side information. The proposed ISS-OFDM system can be used for ultra-wideband communications. It is also expected to be used in cognitive radio adaptive modulation techniques.

7.2 Diversity Performance

7.2.1 Introduction

Frequency selective fading is a dominant impairment in wireless communications. Channel fading reduces received SNR and degrades the BER. It also causes channel delay spread and introduces ISI. To combat frequency selective fading in wireless communications, diversity techniques must be resilient. The OFDM technique as one of the multi-carrier transmission techniques has extended the symbol duration and effectively reduced the ISI by inserting a cyclic prefix, which is greater than the channel delays, before the signal is transmitted to the channel. OFDM has been considered in a wide range of applications in recent years, but its diversity potentials have not been fully exploited yet.

Driven by OFDM applications against channel fading and by enabling multipath diversity, some different forms of OFDM systems with different diversity techniques have been proposed, such as the multiple-input multiple-output OFDM

(MIMO-OFDM) systems, the FD-OFDM or adaptive AFD-OFDM systems [103], and the SS-MC-MA [73]. Among these systems, the MIMO-OFDM is one of the most typical ones against channel fading [48]. It adopts a very commonly used method for achieving spatial diversity by employing multiple antennas at both ends of wireless links. It holds the potential to drastically improve spectral efficiency and link reliability in future wireless communications systems, and is regarded as a particularly promising candidate for next-generation fixed and mobile wireless systems. However, an open issue for MIMO-OFDM systems is realizing that technique in real time. The other two methods, FD-OFDM and SS-MC-MA, use the same way of multiplying the transmitted data stream by an orthogonal spreading code before modulation in order to achieve frequency diversity [103, 104] [105]. Spectrum spreading is accomplished by putting the same data on all parallel subcarriers, producing a spreading factor equal to the number of subcarriers. Although these systems enable full multipath diversity, they need a large number of side information transmissions, which causes considerable rate loss.

In this section we analyze system diversity performance including time diversity and frequency diversity. Both time diversity and frequency diversity are enabled by a spread spectrum modulation and interleaving technique, rather than using multiple antennas, orthogonal codes, or other side information. At the transmitter, each data symbol modulates the corresponding subcarriers multiple times, and several replicas bearing the same data information can be obtained. The replicas of the same data information are interleaved into a serial sequence and then transmitted in different time slots, instead of being added together. Thus, time diversity is achieved since the N replicas of a data symbol are placed in different time slots. The interleaving operation also results in the signal spectrum being expanded into multiple subbands, each of which contains the same data information, so that frequency diversity is achieved. After frequency selective channel fading, the receiver can collect signal energy from several signal subbands by using MRC techniques. Thus, the probability that all signal components fade simultaneously is reduced considerably, leading to significant system performance improvement.

7.2.2 Diversity in ISS-OFDM signals

7.2.2.1 Time Diversity

After serial to parallel conversion the $N \times 1$ parallel QPSK symbols modulate the corresponding N subcarriers. In the ISS-OFDM symbol duration T_s, each element of the $N \times 1$ data symbol vector modulates the same corresponding subcarrier N times, so that N elements in the vector generate an $N \times N$ sample matrix after modulation. In consequence, N replicas of each data symbol are produced in symbol duration T_s by CES modulation and transmitted in the multipath fading channels. Thus, the time diversity of the ISS-OFDM symbol is achieved.

7.2.2.2 Frequency Diversity

After CES modulation, the $N \times N$ samples are shifted in time and placed on different time slots to form a serial sequence of length N^2 in the time domain. All N samples in a column of the $N \times N$ matrix are taken out from the $N \times N$ matrix, shifted in time, and then placed in different time slots, instead of being superimposed together as in conventional OFDM systems. Due to the shifting in time for each sample, the phase of each subcarrier is shifted. In the frequency domain, the signal spectrum is expanded to N subbands, each of which contains N orthogonal subcarriers modulated by the same transmitted data symbols. At the receiver, multiple versions of each signal are received and demodulated. Therefore, the ISS-OFDM signal's frequency diversity is obtained. After demodulation, equalization and combination, diversity can be made full use of and system BER performance can be improved effectively.

7.2.3 Scalability of Diversity

A distinct feature in the ISS-OFDM system is scalability of the signal diversities. Since the signal spectrum is very wide and contains N subbands, each of which contains the same data information, any one or more subbands can be used to demodulate the transmitted information according to the system requirement and channel condition. At the transmitter, if we configure the transmitter filter so that the signal spectrum is spread M times, $M \le N$, the system frequency diversity order would be M. The diversity order can be achieved dynamically by adjusting the parameters of modulation and filters, and the diversity capability of the ISS-OFDM system is dependent on the number of subbands or spreading factor. If the number of the subcarriers of the ISS-OFDM is N, then the maximum spectrum spreading factor is N and the maximum diversity capability of the ISS-OFDM system is N. The more the diversity capability is provided by the system, the better BER performance the system can achieve. However, if the diversity capability provided by the system is more than the channel diversity order L, the extra diversity capability provided by the system is redundant. That is to say, if $M > L$ the diversity of the ISS-OFDM system is limited to the channel multipath length L.

The ISS-OFDM system can be used to achieve cognitive communications with dynamic subband allocation. If some of the subbands are interfered by other systems, the ISS-OFDM system can jump to other not-interfered subbands to complete communications and effectively avoid interference. As indicated in Figure 7.3, the system can realize communications by avoiding interference bands or by using some spectrum holes.

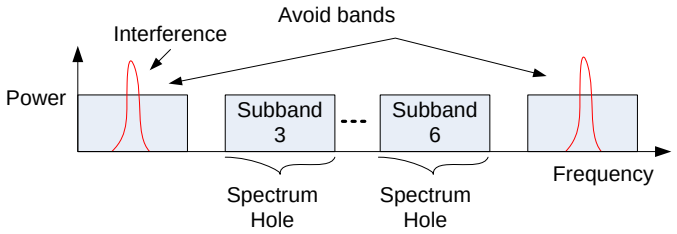

Figure 7.3 Bandwidth reconfigurable system and efficient spectrum usage.

7.2.4 Summary

In this chapter, we have exploited time diversity and frequency diversity of the ISS-OFDM system and investigated its BER performance. The investigation indicates that, by exploiting the diversity provided by the ISS-OFDM system, the performance in terms of BER is improved effectively. The combination of spread spectrum modulation and interleaving techniques is an efficient way of achieving frequency diversity and implementing spread spectrum communications. Furthermore, compared with other previous spread spectrum OFDM systems, the ISS-OFDM signal is superior in terms of BER, peak-to-average power ratio, reconfigurable system structure, and flexible system bandwidth usage. The proposed method of achieving diversity in the ISS-OFDM system can be used in ultra-wideband communications. It is also expected to be used in cognitive radio adaptive modulation techniques.

7.3 System Coexistence Performance

7.3.1 Introduction

Coexistence is the ability of two or more nodes/entities to share a common frequency band. One of the main factors to limit the coexistence between systems sharing a common frequency band is the interference from all sources.

To avoid interference between systems, many techniques have been proposed. Generally, these techniques can be classified into two categories. One is the collaborative mechanism for wireless systems capable of sharing detailed information in real-time about their predefined occupancy of time, frequency, space and power, in which the coexistence is realized by dynamically managing transmission frequency, controlling emission power and rescheduling in time. The other is the non-collaborative one, in which one or more systems must sense the

environment and take a corresponding action. With this method radios scan the channels in a service band and select the channel with the lowest received signal RSSI for data transmission. Since the selected signal band with the lowest RSSI may have interference above the acceptable threshold, this interference will lead to a significant error probability. Of these methods for managing frequency, controlling power and time, the most advanced systems are approaching Shannon's channel capacity limit. Further increase in capacity would require additional system bandwidth.

Cognitive radio, as one of the non-collaborative techniques for improving coexistence, can sense a wireless radio scene and identify interference. It aims at promoting the efficiency of the spectrum utilization and the coexistence between current users and primary users. Based on CR and OFDM techniques, one attempt to avoid interference is to exclude some sub-bands experiencing deep-fading by sculpting the corresponding subcarrier group [106, 107]. However, the reallocation of the transmission signal power for the excluded subbands to the remaining sub-bands increases the power of the remaining subbands and introduces interference to the primary users. Moreover, it requires more advanced techniques to suppress the sidelobes from the rectangular window.

In this section we investigate adaptive subband selection performance of the ISS-OFDM system. This performance is to avoid interference for the coexistence in an OFDM-based system operating in unlicensed ISM bands. Under the assumption that the interference power level and frequency bands can be identified based on CR techniques, the subbands of the transmitted signal are adaptively selected so that interference is avoided and system coexistence is improved.

7.3.2 Adaptive Subband Selection

In Section 4.7, we presented the ISS-OFDM multiple subband signal, which consists of N subbands and each of the subbands contains N subcarriers. When the multiple subband OFDM signal is passing through a multipath fading channel, since

the fading channel dissipates the signal energy, the received signals are faded in different subbands. Meanwhile, an interference signal will be imposed on the transmitted signals.

7.3.2.1 Interference

To avoid interference at the receiver so that system performance can be improved, the interfered subband(s) should be removed from the received signal once the interference power lever is above a predetermined threshold. The mechanism is explained in more detail below.

Assume the value of the threshold is γ_0 (we will discuss how to derive it in the next section). If interference superimposed on a subband is greater than the threshold value γ_0, then this interference would cause severe adverse effects on the desired signal. In order to achieve better system BER performance, the interfered subband should be excluded. If interference is lower than the threshold value γ_0, this interference can be tolerated and the interfered subbands are kept in the transmission bands. Otherwise, if we remove the interfered subbands with interference lower than the threshold, system performance will be worse than that of the system with the interfered subbands, since when we remove the interfered subbands, the signal energy is removed at the same time.

Figure 7.4 shows the fundamental principle of interference avoidance, in which a 4 subband OFDM signal in the unlicensed 2.4GHz ISM frequency band is faded and interfered with, but only two of the subbands with interference over the threshold are removed. Figure 7.4a shows the 4 subbands interfered with different power levels. As shown in Figure 7.4b the subbands with interference over the interference threshold γ_0 are sculpted by using an adaptive filter. The other two interfered subbands remain in the transmission bands since their interference levels are lower than the threshold.

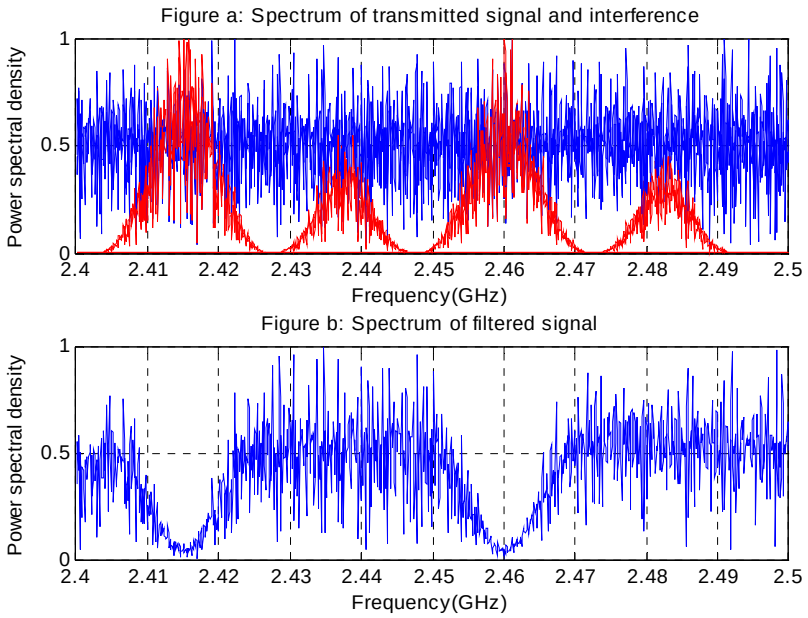

Figure 7.4 Subband selection by using adaptive filter.

7.3.2.2 Determination of Interference Thresholds

7.3.2.2.1 Thresholds in Gaussian Channels

In the previous section the methods of avoiding interference was discussed under the assumption of a known threshold of interference. In this section the thresholds of interference for systems coexistence will be investigated.

Assume that M subbands of the N subband signal are transmitted, and each has signal power P_S . If the noise power spectral density is N_0 , and the total interference signal power is P_J , and it is distributed in l subbands of the transmitted M subband OFDM signal, then, the total signal power of the M subbands is $M \cdot P_S$, and the total signal to interference noise ratio ($SINR$) can be expressed as:

$$SINR_M = \frac{M \cdot P_S}{N_0 M \cdot B + P_J} = \frac{SNR}{1 + INR}, \tag{7.2}$$

where $\frac{MP_S}{MN_0 B} = SNR$, $\frac{P_J}{N_0 MB} = INR$, B is the bandwidth of each subband.

Let G_p denote the processing gain for each subband, the total $SINR$, after considering the processing gain, is the sum of M subbands $SINR^{(1)}$ in (7.2), denoted by

$$SINR^{(1)} = M \cdot G_p \cdot SINR_M = \frac{M \cdot G_p \cdot SNR}{1 + INR}.$$

Similar to $SINR_M^{(1)}$, if the interfered subbands are cut off, the interference energy P_J is correspondingly completely removed. Thus, the total signal-to-interference noise ratio ($SINR$), after the interfered subbands are cut off, can be expressed as:

$$SINR_{M-l} = \frac{(M-l) \cdot P_S}{N_0 (M-l) \cdot B} = SNR. \tag{7.3}$$

Similar to $SINR^{(1)}$, after the l interfered subbands are removed, the total $SINR$, after considering the processing gain, is the sum of M subbands $SINR_{M-l}$ in (7.3), which is denoted by

$$SINR^{(2)} = (M-l) \cdot G_p \cdot SINR_{M-l} = (M-l) \cdot G_p \cdot SNR.$$

Since the signal energy is distributed in the whole bands, after the l interfered subbands are removed, the signal energy distributed in the l subbands is also removed, and the signal energy is correspondingly reduced. In a Gaussian channel, the BER performance is determined by the normalized signal-to-noise ratio. In order to have higher SNR after the interfered subband removal, $SINR^{(2)}$ should be higher than $SINR^{(1)}$, and thus we have the following expression:

$$SINR^{(2)} > SINR^{(1)} \Rightarrow INR > \frac{l}{M-l} = \gamma_0 . \tag{7.4}$$

It can be seen from Equation (7.4) that the threshold γ_0 of the INR is related to the number of transmitted subbands M and the number of interfered subbands l over Gaussian channels. Given the interfered subband number l (l=1, 2, 4, 8), the INR threshold decreases with the increase of the number M of the transmitted subbands. If the number M of the transmitted subbands is given, the INR threshold increases with the increase of the interfered subband number l.

7.3.2.2.2 Thresholds in Multipath Fading Channels

In a multipath fading channel, since channel fading is random, we can not obtain the same thresholds as those in the Gaussian channel. However, it is possible for us to get an estimation of the thresholds by statistically analyzing system BER performance in a multipath fading channel.

Recalling Equation (7.2) and considering the multipath fading effects, system BER performance before the interfered subbands are removed can be expressed by using the Q function as:

$$P_e^{(1)} = E\left[Q\left(\sqrt{\sum_{p=0}^{M-1} \left|H_p\right|^2 SINR^{(1)}} \right)\right] = E\left[Q\left(\sqrt{\sum_{p=0}^{M-1} \left|H_p\right|^2 \frac{SNR}{1+INR}} \right)\right],$$

where $E(\cdot)$ denotes the statistical expectation of the conditional error probability over multipath fading channels, and $\sum_{p=0}^{M-1} \left|H_p\right|^2$ is the sum of the M multipath fading channel coefficients on the M subcarriers. Due to the QPSK modulation, $SNR = \frac{2}{M} E_b / N_0$, which is derived in Section 6.5.3.3, where E_b / N_0 is the signal bit energy to noise spectrum density ratio [104]. The equation above can be rewritten as:

$$P_e^{(1)} = E\left[Q\left(\sqrt{\frac{1}{M}\sum_{p=0}^{M-1} \left|H_p\right|^2 \frac{2 \cdot E_b / N_0}{1+INR}} \right)\right]. \tag{7.5}$$

Similarly, recalling Equation (7.3), the BER performance of the system after the interfered subbands are removed in multipath fading channels can be derived as:

$$P_e^{(2)} = E\left[Q\left(\sqrt{\sum_{p=0}^{M-l-1} \left|H_p\right|^2 \frac{2 \cdot E_b / N_0}{M}} \right)\right], \tag{7.6}$$

where $E(\cdot)$, H_p, E_b / N_0 have the same meanings as defined in Equation (7.5).

According to Equation (7.5), we simulate system BER performance with the increase of the INR when the transmission subband number is 16 and E_b / N_0=10dB, which is displayed in Figure 7.6.

According to Equation (7.6) and with the same E_b / N_0, the BER performance of the system after the interfered subbands (its number is l=1, 2, 4, 8 respectively) are removed is shown as flat lines in Figure 7.6. The cross points are the interference thresholds γ_0 corresponding to l=1, 2, 4 and l =8. It can be seen from Figure.7.6 that the interference thresholds are -11dB, -7.5dB, -4.0dB and 1dB. The corresponding thresholds at the same conditions in a Gaussian channel can be calculated from Equation (7.4).

The interference thresholds in a multipath fading channel with transmission subbands M = 2, 4, 8, 16 and 32 are presented in Table 7.1. It is observed from Table 7.1 that the threshold discrepancies between multipath fading channel and Gaussian channel decrease with the increase of the transmission subband number and the discrepancy is approximately zero when the transmission subband number M = 32. That is to say, we can use thresholds in a Gaussian channel to replace the thresholds in a multipath fading channel if the number of transmitted subbands is more than 32.

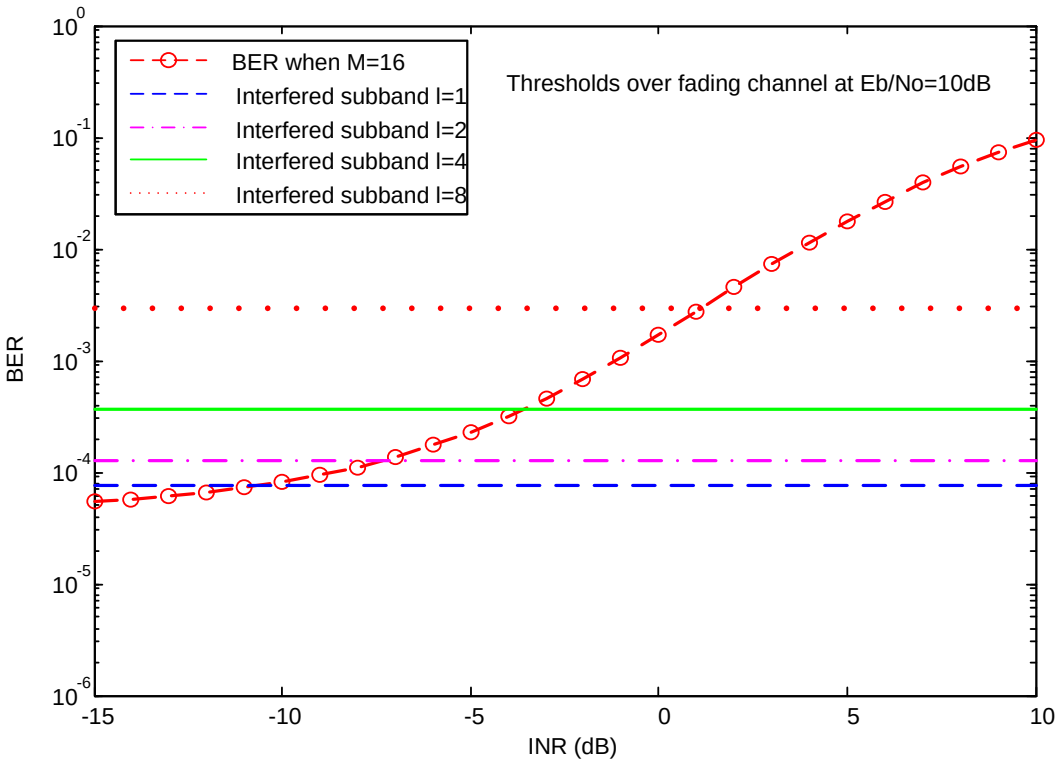

Figure 7.5 *INR* thresholds over multipath fading channel.

Table 7.1 Threshold comparison between Gaussian and multipath channels at $E_b / N_0 = 10$ dB.

Interfered Subbands	M=2		M=4		M=8		M=16		M=32	
	Gauss.	Multi.	Gauss.	Multi.	Gauss.	Multi.	Gauss.	Multi.	Gauss.	Multi.
l = 1	0	4.9	-4.8	-1.7	-8.5	-5.5	-11.8	-11.0	-14.9	-14.5
l = 2	–	–	0	3.3	-4.8	-2.0	-8.5	-7.5	-11.8	-11.5
l = 4	–	–	–	–	0	3.0	-4.8	-4.0	-8.5	-8.5
l = 8	–	–	–	–	–	–	0	1.0	-4.8	-4.5
Discrepancy	≈ 4.9		≈ 3.2		≈ 3		≈ 1.0		≈ 0.3	

7.4 Filtering of Multiple Subband Signal

When the multiple subband signal passes through the adaptive filter, the filtering of the multiple subband signal can be viewed as the convolution between the received multiple subband signal and the filter impulse response.

If the bandwidth of the adaptive filter is designed to be equal to the bandwidth of the signal frequency band with N subbands, after filtering the pass-band signal has N sub-bands, each of which has the whole transmitted information. If the bandwidth of the filter is designed to be M ($M \leq N$, N is the number of the subcarriers of the base band signal) sub-bands, only M subbands of the signal are passed through the filter, or only M subbands of the signal are received. In the case, if the filter pass-band is equal to one subband of the multiple subband signal, the system model is equivalent to a conventional OFDM system.

Assume the value of the threshold is γ_0. If interference superimposed on a subband is greater than the threshold γ_0, then this interference would cause severe adverse effects on the desired signal. In this case the interfered subband should be excluded. If interference is lower than the threshold γ_0, the interference can be tolerated by the system and the interfered subbands should be kept in the transmission bands. These transmission signals with different numbers of subbands are very flexible to match different spectrum holes with different bandwidths.

7.5 System Performance

Once the system *INR* thresholds are obtained, the interfered subbands with INR over the thresholds can be adaptively cut off to avoid interference. In order to verify the effectiveness of the subband adaptation in a multipath fading channel, the BER of the system without interference, with interference, and with interference removed are simulated. These are shown in Figure 7.6, Figure 7.7 and Figure 7.8, respectively.

Figure 7.6 indicates the system BER performance without interference with system transmission subband numbers M = 2, 4, 8, 16 and 32. It is observed that with the increase of M , the system BER performance is improved considerably. After M = 16, a further increase of transmission subbands is not obviously beneficial to the improvement of the BER performance, but is helpful for interference avoidance.

Under the same conditions, the system BER with one subband interfered is displayed in Figure 7.7. The *INR* is 3dB. It is seen that the impact from the interference results in 5 ~6 dB degradation at the BER performance of 10^{-6} compared with the system performance without interference.

As shown in Figure 7.8 after the interfered subband is removed when M = 4, 8, 16 and 32, the system BER is improved by 0.5~ 5 dB compared with the system performance with interference. In this case performance is very close to that without interference. However, when M = 2 system performance becomes worse, since the subband with *INR* lower than the threshold γ_0 = 4.9 dB is removed, which agrees with the previous analysis.

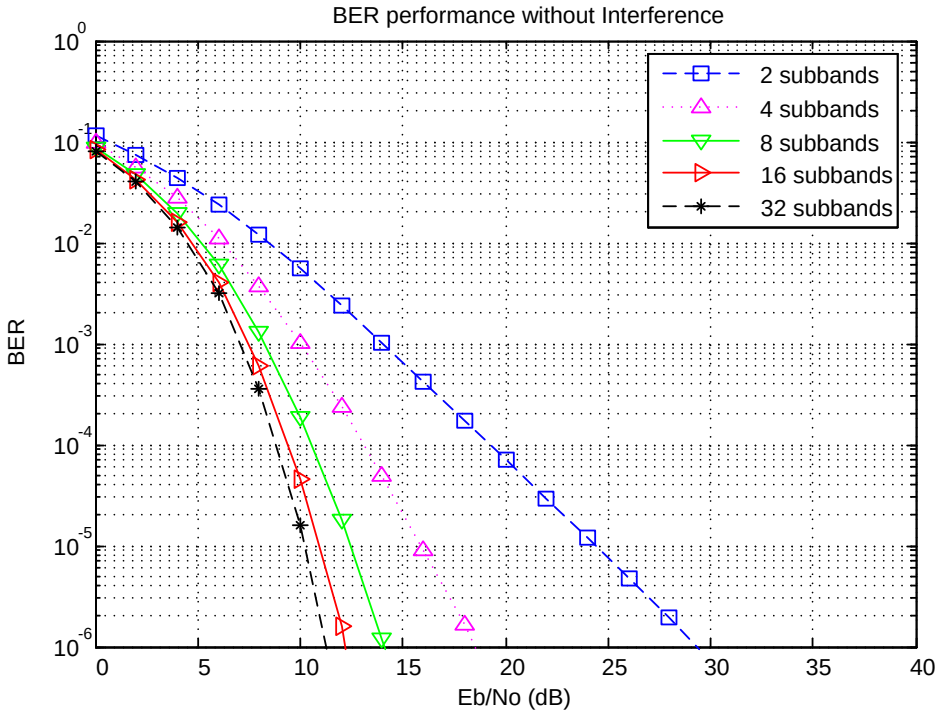

Figure 7.6 BER performance without interferences in fading channel.

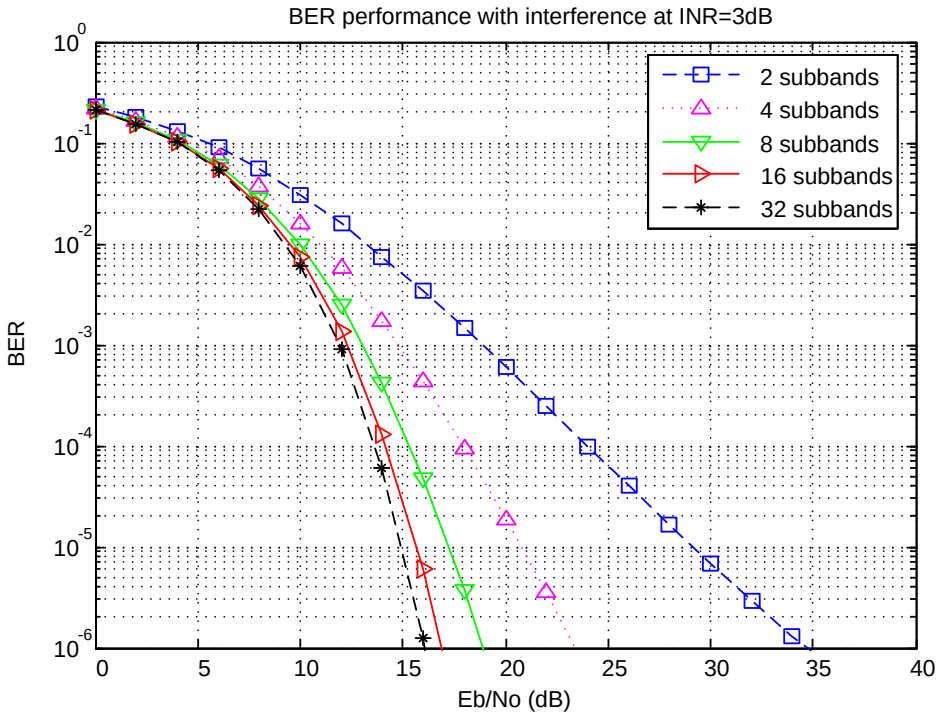

Figure 7.7 BER performance with interferences in fading channel.

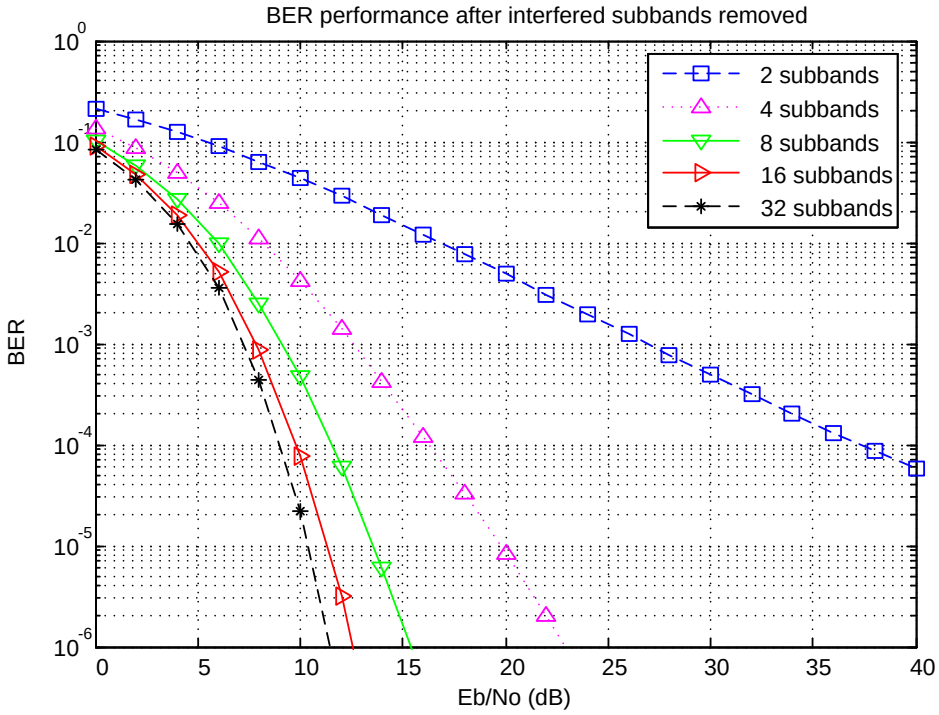

Figure 7.8 BER performance after interfered subbands removed adaptively in the fading channels.

7.6 Summary

In this section we have investigated system performance in a shared spectrum environment. We have discussed the transmission signal PAR, received signal diversity including the diversity in the frequency domain and in the time domain, and coexistence system BER performance when the system transmission band changes with the spectrum environments. The system performance improvement is realized by a proposed algorithm, the adaptive subband selection method. This approach can effectively make use of the interference thresholds in Gaussian and multipath fading channels. We have also shown that the thresholds in a multipath fading channel approach the thresholds in a Gaussian channel when the number of transmission subbands is sufficiently high, which makes the thresholds easy to determine analytically. The proposed algorithms can be used in an agile RF transceiver working over a wide range of frequency bands and the software-defined radio modem in a cognitive way.

Chapter 8

Contribution and Future Work

8.1 Contribution

The contribution of this thesis is made in three main aspects, which are presented as follows.

1. A novel algorithm, the complex exponential spreading method, has been developed to generate a spreading spectrum OFDM signal which can be used for adaptive subband transmission. This signal has unique characteristics. It has multiple subbands, and has both frequency diversity and time diversity, which provides great potential for optimizing receiver system performance.

2. An adaptive subband transmission algorithm has been developed based on the dynamically obtained interference thresholds to avoid coexistence interference between OFDM systems and other narrowband radio systems or ultra-wideband wireless systems. In the adaptive subband transmission, any one of the subbands contains all the transmitted information and any number of subbands can be used to recover the transmitted information.

3. A parallel multiple FFT demodulation method has been proposed to demodulate the received signal to reduce the receiver computation complexity. In this method, N FFT operations are employed in parallel to demodulate the received signal, and the processing rate of demodulation increases efficiently.

Due to the three contributions, great benefits of the ISS-OFDM systems have been brought about. The ISS-OFDM system has five advantages over the conventional OFDM systems. They are described as follows.

1. PAR in the ISS-OFDM system is greatly reduced. Very low PAR in the ISS-OFDM system is one of the distinct characteristics, which is superior to the conventional OFDM systems. As widely known, the biggest problem for OFDM systems is its relatively high peak-to-average power ratio (PAR). Many researchers have done a lot of research on solving the PAR problems. In the ISS-OFDM system, the PAR is effectively reduced by simply interleaving the modulated OFDM subcarriers using a kind of an interleaving algorithm, rather than superimposing the OFDM modulated subcarriers.

2. Both frequency diversity and time diversity of the received signal are distinctively increased. They are increased by N times by interleaving the modulated ISS-OFDM subcarriers. These diversities of the received signal provide the receiver algorithms and transmission system bandwidth with great flexibility, which significantly improves the system bit error rate.

3. Adaptive subband selection makes system transmission bandwidth extremely flexible. Adaptive subband selection is another distinct feature of the ISS-OFDM system. Since the transmission signal spectrum is spread to a wide band consisting of many subbands, and each subband contains the whole information needed to be transmitted, any one or more subband can be employed as the system transmission bandwidth to transmit information. Thus, system bandwidth can be very flexible and can be adaptively reconfigured according to the radio scene or interference conditions. In the spread spectrum bandwidth of the transmitted signal, if some subbands are interfered with by some interfered frequency band, the wideband

transmission bandwidth can be adaptively tailored for information transmission. In this case, since the system transmission bandwidth contains several subbands, the receiver can receive several versions of the transmission signal. Even if some subbands of the received signal are faded severely, the ISS-OFDM system still can obtaine very good system performance by selecting the subbands without interference. Furthermore, it makes the ISS-OFDM system available to cognitive radio communications and ultra-wideband radio communications.

4. System coexistence interference is effectively avoided.

5. Transmission signal power is greatly reduced. Due to the spectrum spreading of the transmitted ISS-OFDM signal, the signal transmission power is very low, which well prepares the ISS-OFDM system for use in sensor networks and wireless body area networks. It can realize this without interfering with other users.

8.2 Applications

The ISS-OFDM system has many applications in wireless communications. In the following, we just list some of the most important applications of the ISS-OFDM system.

1. Application to coexisting systems working in ISM frequency bands. The ISS-OFDM system can be applied to improve coexistence system performance of wireless communications by avoiding interference produced by the coexisting systems. Adaptive subband selection in the ISS-OFDM system can be applied to avoid interference according to the scanned interference frequency bands. Especially in ISM unlicensed frequency bands, every user can use the frequency bands without frequency limits and operate separately without cooperation with other systems. Some of the frequency bands may be already used by the primary users, some of the frequency bands may not. It is desirable for the secondary users to scan the interference subbands and avoid the frequency bands according to the scanned

results. The ISS-OFDM system can satisfy the requirements for avoiding interference.

2. Application to cognitive radios. The ISS-OFDM system applying to cognitive radios is another application. Cognitive radios require the radio frequency front end to be agile, and to transmit various waveforms of the signal including OFDM and DSSS waveforms. ISS-OFDM can generate these two signals by reconfiguring the parameters of the modulation. The method of generating the OFDM signal is discussed above in detail. For generating the DSSS signal, in the low band of the ISS-OFDM system when the interleaving algorithm is performed, a piconet channalization can be achieved by code division multiple access (CDMA) techniques. A piconet is multiplied by a different pseudorandom orthogonal code when using the interleaving technique, so that each data symbol is spread by its CDMA code for the interleaving algorithm. After ISS-OFDM subcarrier interleaving, the modulated signal is a multicarrier CDMA (MC-CDMA) signal, and the DSSS signal can be generated.

3. Embedding in WBANs. The ISS-OFDM system can also be applied to WBANs. WBAN is a kind of wireless personal area network which realizes ultra-wideband low-data rate wireless body area communications. By placing a lot of sensors around the body, the information of interest is sent to the central devices such as a personal digital assistant (PDA) to be processed, so that the body performance can be monitored, diagnosed, and treated. However, since the transmitted signal power is very low, even the hand movements may cause signal degradation, so it is desirable for the system to overcome signal degradation. The characteristics of very lower power transmission and signal diversity can be applied to WBANs to solve the signal fading problems.

8.3 Future Work

The work presented in this thesis has opened up some possible areas for ongoing research. A brief discussion of these topics is presented in the following.

1. Adaptively selecting transmission subbands can be further optimized by considering interference thresholds jointly with the game theory. Dynamically and quantitatively determining interference thresholds has effectively solved issues of adaptive subband selection for system coexistence. However, for the purpose of higher intelligence, the adaptive subband selection is necessary to be considered with the new emerging technique, the game theory. Jointly with the game theory, the system coexistence issues can be dealt with qualitatively, and the coexistence issues are handled cooperatively and competitively so that some models with ambiguous situations can be developed.

2. Radio detection and scanning in practical radio scenes will be considered for further improvement of the system coexistence ability.

In the ISS-OFDM system, work presented in this dissertation is based on the knowledge of interference including the interference type and interference power, which ignores some accuracy of the practical radio scenes and the complexity to sense the radio environments. In practice, the interference signal dynamically varies with the radio scene and it is difficult to capture.

Since the radio scanning and interference detection is closely related to cognitive radio techniques, we will work on the radio scanning and interference detection jointly with cognitive radio techniques. Thus, the future work may include human machine interactive techniques, intelligent decision techniques, and mode pattern recognition techniques.

Scanning and detection of the inference signal needs employing a wide range of technologies such as human intelligence or human machine interactive techniques. In this area, a large number of topics related to the ISS-OFDM system are waiting to be investigated.

3. Synchronization issues will be considered for future applications.

Some results on system coexistence performance are simulated and realized under the assumption of perfect synchronization. The system simulation and implementation are completed under the assumption of transmitter and receiver being perfectly synchronized. The simulation results on system BER performance under this assumption are satisfactory and close to the theoretical analysis results. However, to some extent, we idealize the system without considering the impacts of frequency offset and synchronizations. If we add the impacts from system synchronization, system performance may degrade to some extent. Synchronization is a complex question waiting to be solved. Any fault in one of the issues of frame synchronization, symbol synchronization and subcarrier synchronization may cause the system bit error rate to be come worse. Sometimes it may result in the malfunction of the system. Therefore, ignoring system synchronization to simulate the ISS-OFDM system may not be perfect.

In addition, commercialization of the ISS-OFDM system should be considered. We will seek cooperation with the industry to promote the commercialization of the ISS-OFDM techniques.

References

[1] Y. K. Kim and R. Prasad, *4G Roadmap and Emerging Communication Technologies*, Boston, MA: Artech House, 2006.

[2] S. Haykin, "Cognitive Radio: Brain-Empowered Wireless Communications," in *IEEE Journal on Selected Areas in Communications,* vol. 23, pp. 201-219, 2005.

[3] J. Lansford, "UWB Coexistence and Cognitive Radio: How Multiband-OFDM Leads the Way," in Joint UWBST & IWUWBS.2004, International Workshop on Ultra-Wideband Systems, pp. 35-39, 2004.

[4] T. Cooklev, *Wireless Communication Standards*, NewYork: Standards Information Network, IEEE Press, 2004.

[5] Y. Liu and Y. Yang, "Efficient Adaptive Array Receiver for OFDM Based Wireless Local Area Networks (WLAN)," in *IEEE Transactions on Consumer Electronics,* vol. 50, pp. 1101-1106, 2004.

[6] D. Cabric and R. W. Brodersen, "Physical Layer Design Issues Unique to Cognitive Radio Systems," in IEEE 16th International Symposium on Personal, Indoor and Mobile Radio Communicaitons, vol. 2, pp. 759-763, 2005.

[7] K. E. Nolan, P. D. Sutton, L. E. Doyle, T. W. Rondeau, B. Le, and C. W. Bostian, "Dynamic Spectrum Access and Coexistence Expericences Involving Two Independently Developed Cognitive Radio Testbeds," in 2nd

IEEE International Symposium on New Frontiers in Dynamic Spectrum Access Networks, pp. 270-275, 2007.

[8] N. Fourty, T. Val, P. Fraisse and J. -J. Mercier, "Comparative analysis of new high data rate wireless communication technologies "From Wi-Fi to WiMAX"**,** in Joint International Conference on Autonomic and Autonomous Systems and International Conference on Networking and Services, pp. 66-66, 2005.

[9] A. R. S. Bahai, B. R. Saltzberg and M. Ergen, *Multi-Carrier Digital Communications Theory and applications of OFDM,* 2ed., Springer Science Business Media, Inc, 2004.

[10] W. G. Jeon, K. H. Chang and Y. S. Cho, "An Equalization Technique for Orthogonal Frequency Division Multiplexing Systems in Time-Variant Multipath Channels," in *IEEE Transactions on Communications,* vol. 47, pp. 27-32, 1999.

[11] E. G. Lundin, F. Gunnarsson and F. Gustafsson, "Adaptive Filtering Applied to an Uplink Load Estimate in WCDMA," in The 57th IEEE Semiannual Vehicular Technology Conference, VTC 2003 Spring, vol. 1, pp. 452-456, 2003.

[12] N. Benvenuto, R. Corvaja, T. Erseghe and N. Laurenti, *Communication Systems Fundamentals and Design Methods*, John Wiley & Sons, Ltd, 2007.

[13] S. B. Slimane, "MC-CDMA with Quadrature Spreading over Frequency Selective Fading Channels," in IEEE Global Telecommunications Conference, GLOBECOM '97, pp. 315-319, 1997.

[14] R. Prasa and S. Hara, "An Overview of Multi-carrier CDMA," in IEEE International Symposium on Spread Spectrum Techniques and Applications Proceedings, vol. 1, pp. 107-114, 1996.

[15] Q. Zhang, A. B. J. Kokkeler and G. J. M. Smit, "Adaptive OFDM System Design for Coginitve Radio," Department of Electrical Engineering, Mathematics and Computer Science University of Twente, http://eprints.eemcs.utwente.nl/2875/01/InOWo06.pdf.

[16] G. Andrea, C. Marco and D. Davide, "Coexistence Issues in Cognitive Radios Based on Ultra-Wide Bandwidth Systems," in 1st International Conference on Cognitive Radio Oriented Wireless Networks and Communications, pp. 1-5, 2006.

[17] R. Brodersen, "Cognitive Dynamic Systems," in IEEE International Conference on Acoustics, Speech, and Signal Processing, ICASSP 2007, vol. 4, pp. IV 1369 - IV 1372, 2007.

[18] J. Mitola, G. Q. mAGUIRE and J. R, "Cognitive Radio: Making Software Radios More Personal," *IEEE Personal Communications,* pp. 13-18, 1999.

[19] S. Lucyszyn, "Review of Radio Frequency Microelectromechanical Systems Technology**,**" in IEE Proceedings on Science, Measurement and Technology, vol.151, no.2, pp. 93-103, 2007.

[20] H. G. Ryu, T. P. Hoa, N. T. Hieu and J. Jianue, "BER Analysis of Clipping Process in the Forward Link of The OFDM-FDMA Communication System," in *IEEE Transactions on Consumer Electronics,* vol. 50, pp. 1058-1064, 2004.

[21] L. E. Aguado, K. K. Wong and T. O' Farrel, "Coexistence Issues for 2.4GHz OFDM WLANs," in Third International Conference on 3G Mobile Communication Technologies, pp. 400-404, 2002.

[22] J. Foerster, E. Green, S. Somayazulu and D. Leeper, "Ultra-Wideband Technology for Short- or Medium-Range Wireless Communications," in Intel Technology Journal, Q2, pp. 1-11, 2001.

[23] M. Welborn, "Frequency Hoppers and FCC UWB Rules, IEEE P802.15 Wireless Personal Area Networks," in *IEEE P802.15-03/27lr2,* 2003.

[24] X. Dong and T. Luo, *OFDM Mobile Communication Technology_Principles and Applicaitons* (in Chinese), Posts and Telecom Press, China, 2003.

[25] T. F. Detwiler and D. L. Jones, "OFDM Receiver Design for Active Constellation Extension**,**" in Conference Record of the Thirty-Ninth Asilomar Conference on Signals, Systems and Computers, pp.1485-1489, Nov. 2005.

[26] V. F. G. A. Sikora, "Coexistence of IEEE 802.15.4 with Other Systems in the 2.4GHz-ISM-BAND," in IMTC 2005- Instrumentation and Measurement Technology Conference, pp. 1786-1790, 2005.

[27] S. Ranganathan and T. Fiez, "A Variable Gain High Linearity Low Power Baseband Filter for WLAN," in International Symposium on Circuits and Systems, ISCAS '04, Proceedings, vol.1, pp. I 845-848, May 2004.

[28] D. Bartolome and A. I. Perez-Neira, "MMSE Techniques for Space Diversity Receivers in OFDM-based Wireless LANs," in *IEEE Journal on Selected Areas in Communications,* vol. 21, pp. 151-160, 2003.

[29] B. Sujak, D. Kumar Ghodgaonkar, B. Mohd, Ali and S. Khatun, "Indoor Propagation Channel Models for WLAN 802.11b at 2.4GHz ISM Band," in ASIA-PACIFIC conference on applied Electromagnetic Proceedings, pp. 373-377, 2005.

[30] K. Akita, R. Sakata and K. Sato, "A Phase Compensation Scheme Using Feedback Control for IEEE 802.11a Receiver," in 2004 IEEE 60th Vehicular Technology Conference, VTC2004-Fall, vol. 7, 2004.

[31] C. Eklund, R. B. Marks, K. L. Stanwood and S. Wang, "IEEE Standard 802.16: a Technical Overview of the WirelessMAN^{TM} Air Interface for

Broadband Wireless Access," in IEEE Communications Magazine, vol. 40, no. 6, pp.98 - 107, June 2002.

[32] J. S. Lee, Y. W. Su and C. C. Shen, "A Comparative Study of Wireless Protocols: Bluetooth, UWB, ZigBee, and Wi-Fi," in IEEE 33rd Annual Conference of the Industrial Electronics Society, IECON 2007, pp.46-51, Nov. 2007.

[33] C. Woo Cheol, N. J. August and H. D. Sam, "Signaling and Multiple Access Techniques for Ultra Wideband 4G Wireless Communication System," in *IEEE Wireless Communications,* vol. 12, pp. 46-55, 2005.

[34] A. Fort, C. Desset, P. De Doncker, P. Wambacq and L. V. Biesen, "An Ultra-Wideband Body Area Propagation Channel Model-From Statistics to Implementation," in *IEEE Transactions on Micorwave Theory and Techniques,* pp. 1820-1826, 2006.

[35] M. Castrucci, I. Marchetti, C. Nardini, A. Ichimescu, N. Ciulli, G. Landi and P. Neves, "A Framework for Resource Control in WiMAX Networks," in the 2007 International Conference on Next Generation Mobile Applications, Services and Technologies, NGMAST '07, pp. 316 - 321, Sept. 2007.

[36] L. Ophir, Y. Bitran and I. Sherman, "Wi-Fi (IEEE 802.11) and Bluetooth Coexistence: Issues and Solutions," in IEEE 16th International Symposium on Personal, Indoor and Mobile Radio Communicaitons, vol. 2, pp. 847-852, 2004.

[37] Y. Zhe, A. Mohammed, T. Huh and D. Grace, "Optimizing Downlink Coexistence Performance of WiMAX Services in HAP and Terrestrial Deployments in Shared Frequency Bands," in International Waveform Diversity and Design, pp. 79-82, 2007.

[38] S. A. Ghorashi, B. Allen, M. Ghavami and A. H. Aghvami, "An Overview of MB-UWB OFDM," in IEE Seminar on Ultra Wideband Communications Technologies and System Design, pp. 107-110, 2004.

[39] S. Coleri, M. Ergen, A. Puri and A. Bahai, "Channel Estimation Techniques Based on Pilot Arrangement in OFDM Systems," in *IEEE Transactions on Broadcasting,* vol. 48, pp. 223-229, 2002.

[40] M. Wlborn, "Frequency Hoppers and FCC UWB Rules," in IEEE P802.15 Working Group for Wireless Personal Area Networks (DS-UWB), IEEE P802.15-03/271r2, pp1-13, July 2003.

[41] R. S. Blum, Y. Li, J. H. Winters, and Q. Yan, "Improved Space-Time Coding for MIMO-OFDM Wireless Communications," in *IEEE Transactions on Communications,* vol. 49, pp. 1873-1878, 2001.

[42] M. K. Simon, J. K. Omura, R. A. Scholtz and B. K. Levitt, *Spread Spectrum Communications Handbook*, McGraw-Hill, Inc., New York, 1994.

[43] J. Qaddour and D. Leonard, "Beyond 3G: Uplink Capacity Estimation for Wireless Spread-Spectrum Orthogonal Frequency Division Multiplexing (SS-OFDM)," in Global Telecommunications Conference, pp. 4139-4141, 2003.

[44] H. Viittala, M. Hamalainen and J. Iinatti, "The Impact of Co-existing Systems on MB-OFDM and DS-UWB System Perfromances in AWGN and Multipaht Channels," in http://www.sgo.fi/Events/ursi-2006/URSI2006_abstracts/Viittala_etal_abstract.pdf, Centre for Wireless Communications, Oulu, Finland, Oct. 2006.

[45] Z. Xu and L. Liu, "Power Allocation for Multi-band OFDM UWB Communication Networks," in IEEE 60th Vehicular Technology Conference, VTC2004-Fall, vol. 1, pp. 368-372, 2004.

[46] B. Ackland, D. Raychaudhuri, M. Bushnell, C. Rose and I. Seskar, "High Performance Coginitive Radio Platform with Intergeated Physical and Network Layer Capabilities (Interim Technical Report)," in Network Centric Cognitive Radio, WINLAB, Rutgers University, pp. 1-13, 2005.

[47] G. L. Stuber, J. R. Barry, S. W. McLaughlin, L. Ye, A. Lngram and G. Pratt, "Broadband MIMO-OFDM Wireless Communications," in Proceedings of the IEEE, pp. 271-294, 2004.

[48] P. Uthansakul and M. E. Bialkowski, "Multipath signal effect on the capacity of MIMO, MIMO-OFDM and spread MIMO-OFDM**,**" in 15th International Conference on Microwaves, Radar and Wireless Communications, MIKON-2004, vol.3, pp. 989 - 992, May 2004.

[49] J. G. Proakis, *Digital Communications,* 4ed, New York, USA, Mc Graw Hill, 2000.

[50] Y. Jia and S. Hara, "Coexistence of OFDM-Based WLANs by VIrtual Subcarrier Assignment (VISA) with Multiple Sibcarrier Puncturing," in IEEE 60th Vehicular Technology Conference, VTC2004-Fall, vol. 6, pp. 4330-4334, 2004.

[51] X. Jing, S. Mau, D. Raychaudhuri and R. Matyas, "Reactive Cognitive Radio Algorithms for Co-Existence between IEEE802.11b and 802.16A Networks," in Global Telecommunications Conference, vol. 5, pp. 2465-2469, 2005.

[52] J. Chiang and J. Lansford, "Use of Cognitive Radio Techniques for OFDM Ultra Wideband Coexistence with WiMAX," in http://www.utdallas.edu/~cpb021000/shared/pdfs/0000091.pdf, Texas Wireless Symposium, pp.91-95, 2005.

[53] K. Kim, J. Park, J. Cho, K. Lim, Razzell, C. J., C. Lee, H. Kim and L. J., "Interference Analysis and Sensing Threshold of Detect and Avoid (DAA)

for UWB Coexistence with WiMAX," in IEEE 66th Vehicular Technology Conference, VTC-2007 Fall, pp. 1731-1735, 2007.

[54] I. D. M. Patel, "Investigation of the Performance of a Multimode, Multiband Receiver for OFDM and Cellular Systems," in IEEE 58th Vehicular Technology Conference, VTC 2003-Fall, vol. 1, pp. 284-288.

[55] Z. Li and G. Kuo, "Layered MAC for High-Rate UWB WPAN System," in IEEE 64th Vehicular Technology Conference, VTC2006 Fall, pp. 1-5.

[56] M. L. Roberts, M. A. Temple, R. F. Mills and R. A. Raines, "Interference suppression characterisation for spectrally modulated, spectrally encoded signals," in *Electronics Letters*, vol. 42, pp. 1103-1104, 2006.

[57] A. Duratini, R. Giuliano and F. Mazzenga, "UWB Interference Mitigation Technology in a Cooperative Scenario," in IEEE 18th International Symposium on Personal, Indoor and Mobile Radio Communications, pp. 1-5, 2007.

[58] P. Xia, S. Zhou and G. B. Giannakis, "Bandwidth- and Power-Efficient Multicarrier Multiple Access," in *IEEE Transations on Communications,* vol. 51, pp. 1828-1836, 2003.

[59] Y. Wang, H. M. Lam, C. Y. Tsui, R. S. Cheng and W. H. Mow, "Low Complexity OFDM Receiver Using Log-FFT for Coded OFDM System," in IEEE International Symposium on Circuits and Systems, vol. 3, pp. III 445-III 448, 2003.

[60] L. Dong, H. Choo, R. W. Heath and H. Ling, "Simulation of MIMO Channel Capacity with Antenna Polarization Diversity," in *Transactions on Wireless Communications*, pp. 1869-1871, 2005.

[61] M. Soyuer, H. A. Ainspan, J. N. Burghartz, J. O. Plouchart, B. P. Gaucher, T. J. Beukema, F. J. Canora, E. Pilmanis and M. M. Oprysko, "A Cost-Effective

Approach to a Short-range, High-Speed Radio Design in the U-NII 5.x GHz Band," in IEEE Radio and Wireless Conference, pp.133 - 136, August 1998.

[62] B. A. Forouzan, *Data Communication and Networking,* Mc Graw Hill Higher Education, 2004.

[63] J. Del Prado and S. Choi, "Experimental Study on Coexistence of 802.11b with Alien Devices," in IEEE VTS 54th Vehicular Technology Conference, VTC 2001 Fall, vol. 2, pp. 977-981, 2001.

[64] W. G. Chung, H. S. Jo, H. G. Yoon, J. W. Lim, J. G. Yook and H. K. Park, "Advanced MCL Method for Sharing Analysis of IMT Advanced System," in *Electronics Letters,* vol. 42, pp. 1234-1235, 2006.

[65] D. Torrieri, *Principles of Spread-Spectrum Communication Systems,* Springer Science +Business Media, Inc., 2005.

[66] T. A. Weiss and F. K. Jondral, "Spectrum Pooling: An Innovative Strategy for the Enhancement of Spectrum Efficiency," in *IEEE Communications Magazine,* vol. 42, pp. S8-S14, 2004.

[67] T. S. Rappaport, *Wireless Communcations_Principles and Practice,* vol. 2: Prentice Hall PTR, 2002.

[68] M. Munoz and C. G. Rubio, "A New Model for Service and Applicaiton Convergence in 3G/4G Networks," in *IEEE Wireless Communications,* vol. 11, pp. 6-12, 2004.

[69] J. Mitola, "Software Radio Architecture: A Mathematical Perspective," in *IEEE Journal on Selected Areas in Communications,* vol. 17, pp. 514-538, 1999.

[70] D. S. Mandyam, *Statistical Signal Processing with Applications*, New Jersey, Prentice-Hall, Inc., 1996.

[71] Y. Wang, H. M.Lam, C. Y. Tsui, R. S. Cheng and W. H. Mow, "Performance Study of OFDM Receiver Using FFT Based on Log Number System," in IEEE 55th Vehicular Technology Conference, VTC Spring, vol. 3, pp. 1257-1259, 2002.

[72] G. Zha and X. Xiong, *Spread Spectrum Communications*, 1 ed., University of Electronics Technology, Xi'an, China, 1999.

[73] S. Kaiser and K. Fazel, "A Flexible Spread-Spectrum Multicarrier Multiple-Access System for Multi-Media Applications," in Personal, Indoor and Mobile Radio Communications, vol. 1, pp. 100-104, 1997.

[74] A. Tanka and A. Kasamatsu, "Noise Amplifier with Center Frequency Hopping for an MB-OFDM UWB Receiver," in International Workshop on Ultra Wideband Systems, Joint with Conference on Ultra-wide band Systems and Technologies, pp. 420-423, 2004.

[75] S. Haykin and B. V. Veen, *Signal and Systems,* 2ed., John Wiley & Sons, Inc., 2003.

[76] K. Fazel and S. Kaiser, *Multi-Carrier Spread-Spectrum,* Kluwer Academic Publishers, 2003.

[77] E. G. Larsson and J. Li, "Preamble Design for Multiple Antenna OFDM-Based WLANs with Null Subcarriers," in *IEEE Transactions on Consumer Electronics,* vol. 44, p. 7, 2001.

[78] A. Batra, "Multi-band OFDM Physical Layer Proposal Area Networks (WPAN)," in IEEE P802.15-03/26r2, IEEE p802.15 Wireless Personal Area Networks, pp.1-69, 2003.

[79] O. P. Sharma, V. Janyani and S. Sancheti, "Analysis of Raised Cosine Filtering in Communication Systems**,**" in Third International Conference on

Wireless Communication and Sensor Networks, WCSN '07, pp. 9 – 12, Dec. 2007.

[80] Y. S. Choi, P. J. Voltz and F. A. Cassara, "On Channel Estimation and Detection for Multicarrier Signals in Fast and Selective Rayleigh Fading Channels," in *IEEE Transactions on Communications,* vol. 49, pp. 1375-1387, 2001.

[81] T. Yao and T. Jiang, *Digital Signal Processing,* Huazhong Univeristy of Science and Technology Press, Wuhan, China, 1993.

[82] D. R. Smith, *Digital Transmission Systems,* Kluwer Academic Publishers Boston, 2004.

[83] J. J. Van De Beek, O. Edfors and M. Sandell, "On Channel Estimation in OFDM Systems," in Vehicular Technology Conference (VTC'95'), vol. 2, pp. 815-819, 1995.

[84] L. Wan and V. K. Dubey, "BER Performance of OFDM System Over Frequency Nonselective Fast Ricean Fading Channels," in *IEEE Transaction Letters,* vol. 5, pp. 19-21, 2001.

[85] M. K. Simon and M. S. Alouini, *Digital Communication over Fading Channels,* John Wiley & Sons, Inc., 2000.

[86] E. Saberinia and A. H. Tewfik, "Pulsed and non-pulsed OFDM ultra wideband wireless personal area networks," in 2003 IEEE Conference on Ultra Wideband Systems and Technologies, pp. 275-279, Nov. 2003.

[87] S. B. Slimane, "Peak-to-Average Power Ratio Reduction of OFDM Signals Using Broadband Pulse Shaping," in 2002 IEEE 56th Proceedings on Vehicular Technology Conference, VTC 2002-Fall, vol. 2, pp. 889-893, 2002.

[88] G. Lu, P. Wu and C. Carlemalm-Logothetis, "Peak-to-average power ratio reduction in OFDM based on transformation of partial transmit sequences," in Electronics Letters, vol.63, no.10, pp.105-106, 2006.

[89] C. Schurgers and M. B. Srivastava, "A Systematic Approach to Peak-to-Average Power Ratio in OFDM," in Proccedings of SPIE, pp. 454-464, 2001.

[90] R. Novak and W. A. Krzymien, "An Adaptive Downlink Spread Spectrum OFDM Packet Data System with Two-Dimensional Radio Resource Allocation: Performance in Low-Mobility Cellular Environments," in The 5th International Symposium on Wireless Personal Multimedia Communications, vol.1, Edmonton, Albert, Canada, pp. 163-167, 2002.

[91] M. Debbah, P. L. oubaton and M. D. Courvelle, "Spread OFDM Performance with MMSE Equalization," in Acoustics, Speech, and Signal Processing, vol. 4, pp. 2385-2388, 2001.

[92] D. L. Goeckel and G. Ananthaswamy, "On the Design of Multidimensional Signal Sets for OFDM Systems," in *IEEE Transactions on Communications*, vol. 50, pp. 442-452, 2002.

[93] S. Suyama, Y. Hara, H., Suzuki, Y., Kamio and K. Fukawa, "A Maximum Likelihood OFDM Receiver with Smoothed FFT-Window for Large Multipath Delay Difference over the Guard Interval," in IEEE 55th Vehicular Technology Conference, VTC Spring 2002, vol.3, pp.1247 - 1251, 2002.

[94] A. D. S Jayalath and C. Tellambura, "Use of data permutation to reduce the peak-to-average power ratio of an OFDM signal," in *Wireless Communications and Mobile Computing,* vol. 2, pp. 187-203, 2002.

[95] J. G. Proakis, "Implementation of Square Root Raised Cosine Filter," in http://140.117.160.140/CommEduImp/pdfdownload/9222/BBIC-2-

SRRC.pdf, Wireless Information Transmission Lab, National Sun Yat-Sen Univeristy, 2006.

[96] J. Tsui, *Digital Techniques for Wideband Receivers,* Artech House, Inc., 1995.

[97] P. Sioban and F. M. d. Saint-Martin, "New Designs of Linear-phase Transmitter and Receiver Filters for Digital Transmission Systems," in *IEEE Transactions on Circuits and Systems II: Analog and Digital Signal Processing*, vol. 46, pp. 428-433, 1999.

[98] C. E. Shannon, "A Mathematical Theory of Communication," in *The Bell System Technical Journal,* vol. 27, pp. 379-423, 1948.

[99] O. Edfors, M. Sandell, J. J. V. D. Beek, S. K. Wilson and P. O. Borjesson, "OFDM Channel Estimation by Singular Value Decomposition," in *IEEE Transactions on Communications,* vol. 46, pp. 931-938, 1998.

[100] O. P. Sharma, V. Janyani and S. Sancheti, "Analysis of Raised Cosine Filtering in Communication Systems," in Third International Conference on Wireless Communication and Sensor Networks, pp. 9-12, 2007.

[101] V. G. S. Prasad and K. V. S. Hari, "Interleaved Orthogonal Frequency Division Multiplexing System," in Acoustics, Speech and Signal Processing, vol. 3, pp. III-2745-III-2748, 2002.

[102] A. D. S Jayalth and C. Tellambura, "Interleaved PC-OFDM to Reduce the Peak-to-Average Power Ratio," in Advanced Signal Processing for Communication Systems, Springer Netherlands, pp. 224-228, 2007.

[103] R. Novak and W. A. Krzymien, "Diversity Combining Options for Spread Spectrum OFDM in Frequency Selective Channels," in Wireless Communications and Networking Conference, vol. 1, pp. 308-314, 2005.

[104] P. Tu, X. Huang and E. Dutkiewiz, "Diversity Performance of an Interleaved Spread Spectrum OFDM System over Frequency Selective Multipath Fading Channels," in 7th International Symposium on Communications and Information Technologies, Sydney, pp. 184-189, 2007.

[105] S. W. Kim, K. H. Yoon, R. G. Jung, J. W. Son and H. G. Ryu, "Adaptive Frequency Diversity OFDM (AFD-OFDM) Communication Narrow-Band," in Joint Conference of 10th Asia-Pacific Conference on Communications and 5th International Symposium on Multi-Dimensional Mobile Communicaitons, pp. 834-838, 2004.

[106] B. C. Jung, Y. J. Hong, D. K. Sung and S. Y. Chung, "Adaptive Sub-band Nulling for OFDM-Based Wireless Communication Systems," in IEEE Wireless Communications and Networking Conference, WCNC, pp. 1491-1495, 2007.

[107] H. Hamazumi, Y. Ito and H. Miyazawa, "Performance of Frequency Domain Sub-band Diversity Combination Technique for Wide-band Mobile Radio Reception: An Application to OFDM Reception," in *Electronics and Communications in Japan,* vol. 81, pp. 32-41, 1998.